Quantum mechanical tunneling between magnetic states

Sergei M. Vlasov

Faculty of Physical Sciences
School of Engineering and Natural Sciences
University of Iceland
2017

Quantum mechanical tunneling between magnetic states

Sergei M. Vlasov

Dissertation submitted in partial fulfillment of a
Philosophiae Doctor degree in Chemistry

PhD Supervisors:
Hannes Jónsson
Valery M. Uzdin

PhD Committee:
Hannes Jónsson
Valery M. Uzdin
Viðar Guðmundsson

Opponents:
Dmitrii E. Makarov
Oleg A. Tretiakov

Faculty of Physical Sciences
School of Engineering and Natural Sciences
University of Iceland
Reykjavík, December 2017

Quantum mechanical tunneling between magnetic states
Dissertation submitted in partial fulfillment of a *Philosophiae Doctor* degree in Chemistry

Faculty of Physical Sciences

School of Engineering and Natural Sciences
University of Iceland
Dunhagi, 5
107, Reykjavík, Reykjavík
Iceland

Telephone: +354 525 4700

Bibliographic information:
Sergei M. Vlasov, 2017, *Quantum mechanical tunneling between magnetic states*, PhD dissertation, Faculty of Physical Sciences, University of Iceland, 94 pp.

ISBN 978-9935-9383-3-6

Printing: Háskólaprent, Fálkagata 2, 107 Reykjavík
Reykjavík, Iceland, December, 2017

Abstract

Nanomagnetic systems and transitions between magnetic states are currently an active topic of research. Spintronics is, in particular, a new branch of science and technology where spin degrees of freedom and spin currents are used in an analogous way as electron current in electronic devices. The development of techniques for constructing magnetic systems with near atomic-scale precision opens the possibility of using quantum coherence in magnetic states for quantum computing devices. Quantum mechanical tunneling from one magnetic state to another is an important topic in that context. In this thesis, the tunneling between magnetic states is studied from the point of view of instanton theory. An instanton is an optimal tunneling path, corresponding to a solution to the equation of motion in imaginary time. A method for finding instantons in magnetic systems at finite temperature is presented. It is used to find the crossover temperature from over-the-barrier transition mechanism to tunneling. In some cases the crossover is abrupt, a first order transition, while in other cases it is more gradual, a second order transition. The latter is referred to as thermally assisted tunneling. A test problem including a single spin with a easy axis and applied transverse magnetic field is studied where the crossover changes from first to second order as the strength of the applied magnetic field is increased. The instanton is used to estimate the crossover temperature as well as the activation energy for thermally activated tunneling as a function of temperature. A general expression is presented for the crossover temperature in second order transitions where the only input is the second derivative of the energy of the system with respect to the orientation of the magnetic moments at the first order saddle point in the energy surface. The over-the-barrier transition rate and crossover temperature for tunneling is estimated for a monomer and dimer of a molecular magnet containing a Mn_4 group and the results found to agree well with experimental data. An application to the annihilation of a magnetic skyrmion shows that a crossover temperature for tunneling can be obtained at over 1 K for a certain range of values for the parameters in the Hamiltonian.

Útdráttur

Nanósegulkerfi og breytingar á milli segulástanda eru öflugt rannsóknasvið um þessar mundir. Spunatækni er t.a.m. ný grein vísinda og tækni þar sem spunafrelsisgráður og spunastraumur eru notuð á svipaðan hátt og rafstraumur í rafeindatækni. Tæknin sem hefur verið þróuð til að búa til segulkerfi með næstum atóm nákvæmni gerir það mögulegt að nota skammtasamspil segulkerfa í skammtatölvum. Skammtafræðilegt smug frá einu segulástandi til annars er einnig mikilvægt atriði í þessu samhengi. Í þessari ritgerð er smug milli segulástanda rannsakað með snareindaaðferðinni. Snareind er besti smugferillinn og samsvarar lausn á hreyfijöfnunni í tvinntölu tíma. Aðferð til að finna snareindir í segulkerfum við endanlegt hitastig er þróuð og notuð til að finna umbreytingarhitastigið þar sem hvarfgangurinn breytist úr hoppi yfir orkuhólinn í smug gegnum hólinn. Í sumum tilfellum er umbreytingin skörp, þ.e. fyrsta stigs, en í öðrum tilfellum er hún meira aflíðandi, þ.e. annars stigs. Í síðara tilfellinu er um að ræða varamadrifið smug. Prófdæmi þar sem stakur spuni er með auðveldan stefnuás og segulsvið er lagt þvert á ásinn er rannsakað en þar færist umbreytingin úr því að vera fyrsta stigs í að vera annars stigs við það að styrkur sviðsins er aukinn. Snareindin er notuð til að meta umbreytingarhitastigið sem og virkjunarorkuna fyrir varamadrifið smug sem fall af hitastigi. Almenn líking fyrir hitastigið við annars stigs umbreytingar er leidd út þar sem koma fyrir aðrar afleiður orkunnar með tilliti til stefnuhorna segulvigursins í fyrsta stigs söðulpunktinum á orkuyfirborðinu. Hraði hopp-yfir-hól hvarfgangsins og umbreytingarhitastigið er metið fyrir stakan Mn_4 sameindarsegul sem og tvennu og niðurstöðurnar eru í góðu samræmi við tilraunaniðurstöður. Reikningar á eyðingu segulskyrmeindar sýna að umbreytingarhitastigið fyrir smug getur verið yfir 1 K fyrir tiltekin gildi á stikunum í Hamiltonvirkjanum.

Table of Contents

Abstract iii

Útdráttur v

Table of Contents vii

List of publications ix

Acknowledgments xi

1 Introduction 1

2 Classical Transitions 5

2.1 Molecular Magnets . . . 6

2.1.1 Macrospin approximation . . . 6

2.2 Transition State Theory for Magnetic Systems . . . 7

2.2.1 Calculation of the pre-exponential factor in the transition rate . . . 10

2.2.2 Quantum corrections to HTST . . . 11

3 Tunneling in magnetic nanosystems 13

3.1 Coherent States . . . 15

3.1.1 Spin coherent states . . . 16

3.2 Spin Coherent State Path Integral (SCSPI) . . . 17

3.3 Semiclassical approximation, instantons . . . 20

3.4 Applications . . . 26

3.4.1 Uniaxial single spin system . . . 26

4 Calculation of the onset temperature for tunneling in magnetic systems 29

4.1 Derivation of the onset temperature formula . . . 30

4.2 Applications . . . 32

4.2.1 Mn_4 molecular magnet . . . 32

4.2.2 Magnetic skyrmion . . . 33

5 Conclusions 37

Article I 39

Article II 59

Article III 69

References 89

List of publications

Publications included in the thesis

1. S. Vlasov, P. F. Bessarab, V. M. Uzdin and H. Jónsson, *Classical to quantum mechanical tunneling mechanism crossover in thermal transitions between magnetic states*, Faraday discussions **195**, 93 (2016).

2. S. M. Vlasov, P. F. Bessarab, V. M. Uzdin and H. Jónsson, *Calculations of the onset temperature for tunneling in multispin systems*, Nanosystems: Physics, Chemistry, Mathematics **8**, 454 (2017).

3. S. M. Vlasov, P. F. Bessarab, V. M. Uzdin and H. Jónsson, *Instantons describing tunneling between magnetic states at finite temperature*, (submitted for publication).

Publications not included in the thesis

1. S. M. Vlasov, P. F. Bessarab, V. M. Uzdin and H. Jónsson, *Crossover temperature for quantum tunnelling in spin systems*, Journal of Physics: Conference Series **741**, 012183 (2016).

Acknowledgments

Above all else, I would like to thank my scientific advisors, professor H. Jónsson and professor V. M. Uzdin. They provided me with this fascinating project some years ago and have been navigating me through the deep sea of science for all this time.

I want to acknowledge I. Lobanov and P. Bessarab for the helpful discussions and significant extending my understanding of the subject. In addition, I am grateful to my colleagues and mates, S. Liashko, G. Müller, E. Jónsson and many others who helped me to keep the motivation strong and without whom this road would not have been so exciting. Their contribution hardly can be overestimated.

Finally, I want to express my sincerest appreciation to my dear family and all my friends who have supported me through the years.

1 Introduction

From its foundation in the 1920s, quantum mechanics has changed our understanding of the world at the atomic scale. When the distance between atoms is of the order of the de Broglie wavelength, quantum laws take over and the classical description of the world does not valid anymore. It is not possible to measure both position and momentum of a particle simultaneously with infinite precision as described by the Heisenberg uncertainty principle. Moreover, two or more identical particles with a half-integer spin cannot occupy the same state according to the Pauli exclusion principle. This leads to the exchange interaction, a purely quantum phenomenon.

Although quantum effects in macroscopic systems need to be considered in order to provide an adequate description of the system, it is usually enough to use a quasi-classical description. For instance, electrons in metals have a wavelength of $\lambda = \hbar/\sqrt{mkT}$ in the free particle approximation. This is of the same order as the distance between atoms even up to a temperature of 10^4 K. Thus, electrons in metals form a degenerate Fermi gas within the most relevant temperature range and the Fermi-Dirac distribution of the occupation of energy levels has the form of a step function. Nevertheless, the quasi-classical theory of Drude-Lorentz based on a phenomenological description of quantum effects describes the conductivity in metal systems quite well in most cases. There are, however, important cases where quantum behaviour manifests itself at the macroscopic level. One of such example is quantum mechanical tunnelling through a potential barrier.

The scanning tunneling microscope is made possible by the tunneling of electrons between a metal surface and a tip. As a result, crystal surfaces can be imaged with atomic resolution. Also, tunneling through a thin dielectric layer in three-layer systems and the effect of tunnel magnetoresistance, is the basis of recording and magnetic sensor devices. The functionality of these systems is based on the tunneling of electrons — microscopic particles. Their quantum mechanical behaviour can be observed only when they interact with macroscopic measuring devices.

Quantum tunneling can also be responsible for the change in the orientation of magnetic moments from one stable magnetic state to another. This has, for example been observed for molecular magnets – compounds of several 3d metal atoms that form a single macrospin, also known as a giant spin. The quantum mechanical behaviour can, in particular, been seen in ”steps” in the hysteresis loops.

Spin systems and transitions between magnetic states are receiving growing attention not only from a theoretical but also practical point of view. They are used in computer memory devices and vairous other applications. A new branch of science and technology has appeared recently – spintronics spin degrees of freedom are used in an analogous way as electrons in electronics. Spin dynamics are governed by Landau-Lifshitz equations

of motion within a quasi-classical approximation. These are first order equations and as a result, spin systems have no inertia. Therefore, devices based on spintronics can operate faster than their analogs based on electron current. The storage of information in non-volatile memory devices, where information is kept even when the device is switched off, is one important application area. Another area is the technology of atomic-scale magnetic systems [1, 2] that can keep and use quantum coherence of magnetic states for use in devices for quantum computing. At the present time, there are several of candidates for such devices ranging from metals to organic semiconductors [3, 4, 5].

As magnetic devices are becoming smaller and smaller, the question arises about stability of the magnetic states. The stability of a magnetic state against thermal fluctuations at a finite temperature is an important issue in the theory of magnetism [6, 7]. If a system escapes from a prepared stable or metastable state due to thermal fluctuations, the information recorded will be lost. For reasonably stable states, thermally activated transitions over an energy barrier are rare events on the time scale of the vibrations of the spins. This makes direct simulations of such transitions to evaluate the transition rate difficult or even impossible. However, the separation of time scales makes it possible to use transition rate theory (TST). Furthermore, by harmonic TST (HTST) can in many cases be applied in a harmonic to estimte magnetic transition rates and the lifetime of a magnetic state [7, 8, 9, 10]. This approach is based on an analysis of the multidimensional energy surface, i.e. the energy as a function of the direction of the magnetic moments (or spins), represented by spherical angles or cartesian coordinates. Stable and metastable states correspond to minima on the energy surface. The minimum energy path (MEP) between two local minima represents the mechanism for the transition between the corresponding states. Within an adiabatic approximation, the length of the magnetic vector is assumed to be constant or is calculated using self-consistent calculations for fixed values of the angles specifying the orientation which are treated as slow variables [10, 11, 12].

The maximum along an MEP corresponds to a first-order saddle point on the energy surface. The MEP does not correspond to a dynamical trajectory but it is the path with highest statistical weight. The lifetime of a magnetic state typically has an Arrhenius dependence on the temperature. By using HTST, it is possible to obtain the parameters in the Arrhenius law, both the activation energy and the pre-exponential factor, from an analysis of the energy surface of the system. The activation energy, i.e. the height of the energy barrier, is the difference between the energy at the saddle point and at the initial state minimum. The pre-exponential factor depends on the eigenvalues of the Hessian evaluated at the saddle point and at the minimum. In many cases, HTST has been shown to give accurate estimates for rates of magnetic transitions. However, it is approximate and the most severe approximation is typically the no-recrossing assumption of TST. Corrections to the HTST rate estimate can be evaluated from short time trajectories started at the transition state. Efficient methods for evaluating such dynamical corrections even for flat energy barriers have been presented [13].

At low enough temperature, quantum tunneling through the energy barrier becomes the dominant mechanism of a transition between stable states (or escape from the metastable state). In this low temperature tunneling regime, the rate depends only weakly on temperature or is independent of temperature. Thus, it is important to the

temperature at which tunneling becomes the dominant transition mechanism. This is referred to as the crossover temperature between over-the-barrer mechanism to quantum mechanical tunneling. At below the crossover temperature, T_c, quantum tunneling is the dominant transition mechanism, while above T_c the over-the-barrier transition mechanism dominates. This crossover can in some cases be abrupt to a temperature independent rate and is then referred to as first order. In other cases, it is smooth and activation energy drops more gradually to zero, in which case it is referred to as second order. There, the tunneling is thermally assisted. The shape of the energy surface determines which type of crossover occurs [14].

In some cases, a mapping can be made between a magnetic system and a corresponding particle system [15]. Then, methods developed for particle systems can be applied to estimate rates of magnetic transitions. This approach is known as the effective potential (EP) method and it has been used in several theoretical studies of systems with uniaxial and biaxial anisotropy [16, 17, 18, 19, 20]. However, there are no known methods for EP for systems with higher-order anisotropy, such as fourth-order [21], while it can affect the tunneling rate significantly [22, 23].

As part of this thesis work, a method was developed for evaluating the second order onset temperature for tunneling in a system with an arbitrary number of spins, see articles I and II. The required input for the calculation are the second derivatives of the energy with respect to the orientation of the magnetic vectors at the first order saddle point on the energy surface characterizing the classical remagnetization mechanism [24, 25]. The method is general and is applicable to Hamiltonians with higher-order terms. The application of the method to a monomer and a dimer of molecular magnets containing a Mn_4 group gave excellent agreement with reported experimental measurements.

Instanton theory is frequently used to estimate quantum tunneling rates in particle systems. The theory is based on the quasi-classical approximation of Feynman's path integrals (FPI). In this approach, diagonal elements of the density matrix $\rho(\beta) = e^{-\beta H}$, included in the partition function expression, are split into multipliers by dividing the interval $\beta = 1/T$ on N segments $\varepsilon = \beta/N$

$$\rho(\beta) = e^{-\varepsilon H} \cdot e^{-\varepsilon H} \ldots e^{-\varepsilon H}. \tag{1}$$

One can think of β as an imaginary "time" interval in this case, and the particles move in closed trajectory with the period β. This trajectory is a classical path, i.e. a solution of the equation of motion in "imaginary" time, $\tau = it$. It is referred to as instanton. When in the classical case there is no classical trajectory for which a particle appears on the other side of the barrier, the quantum mechanical theory provides such a solutions via tunneling.

The instanton approach is widely used in quantum field theory and is increasingly used in chemistry and condensed matter physics. It has, however, not been used significantly for the analysis of magnetic transitions. There, it is necessary to use coherent state path integrals (CSPI) CSPIs for magnetic systems contain a topological term, a Wess-Zumino term corresponding to a Berry phase. It can cause interference between different instantons. In practice, this effect can be observed as oscillation of the tunneling rate. Such behavior was seen in an Fe_8 molecular magnet [23].

The task of finding instantons is non-trivial but important for an analysis of the crossover temperature and the tunneling rate. In particle systems, instantons are first-

order saddle points on the Euclidean action surface. They can, therefore, be located using NEB method as the point of maximum action along the minimum action path (MAP) [26] or by using saddle point search methods such as the minimum mode following method. However, methods developed for finding instantons in particle systems do not work for magnetic systems because the action corresponding to CSPIs is a complex-valued function. The taks is there to find stationary points of the complex-valued action. A method for doing that was developed in the thesis project and it was applied to the uniaxial spin system (see article III). The method can readily be extended to multi-spin systems.

2 Classical Transitions

This chapter deals with classical thermally activated transitions in magnetic systems, i.e. the over-the-barrier transition mechanism. First, the methodology for analysis of transitions in atomic systems is reviewed briefly. The transition from one stable state of the system to another is typicalle a rare event, in the sense that transitions occur rarely on the time-scale of the vibrations. Thus, the problem of time scales arises: The calculations of classical dynamical trajectories cannot be carried out long enough to be used for analysis of the transitions. Instead, a statistical approach is needed. One such approach is transition state theory (TST). It was initially formulated for chemical reactions by Wigner [27]. A key concept is the dividing surface, a $(D-1)$-dimensional subspace, where D is the dimensionality of the system, dividing the initial state configurations from all other configurations. The dividing surface should be located in such a way that every classical trajectory going from the initial state to some other state needs to go through it. TST assumes that if the system is at the dividing surface and is moving away from the initial state, then it is a reactive trajectory abd a transition will occur. Thereby, TST ignores recrossing transitions where a trajectory crosses the dividing surface two or more times. Other assumptions of TST are: Adiabatic separation of electronic and nucleiar degrees of freedom, classical equations of motion and thermal equilibrium with a heat bath, i.e. the energy is Boltzmann distributed in the initial state. If one approximates the energy function in the vicinity of the initial state minimum and in the vicinity of the saddle point on the energy surface then an analytical expression for the transition rate can be obtained. The expression contains eigenvalues of the Hessian of the energy function at the minima and the saddle point.

The theory developed by Kramers is similar although it starts from a different formulation [28]. The main difference is that the expression by Kramers includes an estimate of the effect of recrossing trajectories within an approximation based on a Brownian motion approach. Using Langevin dynamics, he showed the rate in a presence of a buffer gas or a solvent is a function of solvent viscosity. This theory was generalized to multidimensional systems by Langer [29]. Subsequently, the theory of activation transitions was reformulated for the description of different processes, like first-order phase transitions, a relaxation of liquid crystals, etc. It should be pointed out that the approach by Kramers only takes into account part of the recrossing trajectories. The shape of the energy surface, in particular curvature of the MEP, can lead to recrossings which are not taken into account in Kramers theory. The full effect of recrossing trajectories is, however, included when dynamical corrections to TST are calculated from short time trajectories started at the transition state.

These rate theories that were developed originally for estimating rates of chemical reactions have been adapted to magnetic transitions. By using Langer's method, Braun

investigated domain wall propagation in magnetic systems [7]. Recently, an expression for the rate of magnetic transitions within HTST where the flux through the transition state is obtained from Landau-Lifshitz equations of motion has been presented [10]. It has, for example, bee applied to transitions involving non-collinear magnetic systems such as skyrmions.

2.1 Molecular Magnets

Molecular magnets or single-molecule magnets (SMM) are compounds with a magnetic core that contains one or several metal ions with unpaired electrons surrounded by organic ligands. The strong spin-spin interaction leads to conservation of the relative spin direction of the electrons in the metal atmoms. The the SMM can therefore be represented by a single magnetic momentum vector. Various differenent SMMs have been synthesized. However, most studies have been carried out for three types. Perhaps the most popular type are compounds continaining twelve manganese atoms and acetate ligands – [Mn_{12}-ac] [30]. The other two types are [Fe_8] [31] and [Mn_4] [32].

From a physical point of view, SMMs exhibit both classical and quantum properties. They demonstrate the whole series of quantum effects from quantum tunneling of magnetization [33, 34] and Berry phase interference [23] to quantum coherence[35] that can be useful in spintronics. SMMs can be used as two-level qubits in quantum computers and also as magnetic refrigerators (magnetocaloric effect) in electronic devices at cryogenic temperature.

2.1.1 Macrospin approximation

SMMs are usually described within the macrospin approximation, also known as the giant spin approximation. For example, the Mn_4 compounds have one Mn^{4+} ion with spin of $j = 3/2$ and three Mn^{3+} ions with spin of $j = 2$. The cluster has a total spin of $j = 9/2$, due to ferromagnetic interaction between the Mn^{III} ions and antiferromagnetic coupling with the Mn^{IV}. The effective Hamiltonian for the description of the energy levels is

$$\hat{H} = -D\hat{S}_z^2 - B\hat{S}_z^4 + C\left(\hat{S}_+^4 + \hat{S}_-^4\right) - g\mu_B \mathbf{H}\cdot\hat{\mathbf{S}}, \tag{2}$$

where D, B, and C are parameters for anisotropy energy terms up to fourth order. The **z** axis coincides with the axis of quantization and is responsible for the appearance of an energy barrier between the two degenerate ground states. This approximation works at temperature below 30 K [36].

In the present work, the macrospin approximation and an effective Heisenberg Hamiltonian is used, using parameters obtained mainly from experimental measurements. A more fundamental description of the states of a magnetic system can be based on the non-collinear Alexander-Anderson model (NCAA) [37, 38] or density functional theory (DFT) [39, 40]. Atomic units are used with $e = m_e = \hbar = 1$, Bohr magneton of $\mu_B = 1/2$. The magnetic moment of the SMM is $\mu = gj\mu_B/\hbar = gj/2j$, where g is Lange's factor.

2.2 Transition State Theory for Magnetic Systems

Let us consider a magnetic system with multiple spins interacting with each other. It is convenient to switch to phase variables when describing the energy of the system. We will use a unit vector $\hat{\mathbf{n}}$ defining the direction of the spin in space. The operators $\hat{S}_x$, $\hat{S}_y$ and $\hat{S}_z$ correspond to spin projections onto x-, y-, and z-axis. We will use spherical polar coordinates $\omega = \{\theta_1, \theta_2, \ldots, \theta_N, \phi_1, \phi_2, \ldots, \phi_N\}$. The length of $\hat{\mathbf{n}}$ is always equal to one and spin operators have the following form

$$\begin{aligned} \hat{S}_x &= j \sin\theta \cos\phi, \\ \hat{S}_y &= j \sin\theta \sin\phi, \\ \hat{S}_z &= j \cos\theta. \end{aligned} \tag{3}$$

The energy of the system is a smooth function of ω.

The classical over-the-barrier transition rate can be evaluated by using HTST adapted to magnetic systems. The equation is

$$\Gamma^{HTST} = \nu_0 e^{-\Delta E / k_B T}, \tag{4}$$

where ν_0 is the pre-exponential factor depending on the curvature of the energy surface in the initial state and in the transition state. ΔE is the activation energy of the transition from the initial state to the final state.

In order for the intial state to have long enough lifetime for Boltzmann distribution to be established and maintained, the height of the barrier has to be significantly higher than thermal energy, $\Delta E \gg k_B T$. Nevertheless, owing to thermal fluctuations, the system can receive enough energy to jump over the barrier. In order to estimate the rate of such rare events, we need to evaluate the activation energy and the pre-exponential factor.

The initial and final states correspond to minima on the energy surface. The transition between these states can be characterized by the path in the configuration space where the energy along is minimal with respect to transverse directions. Such a path is called minimum energy path (MEP). According to HTST, the point on the MEP with the highest energy, $E^{\dagger}$, a first-order saddle point $\omega = \omega^{\dagger}$ on the energy surface, gives an estimated of the activation energy $\Delta E = E^{\dagger} - E_m$, where E_m is the energy at the initial state minimum. The transition rate has an Arrhenius dependence on temperature as in (4).

There are several ways to find MEPs and saddle points. One of the most popular is the nudged elastic band (NEB) method [41, 42]. It can be used for finding an MEP when both the initial and final states are known. The method is based on a discrete representation of the path as a sequence of replicas of the system located in the configurational space. As an initial guess, an arbitrary path connecting the two fixed endpoints is used. It usually corresponds to coherent remagnetization. Then, an iterative algorithm is applied to move the replicas to the MEP. The displacements follow the effective force

$$\mathbf{F}_i^{eff} = -\nabla E(\omega_i)|_{\perp} + (\mathbf{F}_{\mathbf{i}}^{\mathbf{s}} \cdot \hat{\tau}_i)\hat{\tau}_i, \tag{5}$$

where $E(\omega_i)|_{\perp}$ is the component of the gradient transverse to the path and $\hat{\tau}_i$ is the unit

vector directed along the path at the i-th replica

$$\begin{aligned}\hat{\tau}_i &= \hat{d}_i/|\hat{d}_i|,\\ \hat{d}_i &= \frac{\omega_{i+1}-\omega_i}{|\omega_{i+1}-\omega_i|}+\frac{\omega_i-\omega_{i-1}}{|\omega_i-\omega_{i-1}|}.\end{aligned} \tag{6}$$

$\mathbf{F}_\mathbf{i}^\mathbf{s}$ is a spring force used to distribute the replicase evenly along the path

$$\mathbf{F}_\mathbf{i}^\mathbf{s} = k(|\omega_{i+1}-\omega_i|-|\omega_i-\omega_{i-1}|), \tag{7}$$

where k is the spring constant. The value of k is chosen to make the two components of the efficient force of the same order of magnitude. The optimization leads to $E(\omega_i)|_\perp = 0$ which means the path becomes an MEP. The relevant saddle point corresponds to the maximum energy along the MEP.

Despite the fact, that spherical coordinates automatically conserve the length of the magnetic moment vector, they have one disadvantage, namely the degeneracy in the ϕ coordinate at the poles, $\theta = 0, \pi$. Therefore, if one of the images lies in the vicinity of a pole, it is better to use Cartesian coordinates. MEPs for magnetic transitions can be found by using the geodesic nudged elastic band method (GNEB) [43]. This is a modification of the original NEB method where the distance between the replicas is the geodesic distance on a sphere and where an additional projection of the tangent and the forces is applied in order to preserve the length of the magnetic momentum.

Saddle points can also be found by starting only from the initial state without including information about a final state. This can, for example, be done with the minimum mode following method where the minimum mode is found using the dimer approach [44], Lanczos [45], or Raileigh-Ritz [46]. These three methods share a common feature, they do not require an explicit form of the objective function and they are based on a modification of the gradient and the Hessian of the energy function in such a way that the modified force around the saddle point corresponds to that of a minimum. Another method for finding a saddle point is the one by Dewar, Healy and Stewart [47] where two images of the system move toward each other from regions of the reactant and product until they met in the saddle point.

An MEP shows how the remagnetization change during a transition. It shows, for instance, whether all spins rotate simultaneously or whether a domain wall or soliton is formed [7, 12]. A remagnetization transition involving the formation of a domain wall in an iron monolayer on W(110) surface is shown in figure 2.1. Two cases are shown, one where the long axis of the island is directed along the anisotropy axis (upper) and in the other where it is orthogonal to the anisotropy axis (lower). In both cases, the energy barrier is nearly flat at the top. The MEP was found using the GNEB method [43].

Sometimes an MEP goes through several intermediate metastable states. This behavior can be seen in a chain of iron atoms on a CuN substrate [49]. The energy of the chain of 8 iron atoms with spin $j = 2$ is described by the function

$$\begin{aligned}E(\omega) = {} & Dj^2\cos^2\theta_1 + Bj\mu_0\cos\theta_1 + \\ & \sum_{i=2}^{8}\left[Dj^2\cos^2\theta_i + Bj\mu_0\cos\theta_i + \right. \\ & \left. Kj^2(\cos\theta_i\cos\theta_{i-1}+\sin\theta_i\sin\theta_{i-1}\cos(\phi_i-\phi_{i-1}))\right],\end{aligned} \tag{8}$$

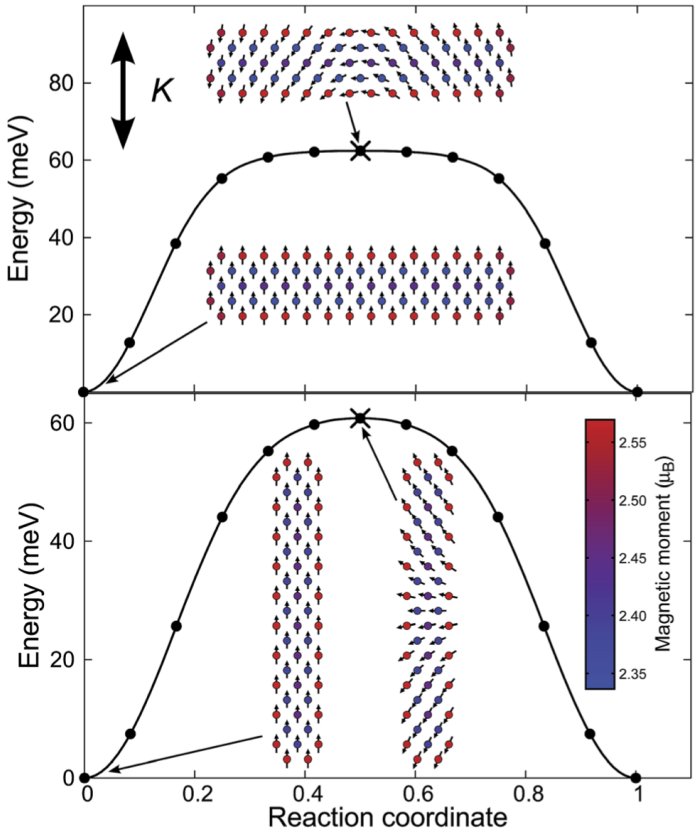

Figure 2.1. Calculated MEP for remagnetization in an iron islands on W(110) surface. Both the direction and length of magnetic moments were obtained using self-consistent calculations within the NCAA model [11, 48]. Color indicates the length of a magnetic moment of a single iron atom. The orientation of the anisotropy axis, K, is also shown. The long axis of the island is along (bottom) or perpendicular (top) to the anisotropy axis. In both cases, the MEP has a plateau at the top of the energy barrier, i.e. the energy is almost constant in this region as the domain wall propagates along the island. The picture is taken from [24].

where $D = 1.55$ meV is the anisotropy constant, $B = 1$ T is the applied magnetic field, and $K = 1.3$ meV is the Heisenberg exchange interaction. The plot of the energy along the calculated MEP has a zigzag form, see figure 2.2. The strong anisotropy leads to a mechanism for the remagnetization where individual spins are flipped one by one.

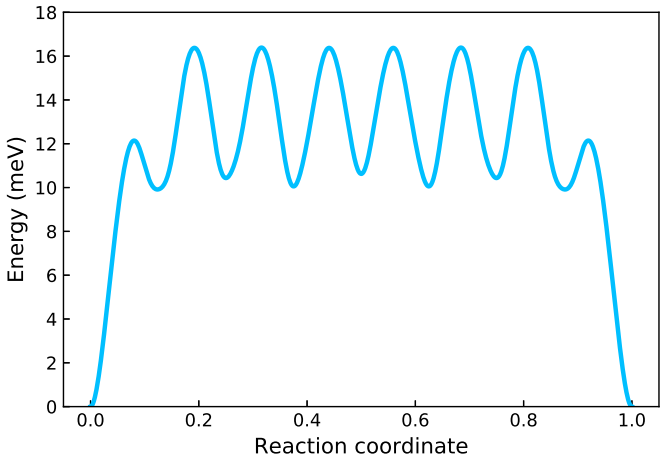

Figure 2.2. Calculated MEP for the remagnetization in a chain of 8 iron atoms on a CuN surface. The parameters of the system are taken from [49]. The graph shows how the system goes through several metastable states (local minima along the MEP). Such behavior is common for systems where the anisotropy energy is significantly larger than the exchange energy.

2.2.1 Calculation of the pre-exponential factor in the transition rate

The HTST expression for the pre-exponential factor contains eigenvalues of the Hessian of the energy at the saddle point $\varepsilon_{\dagger,j}$ and at the initial state minimum $\varepsilon_{m,j}$ [10, 11, 12]

$$\nu_0 = \frac{1}{2\pi}\frac{J_\dagger}{J_m}\sqrt{\sum_{j=2}^{D}\frac{a_j^2}{\varepsilon_{\dagger,j}}\frac{\prod_{i=1}^{D}\sqrt{\varepsilon_{m,i}}}{\prod_{i=2}^{D}\sqrt{\varepsilon_{\dagger,i}}}}. \tag{9}$$

Here, $J^\dagger = J(\omega^\dagger)$ and $J^m = J(\omega^m)$ are Jacobians evaluated at the saddle point an at the minimum, respectively, and $\beta = 1/k_B T$. The lowest eigenvalue of the Hessian at the saddle point $\varepsilon_{\dagger,1}$ is negative and is excluded from the sum in (9). Coefficients a_j in (9) are normal components of the velocity within the dividing surface. They can be found from the Landau-Lifshitz equation of motion

$$\frac{d\hat{\mathbf{n}}_j}{dt} = \hat{\mathbf{n}}_j \times \frac{\partial E^\dagger}{\partial \hat{\mathbf{n}}_j}, \tag{10}$$

or, in spherical coordinates with a quadratic expansion

$$\begin{aligned}\dot{\phi}_i &= \frac{1}{j\sin\theta_i}\sum_{k=1}^{N}\left(\frac{\partial^2 E^\dagger}{\partial\theta_i\partial\phi_k}\phi_k + \frac{\partial^2 E^\dagger}{\partial\theta_i\partial\theta_k}\theta_k\right), \qquad i = 1\ldots N,\\ \dot{\theta}_i &= -\frac{1}{j\sin\theta_i}\sum_{k=1}^{N}\left(\frac{\partial^2 E^\dagger}{\partial\phi_i\partial\phi_k}\phi_k + \frac{\partial^2 E^\dagger}{\partial\phi_i\partial\theta_k}\theta_k\right), \qquad i = 1\ldots N.\end{aligned} \tag{11}$$

Let V be the matrix corresponding to the system of equations (11)

$$V = \left(\begin{array}{ccc|ccc} \frac{E^\dagger_{\theta_0\phi_0}}{j\sin\theta_0} & \cdots & \frac{E^\dagger_{\theta_0\phi_N}}{j\sin\theta_0} & \frac{E^\dagger_{\theta_0\theta_0}}{j\sin\theta_0} & \cdots & \frac{E^\dagger_{\theta_0\theta_N}}{j\sin\theta_0} \\ \vdots & \ddots & \vdots & \vdots & \ddots & \vdots \\ \frac{E^\dagger_{\theta_N\phi_0}}{j\sin\theta_N} & \cdots & \frac{E^\dagger_{\theta_N\phi_N}}{j\sin\theta_N} & \frac{E^\dagger_{\theta_N\theta_0}}{j\sin\theta_N} & \cdots & \frac{E^\dagger_{\theta_N\theta_N}}{j\sin\theta_N} \\ \hline -\frac{E^\dagger_{\phi_0\phi_0}}{j\sin\theta_0} & \cdots & -\frac{E^\dagger_{\phi_0\phi_N}}{j\sin\theta_0} & -\frac{E^\dagger_{\phi_0\theta_0}}{j\sin\theta_0} & \cdots & -\frac{E^\dagger_{\phi_0\theta_N}}{j\sin\theta_0} \\ \vdots & \ddots & \vdots & \vdots & \ddots & \vdots \\ -\frac{E^\dagger_{\phi_N\phi_0}}{j\sin\theta_N} & \cdots & -\frac{E^\dagger_{\phi_N\phi_N}}{j\sin\theta_N} & -\frac{E^\dagger_{\phi_N\theta_0}}{j\sin\theta_N} & \cdots & -\frac{E^\dagger_{\phi_N\theta_N}}{j\sin\theta_N} \end{array}\right) \tag{12}$$

Then, it is necessary to transform V to a new basis consisting of eigenvectors U of the Hessian at the saddle point

$$V_n = U^{-1}VU, \tag{13}$$

where coefficients a_j are placed in the row in V_n that corresponds to the negative mode.

Calculations of the rate of remagnetization in iron islands on a W(110) surface [11] using this expression gave good agreement with experimental results [50]. The calculations were performed both with the Heisenberg Hamiltonian and the NCAA model[12]. With the NCAA model, it was shown that the length of the magnetic moment of the various iron atoms in the island differ by about 10%, the larger value applying to the rim atoms. Also, this HTST expression for the rate has been used for the analysis of hysteresis loops in spring magnets [51], annihilation of magnetic skyrmions [52] and interaction of a magnetic tip with an antiferromagnetic metal surface [53].

2.2.2 Quantum corrections to HTST

At low temperature and in nano-systems in particular, quantum mechanical effects need to be taken into account even above the crossover temperature for tunneling. The reason for this is the zero point energy due to confinement of the vibrations of the magentic moments. This can, for example, reduce the height of the barrier significantly, analogous to the kinetic isotope effect in chemical reactions. Within HTST this correction can be accounted for by including zero point energy of the vibrational modes (magnon frequencies) both in the initial state and in the transition state. In the transition state the system has one less real magnon frequency than in the initial state. Therefore, the effective activation energy is usually reduced by the zero point energy correction. However, it is also possible that the frequencies at the saddle point are sufficiently higher

than at the initial state minimum that the energy barrier is actually increased. This is referred to as inverse isotope effect. The effective barrier is given by

$$\Delta E^{ZPE} = \left(E(\omega^{\dagger}) + \frac{1}{2} \sum_{i=1}^{N-1} \nu_{\dagger,i} \right) - \left(E(\omega_m) + \frac{1}{2} \sum_{i=1}^{N} \nu_{m,i} \right), \tag{14}$$

where $\nu_{\dagger,i}$ and $\nu_{m,i}$ are magnon frequencies [54, 55], calculated at the saddle point and at the minimum, respectively. In the single spin case, they have the following form

$$\nu = \frac{1}{j \sin\theta} \sqrt{\frac{\partial^2 E}{\partial \theta^2} \frac{\partial^2 E}{\partial \phi^2} - \left(\frac{\partial^2 E}{\partial \theta \partial \phi} \right)^2}. \tag{15}$$

At the saddle point the frequency ν will be purely imaginary and does not appear in (14).

In the case of multi-spin systems, magnon frequencies can be found from the following system of equations

$$det(i\nu \mathrm{I} + V) = 0, \tag{16}$$

where I is the identity matrix and V is the matrix from (11).

3 Tunneling in magnetic nanosystems

From a theoretical point of view, quantum tunneling arises due to non-commuting observables in the system. In the case of a systems of particles, those variables are coordinates and momenta, $[\hat{x},\hat{p}] = i$. For magnetic (spin) systems, they are the components of the spin operator $[\hat{S}_i,\hat{S}_j] = i\varepsilon_{ijk}\hat{S}_k$.

The $\Im F$ formalisn is one way of formulating a quantum mechanical version of transition state theory. There, the transition rate is expressed as

$$\Gamma = -2\Im F, \tag{17}$$

where $\Im F$ is an imaginary part of the free energy $F = -\ln Z/\beta$.

The energy of the system in a metastable state can be described as

$$E_n = E_n^0 - i\frac{1}{2}\Gamma_n. \tag{18}$$

Then, the partition function takes the form

$$Z = \sum_n e^{-\beta\left(E_n^0 - i\Gamma_n/2\right)}. \tag{19}$$

Metastability requires the condition $\Gamma_n \ll E_n^0$ and by virtue of this, the partition function can be rewritten as

$$Z = Z' + iZ'' \approx \sum_n e^{-\beta E_n^0} + i(\beta/2)\sum_n \Gamma_n e^{-\beta E_n^0}. \tag{20}$$

The real part of the partition function is defined by properties of the potential well, but the top of the barrier (a transition state in a multidimensional case) defines the imaginary part of the partition function. Letting $Z' = Z_0$ and $Z'' = \Im Z_b$, we write the resulting expression for the transition rate as

$$\Gamma = \frac{2}{\beta}\frac{\Im Z_b}{Z_0}. \tag{21}$$

Equation (21) can be rewritten using the path integral formalism to find the tunneling rate. This approach has important advantages. First of all, it is based on the intuitive notion of a path along which the system travels from one state to another. Secondly, the amplitude of the transition probability is given by the sum of contributions from all plausible paths as $\exp(-S_E)$, where $S_E = \int d\tau \mathscr{L}_E$ is the Euclidean action that describes the path

$$Z = \int dx(0) \int_{x(0)=x(\beta)} D[x(\tau)] \exp\left(-S_E[x(\tau)]\right). \tag{22}$$

Here, $D[x(\tau)]$ is a measure over all closed paths. The variable τ can be split into intervals $0 = \tau_0 < \tau_1 \ldots \tau_N = \beta$, $N \to \infty$, in this case, $D[x(\tau)]$ can be considered as the product $Qdx(\tau_1)\ldots dx_{N-1}$, where Q plays the role of a normalization constant. Thereby, the path integral approach ties together classical and quantum theories. Another intriguing property of a path integral is that it demonstrates clearly the connection between statistical physics and quantum mechanics.

The partition function in (22) can be expressed through a trace of the density matrix

$$Z = \mathrm{Tr}(\rho) = \int dx \rho(x,x,\beta) = \int dx \langle x|e^{-\beta\hat{H}}|x\rangle, \tag{23}$$

Where Tr stands for the trace. Thereby, if one makes the formal substitution $\tau = it$, one can move from the partition function to an expression for the quantum propagator

$$K = \langle x_b|e^{-i\hat{H}T}|x_a\rangle = \int_{x(0)=x_a}^{x(T)=x_b} D[x(t)] \exp\left(iS[x(t)]\right), \tag{24}$$

that corresponds to the probability amplitude of a transition from the state with coordinate x_a to a state with x_b in time T.

This substitution is known as Wick's rotation and it turns a Minkowski metric $(ds^2 = -(dt)^2 + dx^2)$ into a Euclidean metric $(ds^2 = d\tau^2 + dx^2)$. The Euclidean action, S_E, may be considered as an action in imaginary time $\tau = it$. This technique plays a central role in instanton theory because it makes trajectories that are forbidden in the classical case be possible, i.e. tunneling paths.

In hindsight, it is impossible to formulate the path integral for a spin system in a similar way as for a particle systems. The reason is that the Hilbert space of a spin does not have continuously parameterized eigenstates corresponding to classical variables, such as coordinates and momenta. For a system with spin j, there are $2j+1$ states that are eigenstates of the $\hat{S}_z$ operator: $\hat{S}_z|\mu, j\rangle = \mu|\mu, j\rangle$, where μ runs from $-j$ to j.

At first sight, we only need to formulate the classical Lagrangian $\mathscr{L}$ for the spin system in order to get the path integral. $\mathscr{L}$ requires canonical conjugate variables and in the spin problem, they are $p = \cos\theta$ and $x = \phi$. The Lagrangian then can be written as

$$\mathscr{L} = p\dot{x} - \mathscr{H} = \dot{\phi}\cos\theta - \mathscr{H}(\theta,\phi). \tag{25}$$

Unfortunately, this expression is ill-defined. To get the right formulation of the path integral for magnetic systems one needs to use the basis of coherent states.

Many spin systems, such as the model of a uniaxial single ferromagnetic spin in a transverse magnetic field [16], have been studied using the method of effective potential [56, 15]. In the this method, one introduces a spin wave function using the $\hat{S}_z$ eigenstates and then transforms an eigenvalue equation $\hat{H}|\psi\rangle = E|\psi\rangle$ to a differential equation, which is then reduced to a Schroedinger equation with an effective potential and a possibly coordinate dependent mass. The energy spectrum of the spin system coincides with the first $2j+1$ levels of the resulting particle system, where j is the spin number. Thereby, one can use the whole range of techniques developed for particle systems to investigate spin systems. This technique is also referred as the spin-particle mapping method.

However, the effective potential method has several disadvantages. First of all, this method is not universal, there is no general way to construct the corresponding potential

and one needs to find it from scratch for each spin system. Furthermore, for a spin systems described by a Hamiltonian with higher-order terms (cubic and higher), there are no known strategies for the spin-particle mapping. However, many spin systems, e.g. molecular magnets, are described by such Hamiltonians. Also, multi-spin systems are difficult to treat. Apparently, only one study of spin-particle mapping for a two-spin system has been reported [20]. Finally, the action of the corresponding particle system does not contain a topological term (49) that is responsible for known interference effects in magnetic systems [57, 58, 59]. This phenomenon cannot be investigated using the effective potential method. Thereby, it is essential to have an efficient method for studying tunneling in spin systems without spin-particle mapping.

3.1 Coherent States

Coherent states were discovered by Schroedinger as harmonic oscillator states that describe the dynamics as closely to the classical dynamics as possible. Today they are actively used in various fields of physics, such as quantum optics, physics of superfluids and superconductors, quantum field theory, and string theory. Coherent states, in most cases, are a useful addition to or substitute for other physical representations of a system, but in the case of spins, they are the only known way to develop path integrals.

The term – coherent states – was introduced by Glauber in his work on laser beams [60]. Then, Perelomov elaborated and expanded on coherent states for different physical and mathematical objects. He showed that it is possible to consider the task of formulating coherent states as the part of group theory [61]. Thus, the mathematical machinery was developed for the various tasks in mathematical physics. That is why nowadays the coherent states of a harmonic oscillator are referred to as canonical coherent states, in order to distinguish them from other systems.

These states form a basis of the annihilation operator $\hat{a}$

$$\hat{a}|z\rangle = z|z\rangle, \tag{26}$$

and because $\hat{a}$ is not a Hermitian operator ($\hat{a} \neq \hat{a}^\dagger$), the eigenvalues, z, are in general complex.

States (26) have the important feature that they minimize the Heisenberg uncertanty

$$\langle(\Delta\hat{x})^2\rangle_z \langle(\Delta\hat{p})^2\rangle_z = \frac{1}{4}, \quad \forall z \in \mathbb{C}. \tag{27}$$

If one rewrites $z = \alpha e^{i\theta}$, then the position of a coherent state in phase space can be tracked by the coordinate and momentum of the classical oscillator with phase θ and amplitude $|\alpha|$. As is shown in figure 3.3, the uncertainty is equal to the diameter $1/2$ of the disk in phase space. With a variation of a phase or an amplitude, the disk moves in phase space without any deformartion. Thereby these quantum states are the nearest thing to classical points in phase space.

A coherent state can be obtained by acting the displacement operator $D(z) = \exp\left(z\hat{a}^\dagger - z^*\hat{a}\right)$ on the vacuum state

$$|z\rangle = D(z)|0\rangle = e^{z\hat{a}^\dagger - z^*\hat{a}}|0\rangle. \tag{28}$$

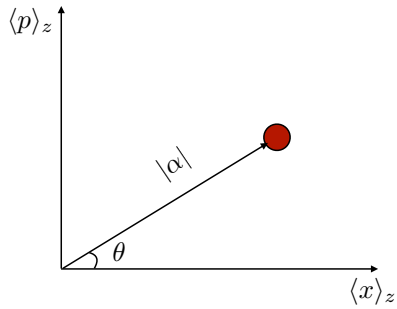

Figure 3.3. The coherent state in phase space. The area of the disk remains constant as it movemes and the Heisenberg uncertainty remains minimal.

Another property of coherent states is that they form an overcomplete basis. That means the set remains complete even after removing at least one eigenvector. Also, the states $|z\rangle$ are not orthogonal. The scalar product (overlap) of coherent states can be written as

$$\langle z|z'\rangle = \exp\left\{-(|z|^2+|z'|^2)/2+z^*z'\right\}, \tag{29}$$

and therefore

$$|\langle z|z'\rangle|^2 = e^{-|z-z'|^2}. \tag{30}$$

3.1.1 Spin coherent states

As it was mentioned before, the basis of coherent states can be constructed for the group other than Heisenberg group corresponding to the canonical coherent states. One such group is the special unitary group $SU(2)$ which describes a spin. The unitary irreducible representation of this group is set by the integer or half-integer number j and has the canonical basis $|\mu, j\rangle$. Generators of the group $\hat{S}_x$, $\hat{S}_y$, and $\hat{S}_z$ define the algebra and satisfy to commutation relations

$$[\hat{S}_z, \hat{S}_\pm] = \pm\hat{S}_\pm, [\hat{S}_-, \hat{S}_+] = -2\hat{S}_z, \tag{31}$$

where $\hat{S}_\pm = \hat{S}_x \pm i\hat{S}_y$ are raising/lowering operators. Spin coherent states can be established from the state $|\mu, j\rangle$ with arbitrary μ, however, we choose the state $|j, j\rangle$ because it minimizes the dispersion of the Kasimir operator $\hat{\mathbf{S}}^2 = \hat{S}_x^2 + \hat{S}_y^2 + \hat{S}_z^2$:

$$\Delta\hat{\mathbf{S}}^2 = j(j+1) - j^2 = j. \tag{32}$$

After that, consider the state labeled by the vector $\hat{\mathbf{n}}$ with unit length [62, 61],

$$|\hat{\mathbf{n}}\rangle = e^{i\theta(\hat{n}_0\times\hat{n})\cdot\hat{S}}|-j,j\rangle, \tag{33}$$

where $\hat{n}_0$ is a unit vector parallel to the quantization axis. It is convenient to choose $\hat{n}_0 = \hat{\mathbf{z}} = (0,0,1)$ and $\theta = \hat{n}_0 \cdot \hat{n}$. Operator $D(\hat{\mathbf{n}}) = \exp(i\theta(\hat{n}_0\times\hat{n})\cdot\hat{S})$ is the displacement operator similar to (28). Indeed, if we assume $\xi = -(\theta/2)e^{-i\phi}$, then we get

$$D(\xi) = \exp\left(\xi\hat{S}_+ - \xi^*\hat{S}_-\right). \tag{34}$$

The state $|\hat{\mathbf{n}}\rangle$ can be expanded in the basis of $|\mu, j\rangle$. By using spherical angular coordinates θ and ϕ for the parametrization of $\hat{\mathbf{n}}$ we obtain

$$|\theta,\phi\rangle = \sum_{m=-j}^{j}\sqrt{\frac{(2j)!}{(j+m)!(j-m)!}}\left(\sin\frac{\theta}{2}\right)^{j+m}\left(\cos\frac{\theta}{2}\right)^{j-m}e^{-i(j+m)\phi}|m,j\rangle. \tag{35}$$

Or, with the substitution $z = -\tan\frac{\theta}{2}e^{i\phi}$,

$$|z\rangle = \frac{1}{(1+z\bar{z})^j}\sum_{m=-j}^{j}\sqrt{\frac{(2j)!}{(j+m)!(j-m)!}}z^{j+m}|m,j\rangle. \tag{36}$$

Also we will need the closure relation (resolution of unity) that is given as

$$1 = \frac{2j+1}{4\pi}\int d^3\hat{n}|\hat{\mathbf{n}}\rangle\langle\hat{\mathbf{n}}|. \tag{37}$$

Hence, we have enough instruments in our toolbox to derive the expression for the path integral for magnetic systems.

3.2 Spin Coherent State Path Integral (SCSPI)

In this section we will briefly derive the expression for SCSPI. Mostly, we will follow the presentation by Fradkin [62]. For an alternative derivation, see [63]. We will start our analysis with the expression for the partition function

$$Z = \mathrm{Sp}(e^{-\beta\hat{H}} = \int d\hat{\mathbf{n}}\langle\hat{\mathbf{n}}|e^{-\beta\hat{H}}|\hat{\mathbf{n}}\rangle. \tag{38}$$

As in the case of Feynman path integrals, we split the interval β in N parts

$$\langle\hat{\mathbf{n}}|e^{-\beta\hat{H}}|\hat{\mathbf{n}}\rangle = \lim_{N\to\infty}\langle\hat{\mathbf{n}}|\left(1-\varepsilon\hat{H}\right)^N|\hat{\mathbf{n}}\rangle, \tag{39}$$

where $\varepsilon = \beta/N$. Then, we insert the resolution of identity (37) into every segment of the interval and thus, the expression for the partition function will get the following form

$$Z = \lim_{N\to\infty}\int\prod_{k=1}^{N}d\mu(\hat{\mathbf{n}}_k)\langle\hat{\mathbf{n}}_k|\left(1-\varepsilon\hat{H}\right)|\hat{\mathbf{n}}_{k-1}\rangle, \tag{40}$$

where $d\mu(\hat{\mathbf{n}}_k) = \left(\frac{2j+1}{4\pi}\right) d^3\mathbf{n}\delta(\mathbf{n}^2-1)$ is the invariant integration measure and $\hat{\mathbf{n}}_0 = \hat{\mathbf{n}}_N = \hat{\mathbf{n}}$, i.e. periodic boundary conditions are fulfilled.

Consider matrix elements from (40), up to the quadratic terms,

$$\begin{aligned}\langle\hat{\mathbf{n}}_k|\left(1-\varepsilon\hat{H}\right)|\hat{\mathbf{n}}_{k-1}\rangle &= \langle\hat{\mathbf{n}}_k|\hat{\mathbf{n}}_{k-1}\rangle\left(1-\varepsilon\frac{\langle\hat{\mathbf{n}}_k|\hat{H}|\hat{\mathbf{n}}_{k-1}\rangle}{\langle\hat{\mathbf{n}}_k|\hat{\mathbf{n}}_{k-1}\rangle}\right)\\ &\simeq \langle\hat{\mathbf{n}}_k|\hat{\mathbf{n}}_{k-1}\rangle\exp\left(-\varepsilon\frac{\langle\hat{\mathbf{n}}_k|\hat{H}|\hat{\mathbf{n}}_{k-1}\rangle}{\langle\hat{\mathbf{n}}_k|\hat{\mathbf{n}}_{k-1}\rangle}\right).\end{aligned} \tag{41}$$

The first term in (41) is not equal to zero since coherent states are not orthogonal. It looks like a disadvantage of this approach, but as we will see later on, this property leads to the important feature of the spin path integral – topological phase equivalent to Berry phase[64]. Let us rewrite this term in a bit more convenient way as

$$\langle\hat{\mathbf{n}}_k|\hat{\mathbf{n}}_{k-1}\rangle = 1-\varepsilon\frac{\langle\hat{\mathbf{n}}_k|(|\hat{\mathbf{n}}_k\rangle-|\hat{\mathbf{n}}_{k-1}\rangle)}{\varepsilon} \simeq \exp\left(-\varepsilon\frac{\langle\hat{\mathbf{n}}_k|(|\hat{\mathbf{n}}_k\rangle-|\hat{\mathbf{n}}_{k-1}\rangle)}{\varepsilon}\right). \tag{42}$$

Finally, in the limit $\varepsilon\to 0$ we get

$$Z = \int D[\hat{\mathbf{n}}(\tau)]e^{-S_E}, \tag{43}$$

where

$$S_E = \int_0^\beta d\tau\left[\langle\hat{\mathbf{n}}|\frac{\partial}{\partial\tau}|\hat{\mathbf{n}}\rangle + \langle\hat{\mathbf{n}}|\hat{H}|\hat{\mathbf{n}}\rangle\right] \tag{44}$$

Now that we have the expression for the spin action, we can examine closely the matrix elements. For the Hamiltonian, we need to obtain expectation values on the basis of coherent states. Let us consider a simple example, $\hat{H} = \hat{S}_z$. Using the expansion from (35) we reformulate it as

$$\begin{aligned}\langle\hat{\mathbf{n}}|\hat{S}_z|\hat{\mathbf{n}}\rangle &= \left(\cos^2\frac{\theta}{2}\right)^{2j}\sum_{m=-j}^{j}\frac{(2j)!}{(j+m)!(j-m)!}\left(\tan^2\frac{\theta}{2}\right)^{j+m}\langle m,j|\hat{S}_z|m,j\rangle\\ &= \left(\cos^2\frac{\theta}{2}\right)^{2j}\sum_{m=-j}^{j}\frac{(2j)!m}{(j+m)!(j-m)!}\left(\tan^2\frac{\theta}{2}\right)^{j+m}\\ &= \left(\cos^2\frac{\theta}{2}\right)^{2j}\left(2j\tan^2\frac{\theta}{2}\left(\cos^2\frac{\theta}{2}\right)^{1-2j} - j\left(\cos^2\frac{\theta}{2}\right)^{-2j}\right)\\ &= -j+2j\sin^2\frac{\theta}{2} = -j\cos\theta.\end{aligned} \tag{45}$$

The same procedure can be performed for $\hat{S}_x$ and $\hat{S}_y$:

$$\begin{aligned}\langle\hat{S}_x\rangle &= -j\sin\theta\cos\phi,\\ \langle\hat{S}_y\rangle &= -j\sin\theta\sin\phi.\end{aligned} \tag{46}$$

Thus, there is a direct correspondence between expectation values of the quantum Hamiltonian and a classical values.

As for the first term in (44), we will show later on that it plays the role of a Berry phase [64, 7] related to the parallel transport of the Hamiltonian along the closed path.

With the parametrization from (35), we can write

$$\langle \hat{\mathbf{n}}| = \sum_{p=0}^{2j} \sqrt{\frac{(2j)!}{p!(2j-p)!}} \left(\cos\frac{\theta}{2}\right)^{2j} \left(\tan\frac{\theta}{2}\right)^{p} e^{ip\phi} \langle -j+p, j|, \tag{47}$$

$$|\frac{\partial \hat{\mathbf{n}}}{\partial \tau}\rangle = \sum_{p=0}^{2j} \sqrt{\frac{(2j)!}{p!(2j-p)!}} \left(\cos\frac{\theta}{2}\right)^{2j} \left(\tan\frac{\theta}{2}\right)^{p} e^{-ip\phi} \left[\left(p\csc\theta - j\tan\frac{\theta}{2}\right)\dot{\theta} - ip\dot{\phi}\right] |-j+p, j\rangle, \tag{48}$$

and

$$\langle \hat{\mathbf{n}}|\frac{\partial}{\partial \tau}|\hat{\mathbf{n}}\rangle = -j\tan\frac{\theta}{2}\dot{\theta} + j\tan\frac{\theta}{2}\dot{\theta} - ij(1-\cos\theta)\dot{\phi} = -ij(1-\cos\theta)\dot{\phi} \tag{49}$$

hence, the partition function (43) gets the phase

$$\begin{aligned} \exp\left(\int_0^\beta d\tau \langle \hat{\mathbf{n}}|\frac{\partial}{\partial \tau}|\hat{\mathbf{n}}\rangle\right) &= \exp\left(-ij\int_0^\beta d\tau(1-\cos\theta)\dot{\phi}\right) \\ &= \exp\left(-ij\int_\Gamma (1-\cos\theta)d\phi\right), \end{aligned} \tag{50}$$

where Γ is a closed path described by the vector $\hat{\mathbf{n}} = \{\theta(\tau), \phi(\tau)\}$. It is easy to see that this term does not depend on the velocity and has a pure geometric origin. It is proportional to the area of the section bounded by Γ (see figure 3.4).

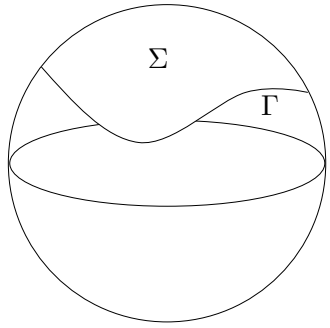

Figure 3.4. For the closed trajectory Γ*, Berry phase* (49) *is proportional to the area of the cap* Σ *bounded by this trajectory.*

There is a mechanical analogy. We can think of $\hat{\mathbf{n}}(\tau)$ as the coordinate of a massless charged particle moving on the unit sphere as time τ evolves, and there is a magnetic monopole with charge j is located at the center of the sphere. The contribution of the electromagnetic exchange to the action usually has the following form

$$S_{em} = \int \vec{A} \cdot d\hat{\mathbf{n}}, \tag{51}$$

where $\vec{A}$ is the vector potential with the singularity at the pole that corresponds to a Dirac string. Using Stokes theorem, we can rewrite (51) as a surface integral. Then, S_{em} is given by the flux of the magnetic monopole through the area Σ multiplied by the charge j.

In examples from real life, the path can go through the pole, hence it is worthwhile to have an expression of the potential $\vec{A}$ in cartesian coordinates

$$\vec{A}[\hat{\mathbf{n}}] = \frac{\hat{\mathbf{n}}_0 \times \hat{\mathbf{n}}}{1 + \hat{\mathbf{n}}_0 \cdot \hat{\mathbf{n}}}, \tag{52}$$

where $\hat{\mathbf{n}}_0$ is an arbitrary unit vector that does not belong to the path $\hat{\mathbf{n}}(\tau)$. Thus, the vector potential $\vec{A}$ is a gauge field.

3.3 Semiclassical approximation, instantons

In the semiclassical approximation, the path with the highest statistical weight in (43) is a stationary point of the action. One needs to expand the action in Taylor series up to the quadratic term. The obtained quadratic form in the exponent leads us to Gaussian integrals that can be evaluated and give a pre-exponential factor. In general, there might be several stationary points, in which case their contributions add up. However, for the sake of simplicity, but without loss of generality, we will assume we have only one stationary point.

The closed trajectory corresponding to the stationary point of the action is called an instatnton. Thus, the integral (43) can be written as

$$Z = \int D[\hat{\mathbf{n}}(\tau)] e^{-S_E} \approx K e^{-S_{inst}}, \tag{53}$$

where K is the pre-factor defined by the curvature of the action surface both in the stable and transition states and S_{inst} is the Euclidean action evaluated at the stationary point – the instanton.

As it was shown in the previous chapter that the Euclidean action describing a spin system with a spin j has the form

$$S[\mathbf{\Omega}] = \int_{-\beta/2}^{\beta/2} d\tau \left[-ij(1-\cos\theta)\dot{\phi} + E(\mathbf{\Omega}) \right], \tag{54}$$

where $\mathbf{\Omega} = \omega(\tau) = (\theta(\tau), \phi(\tau))$ is the closed path on the energy surface $E(\mathbf{\Omega})$. In order to find the instanton, we need to search for stationary paths for (54), i.e. $\delta S = 0$.

Therefyre, a solution to the equation of motion is needed

$$\begin{aligned}\dot{\theta} &= \frac{i}{j\sin\theta}\frac{\partial E}{\partial \phi},\\ \dot{\phi} &= -\frac{i}{j\sin\theta}\frac{\partial E}{\partial \theta},\end{aligned} \tag{55}$$

where θ and ϕ satisfy the boundary condition $\mathbf{\Omega}(0) = \mathbf{\Omega}(\beta)$. These are the Landau-Lifshitz equations in imaginary time.

These equations have two types of solutions. The first one is trivial, $\mathbf{\Omega} \equiv \mathbf{\Omega}(0) = \omega_0$, and corresponds to a stationary point on the energy surface, $E_0 \equiv E(\omega_0)$. If we take the saddle point as the stationary $\omega^\dagger = (\theta^\dagger, \phi^\dagger)$, we get

$$S_{jump} = \beta E(\omega^\dagger) = \beta E^\dagger. \tag{56}$$

This solution corresponds to the classical transitions over the barrier at higher temperature.

The second type is an instanton, it is a closed path connecting two wells of the potential. In the limit of zero temperature $T \to 0$, i.e. $\beta \to \infty$, it corresponds to quantum tunneling from the ground state. With rising temperature, the amplitude of the instanton is reduced until it collapses to a point. It is easy to show how the potential energy $E[\mathbf{\Omega}(\tau)]$ is conserved along the instanton. It suffices to take the time derivative of E and insert it into (55). As a result, we will get

$$\frac{dE}{d\tau} = \frac{\partial E}{\partial \theta}\dot{\theta} + \frac{\partial E}{\partial \phi}\dot{\phi} = \frac{i}{j\sin\theta}\frac{\partial E}{\partial \phi}\frac{\partial E}{\partial \theta} - \frac{i}{j\sin\theta}\frac{\partial E}{\partial \theta}\frac{\partial E}{\partial \phi} = 0. \tag{57}$$

In contrast to atomic systems, where the full energy is conserved, i.e. $T + U = const$, there is no kinetic energy in magnetic systems. Therefore, if we want to find the path that satisfies the boundary conditions and is a solution of (55), we must consider the analytic continuation of the function $E(\mathbf{\Omega})$. There is no nontrivial solution of (55) for real $\mathbf{\Omega}$.

We will represent the path by a set of discrete points $\mathbf{\Omega}(\tau) = \{\omega_0, \omega_1, \ldots, \omega_N\}$ and the integral in (54) will be approximated with the help of the trapezoidal rule

$$\tilde{S} = \beta S = \sum_{k=1}^{N}\left[k(T)\left(1 - \frac{\cos\theta_k + \cos\theta_{k+1}}{2}\right)(\phi_{k+1} - \phi_k) + \frac{E(\omega_k) + E(\omega_{k+1})}{2N}\right], \tag{58}$$

where $k(T) = -ijTk_B$ As a result, our task boils down to finding a stationary point of the function

$$\tilde{S} : \mathbb{C}^N \to \mathbb{C}, \tag{59}$$

that is, to solve the system of differential equations

$$\begin{aligned}\frac{\partial \tilde{S}}{\partial \theta_k} &= \frac{1}{2}k(T)\sin\theta_k(\phi_{k+1} - \phi_{k-1}) + \frac{\partial E}{\partial \theta_k} = 0,\\ \frac{\partial \tilde{S}}{\partial \phi_k} &= \frac{1}{2}k(T)(\cos\theta_{k+1} - \cos\theta_{k-1}) + \frac{\partial E}{\partial \phi_k} = 0, k \in [1, N].\end{aligned} \tag{60}$$

In particle systems, the instanton corresponds to a first order saddle point on the action surface[26], so methods for finding first-order saddle points can be applied for this task, e.g. the minimum mode following method. The main difference between the quantum case from the classical case is that we deal with a chain of replicas of the system rather than a point in configuration space. In fact, this approach is sometimes is referred to as the ring-polymer method since every closed path is a set of replicas of the the system and can be considered as a polymer molecule.

Spin systems have a complex action function defined on a complex field, so methods developed for particle systems are not applicable. There is no natural linear ordering on the set of complex numbers. Moreover, since $\tilde{S}$ is the holomorphic function, i.e. $\tilde{S}$ is analytical with respect to each variable, we cannot just consider the real part. Indeed, consider the function $f(\mathbf{x},\mathbf{y})$ that is the real part of a holomorphic function and $\mathbf{x} = \{x_1 \dots x_N\}$, $\mathbf{y} = \{y_1 \dots y_N\}$, and $z_k = x_k + iy_k$. That is $f : \mathbb{R}^{2N} \to \mathbb{R}$. However, due to the Cauchy-Riemann equations, at every point within the domain Hessian matrix of f has the equal number of positive and negative eigenvalues.

However, we can build a real-valued objective function from the equations in (60). Let us introduce $\tilde{\omega} = (\theta^R, \theta^I, \phi^R, \phi^I)$ with $\theta = \theta^R + \theta^I$ and $\phi = \phi^R + \phi^I$ and the vector function $f(\tilde{\mathbf{\Omega}})$:

$$f(\tilde{\mathbf{\Omega}}) = \begin{pmatrix} f_1(\tilde{\mathbf{\Omega}}) \\ \vdots \\ f_N(\tilde{\mathbf{\Omega}}) \end{pmatrix} \equiv \begin{pmatrix} \frac{\partial S(\tilde{\mathbf{\Omega}})}{\partial \tilde{\Omega}_1} \\ \vdots \\ \frac{\partial S(\tilde{\mathbf{\Omega}})}{\partial \tilde{\Omega}_N} \end{pmatrix}. \tag{61}$$

Then, the objective function can be written as the squared norm of $f(\tilde{\mathbf{\Omega}})$:

$$F(\tilde{\mathbf{\Omega}}) \equiv \frac{1}{2} \bar{f}(\tilde{\mathbf{\Omega}}) \cdot f(\tilde{\mathbf{\Omega}}), \tag{62}$$

Therefore, our task is to find $F(\tilde{\mathbf{\Omega}}) = 0$, a global minimum of the function. We need non-trivial solutions in the sense that $\tilde{\mathbf{\Omega}}$ has to represent a closed path.

Despite the fact that there are several methods for finding global minima such as simulating annealing [65] and methods based on saddle point searches [66], the global optimization remains a challenging problem, requiring large computater power. Also, every stationary point is a global minimum with the value zero, but we are only interested in a small subset of such points. Fortunately, we can avoid these difficulties if we manage to use good enough initial guess for $\tilde{\mathbf{\Omega}}$ in our optimization procedure. Every optimization algorithm requires an initial guess for the point of the optimum, it might be a random point or one can choose it from some heuristic presumptions. If we choose the initial guess for $\tilde{\mathbf{\Omega}}$ lying in the vicinity of the the relevant minimum of $F(\tilde{\mathbf{\Omega}})$, then a local optimization procedure will be good enough.

From (57) we know the energy is preserved along the instanton, that is the instanton lies along an iso-contour of the energy surface, say $E(\tilde{\omega}_k) = E', \forall k \in [1,N]$. We can use this fact for the preliminary search of the isntanton. To do so, we can use a modification of the NEB method for finding optimal paths [67] with the objective function being

$$S^{iso} = \frac{1}{2} \sum_{k=0}^{N} (E(\tilde{\omega}_k) - E')^2. \tag{63}$$

In this method as in the original NEB method, the component of the gradient tangent to the path is removed during the optimization to prevent images from collapsing onto each other at the minima.

Denote the negative gradient of the function (63) as

$$g_k = -\nabla_k S^{iso} = -((E(\tilde{\omega}_k) - E')\nabla_k(E(\tilde{\omega}_k)), \tag{64}$$

where $k = 0, \ldots, N$. The effective forces acted on the system are the same as in NEB

$$g_k^{opt} = g_k^{\perp} + g_k^{sp}, \tag{65}$$

where

$$g_k^{\perp} = g_k - (g_k \cdot \hat{\tau}_k)\hat{\tau}_k, \tag{66}$$

$\hat{\tau}_k$ is the unit vector directed along the path same as in (6) and g_k^{sp} is the spring force parallel to the path provided the equidistant distribution of images along the path. Then, various minimization algorithms can be applied to optimize S^{iso} displacing every point along the path in the direction of g_k^{opt}. For the review of several minimization procedures see [68].

Once, the iso-contour path $\tilde{\mathbf{\Omega}}^{iso}$ is found we can start finding the instanton. First of all we want to be able to find the corresponding temperature. This is possible by calculating the travelling time τ along the closed path $\tilde{\mathbf{\Omega}}^{iso}$. Because

$$\tau = \beta = 1/T \tag{67}$$

the corresponding temperature can be obtained from the period. Since the instanton is the solution of eqn. (55) and $\tilde{\mathbf{\Omega}}^{iso}$ assumed to coincide with the instanton we do not need the exact distribution of the images for the estimation of the period. Thus, we can use Landau-Lifshitz equations to calculate the velocity between each neighbour images in the path and calculate the time it takes the system to make one wind around the path. The algorithm is following, using the fact that $\tilde{\mathbf{\Omega}}^{iso} = \{\tilde{\Omega}_1^{iso}, \tilde{\Omega}_2^{iso} \ldots \tilde{\Omega}_N^{iso}\}$ the Landau-Lifshitz equations can be approximated as

$$\frac{|d_i|}{\Delta\tau_i} = |v_i|, \tag{68}$$

where $|d_i| = |\tilde{\Omega}_{i+1}^{iso} - \tilde{\Omega}_i^{iso}|$ and

$$v_i = \begin{pmatrix} \frac{i}{j\sin\theta_i}\frac{\partial E}{\partial \phi_i} \\ \frac{-i}{j\sin\theta_i}\frac{\partial E}{\partial \theta_i} \end{pmatrix}, \tag{69}$$

with $\theta_i = \theta_i^R + i\theta_i^I$ and $\phi_i = \phi_i^R + i\phi_i^I$. Finally, the total time of traveling along the path is the sum of travelling times between all images:

$$\tau = \sum_{i=1}^{N} \Delta\tau_i. \tag{70}$$

At the end, having both $\tilde{\mathbf{\Omega}}^{iso}$ and $T_0 = 1/\tau$ as the initial guess for the instanton we can perform the minimization of the objective function (62). We have found BFGS

algorithm is more efficient among other in this task. It requires the first derivatives of the function with respect to the coordinates $(\theta^R, \theta^I, \phi^R, \phi^I)$,

$$\begin{cases} \dfrac{\partial F}{\partial \theta_j^R} = \displaystyle\sum_{k=1}^{N} \Re\dfrac{\partial S}{\partial \theta_k}\Re\dfrac{\partial^2 S}{\partial \theta_k \partial \theta_j} + \Im\dfrac{\partial S}{\partial \theta_k}\Im\dfrac{\partial^2 S}{\partial \theta_k \partial \theta_j} + \Re\dfrac{\partial S}{\partial \phi_k}\Re\dfrac{\partial^2 S}{\partial \phi_k \partial \theta_j} + \Im\dfrac{\partial S}{\partial \phi_k}\Im\dfrac{\partial^2 S}{\partial \phi_k \partial \theta_j}, \\ \dfrac{\partial F}{\partial \theta_j^I} = \displaystyle\sum_{k=1}^{N} \Im\dfrac{\partial S}{\partial \theta_k}\Re\dfrac{\partial^2 S}{\partial \theta_k \partial \theta_j} - \Re\dfrac{\partial S}{\partial \theta_k}\Im\dfrac{\partial^2 S}{\partial \theta_k \partial \theta_j} + \Im\dfrac{\partial S}{\partial \phi_k}\Re\dfrac{\partial^2 S}{\partial \phi_k \partial \theta_j} - \Re\dfrac{\partial S}{\partial \phi_k}\Im\dfrac{\partial^2 S}{\partial \phi_k \partial \theta_j}, \\ \dfrac{\partial F}{\partial \phi_j^R} = \displaystyle\sum_{k=1}^{N} \Re\dfrac{\partial S}{\partial \theta_k}\Re\dfrac{\partial^2 S}{\partial \theta_k \partial \phi_j} + \Im\dfrac{\partial S}{\partial \theta_k}\Im\dfrac{\partial^2 S}{\partial \theta_k \partial \phi_j} + \Re\dfrac{\partial S}{\partial \phi_k}\Re\dfrac{\partial^2 S}{\partial \phi_k \partial \phi_j} + \Im\dfrac{\partial S}{\partial \phi_k}\Im\dfrac{\partial^2 S}{\partial \phi_k \partial \phi_j}, \\ \dfrac{\partial F}{\partial \phi_j^I} = \displaystyle\sum_{k=1}^{N} \Im\dfrac{\partial S}{\partial \theta_k}\Re\dfrac{\partial^2 S}{\partial \theta_k \partial \phi_j} - \Re\dfrac{\partial S}{\partial \theta_k}\Im\dfrac{\partial^2 S}{\partial \theta_k \partial \phi_j} + \Im\dfrac{\partial S}{\partial \phi_k}\Re\dfrac{\partial^2 S}{\partial \phi_k \partial \phi_j} - \Re\dfrac{\partial S}{\partial \phi_k}\Im\dfrac{\partial^2 S}{\partial \phi_k \partial \phi_j}, \end{cases} \quad \forall j \in [1, N] \tag{71}$$

Since the function (62) depends on the temperature and it can be seen from (60) that at $T = 0$ components of the gradient of the action coincide with gradient of the energy at each image along the path. Thus, during the minimization each image will be relocated to the nearest stationary point on the extended (complex) energy surface. Therefore, we can say the algorithm of finding instantons works only at finite temperature. A similar consideration applies to particle systems.

One of the fascinating differences between magnetic and particle systems is that in the case of magnetic systems, the period of an instanton sometimes depends on the instanton energy in a non-monotonic way [14] (see figure 3.5). Such behavior corresponds to first-order crossover from the classical over-the-barrier regime to quantum tunneling. This makes the task of finding instantons more tricky because in that case, two or more instantons with different energy can correspond to the same period. Also, instantons corresponding to first-order crossover are not directly connected to the classical saddle point on the energy surface.

Summarizing, the quantum transition rate in semiclassical approximation depends on temperature, thus we need to find instantons for a range of values of the energy from the initial state minimum, E_0, to the first order saddle point, $E^\dagger$, and evaluate the corresponding periods and thereby temperature. The procedure can be divided up into the following steps

1. Find a set of iso-contour paths $\tilde{\mathbf{\Omega}}^{iso}$ for the energy ranging from E_0 to $E^\dagger$ using the modified NEB algorithm.

2. Find τ and T_0 from Landau-Lifshitz dynamics in imaginary time, the period and temperature of each $\tilde{\mathbf{\Omega}}^{iso}$.

3. Using lists of $\tilde{\mathbf{\Omega}}^{iso}$ and T_0 as the set of initial guesses minimize the objective function (62) that gives you the whole set of instantons.

A generalization of the method for multi-spin systems is straightforward.

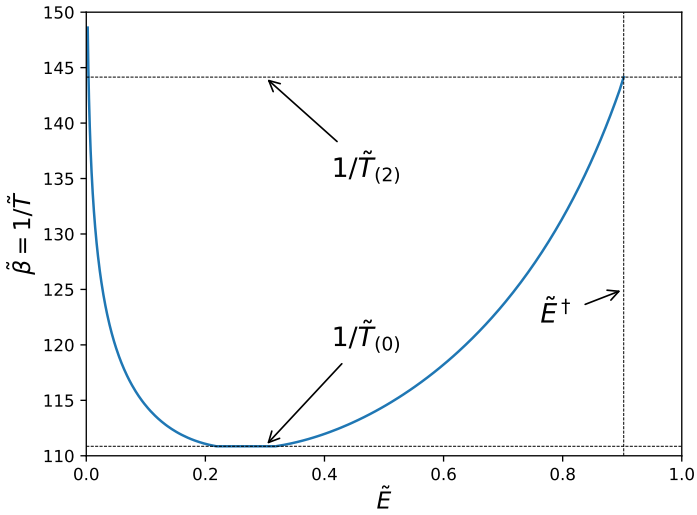

Figure 3.5. Non-monotonic dependance of the period of the instanton on the energy, both in dimensionless units, for a uniaxial single spin system in a transverse applied magnetic field. $\tilde{E}^{\dagger}$ is the energy of the system at the saddle point of the energy surface. $\tilde{T}_{(m)}$ is the highest temperature at which an instanton exists and $\tilde{T}_{(2)}$ is the temperature at which the instanton collapses to the saddle point on the energy surface.

3.4 Applications

3.4.1 Uniaxial single spin system

In this section we will find instantons at different temperature for the uniaxial spin system in a transverse magnetic field. The system with spin j is described by the Hamiltonian

$$\hat{H} = D\hat{S}_z^2 + \mathbf{B}\cdot\mathbf{S}, \tag{72}$$

where D is the anisotropy along $\hat{\mathbf{z}}$ axis and $\vec{B} = B_x$ is the applied magnetic field along $\hat{\mathbf{x}}$ axis.

We can match the differentiable function E of the angle coordinates $\omega = (\theta, \phi)$ to the operator (72)

$$E(\omega) = Dj^2\cos^2\theta + Bj\sin\theta\cos\phi + Dj^2 + \frac{B^2}{4D}, \tag{73}$$

here we have added a constant to make the minimum of the function equal to zero.

For convenience, we rewrite the energy function in dimensionless parameters

$$\tilde{E}(\omega) = -\cos^2\theta - 2h_x\sin\theta\cos\phi \tag{74}$$

where $h_x = B/2Dj$ and $\tilde{E}(\omega) = Dj^2E(\omega)$ and we will use also the dimensionless variable $\tilde{T} = Tk_B/2Dj$.

It is known for this system that it has the first-order crossover for $h_x < 1/4$[16]. Thus, we can expect non-monotonic dependence of the instanton period on the energy for small enough field. We will find instantons for two cases: $h_x = 0.05$ and $h_x = 0.5$

As was discussed before, we need to analytically continue the energy function (73), i.e. switch $\omega = (\theta, \phi)$ to the $\tilde{\omega} = (\theta^R, \theta^I, \phi^R, \phi^I)$, and use

$$\tilde{E}(\tilde{\omega}) = -\cos^2(\theta^R + i\theta^I) - 2h_x\sin(\theta^R + i\theta^I)\cos(\phi^R + i\phi^I). \tag{75}$$

Due to the fact that each point along the instanton lies in $\mathbb{R}^4$, a graphical representation of both the energy function and the instanton is impossible in general. However, the numerical calculations of (75) in the present case show that some coordinates along the instanton are constant, namely $\phi^R = 0$ and $\theta^I = 0$, and the energy is real

$$\tilde{E}_{inst} = -\cos^2(\theta^R) - 2h_x\sin(\theta^R)\cosh(\phi^I). \tag{76}$$

This makes it possible to illustrate the path, as in figure 3.6, where several instantons at varlious temperatures are shown.

When the applied magnetic field is small enough, $h_x = 0.05$, the system shows non-monotonic dependence of the instanton period on the energy (see figure 3.5), however, at a higher field $h_x = 0.5$, the the instanton period decreases monotonically with increasing energy, as shown in figure 3.7

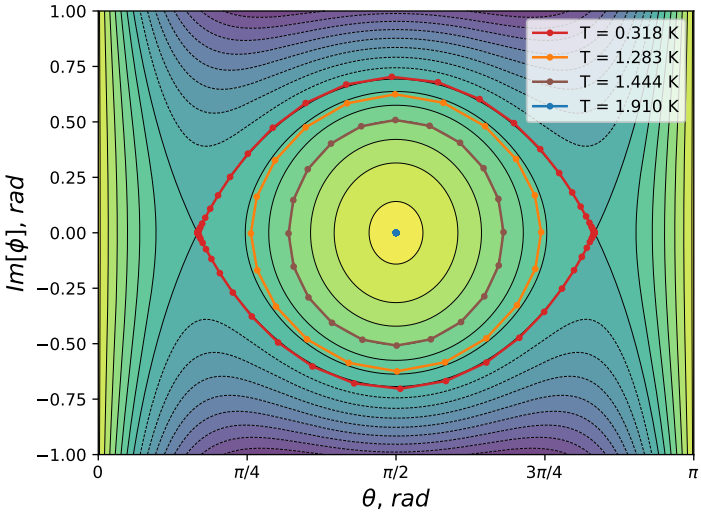

Figure 3.6. Calculated instantons (red, orange, brown, and blue lines with dots) at various values of the temperature for a system described by (74) *in transverse field corresponding to* $h_x = 0.5$. *The contour graph shows the energy surface* (76).

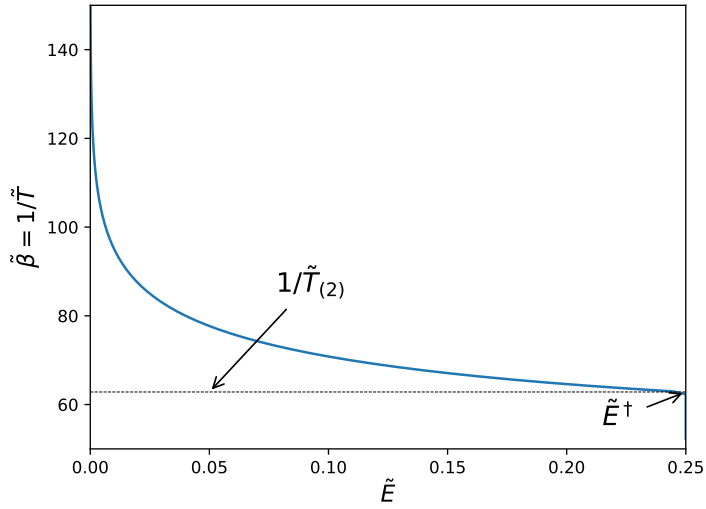

Figure 3.7. The monotonic dependance of the instanton period on energy, both in dimensionless units, for a uniaxial single spin system in transverse applied magnetic field. $\tilde{E}^{\dagger}$ *is the energy of the system at the saddle point on the energy surface. At temperature* $\tilde{T}_{(2)}$ *the instanton collapses to the saddle point on the energy surface.*

4 Calculation of the onset temperature for tunneling in magnetic systems

At sufficiently high temperature, the direction of the magnetic moment can change by thermal activation and its rate Γ obeys the Arrhenius law $\Gamma \sim \exp(-\Delta E/k_B T)$ with ΔE being the height of the energy barrier, whereas, at low temperature, quantum tunneling is the dominant transition mechanism where the rate is $\Gamma \sim \exp(-S_{inst})$ with S_{inst} being the instanton action. At the crossover temperature, T_c, the dominant mechanism changes from over-the-barrier hop to and quantum tunnelling.

The crossover can either be abrupt (first-order) or smooth (second-order). The transition rate, $\Gamma(T)$, and its first derivative $\Gamma'(T)$ are continuous in second order crossober, but for first-order crossover the first derivative $\Gamma'(T)$ is apparently discontinuous as the rate changes abruptly from thermally activated over-the-barrier to nearly temperature independent tunneling. The two types of crossover were considered by Chudnovsky [14], who studied the shape of the potential barrier and dependencies of the oscillation period $\tau(E)$ on E, the energy of the instanton.

Many theoretical studies of the crossover for uniaxial and biaxial models have been performed on spin systems in the presence of an external field in various situations [17, 18, 19]. However, usually due to the spin-particle mapping approach, they have been studied for the spin Hamiltonians without higher-order terms in anisotropy. In fact, such terms are important in quantum resonant tunnelling [22], and quantum phase interference [23]. Recently, the crossover for a uniaxial and biaxial spin systems with higher-order terms in an anisotropy energy was studied numerically with direct diagonalization of the Hamiltonian[69, 70]. Experimental studies of the crossover in spin systems have been performed by many groups[71, 22, 72].

As discussed in the previous chapter, there are two types of crossover from the classical to quantum regime. In the case of first order crossover, the onset temperature for tunneling can be roughly estimated from the comparison of the Boltzmann factor $\Delta E/k_B T$ and the real part of the instanton action at a given temperature, $\Re S_{inst}$. At temperature when the real part of the action becomes smaller than the $\Delta E/k_B T$, tunneling is expected to become dominant. However, when the crossover is of second order, an analytical solution for the onset temperature can be obtained.

For particle systems, the mechanism of the crossover from the classical regime to the quantum regime has been studied extensively. There, a second order crossover is most common. The onset temperature for tunneling in a particle system has been given by [73]

$$T_c = \frac{\omega_b}{2\pi k_B}, \quad \omega_b^2 = -\frac{U''(x_s)}{m}, \tag{77}$$

where ω_b is the oscillation frequency at the bottom of the inverted potential $-U(x)$ corresponding to the negative mode of the Hessian matrix at the saddle point. Below, we derive equations for the second-order crossover temperature for magnetic systems.

4.1 Derivation of the onset temperature formula

The Hilbert space of a many-spin system is a tensor product of the Hilbert space of the individual spins. The Euclidean (imaginary-time) action for a system with N spins of length j is defined by

$$S(\mathbf{\Omega}) = \int_{-\beta/2}^{\beta/2} d\tau \left[-ij \sum_{k=1}^{N} (1-\cos\theta_k)\,\dot{\phi}_k + \mathscr{H}(\mathbf{\Omega}) \right], \tag{78}$$

where the first term is the sum of the Berry phases of the individual spins and $\mathbf{\Omega} = \mathbf{\Omega}(\tau)$ represents a closed path with the period β.

In order to find the onset temperature for tunneling, T_c, the action is expanded to second order in the vicinity of the first order saddle point on the energy surface, $\mathbf{\Omega} = \mathbf{\Omega}^\dagger + \varepsilon\delta\mathbf{\Omega}$

$$S(\mathbf{\Omega}) = \beta U(\mathbf{\Omega}^\dagger) + \delta S + \frac{1}{2}\delta^2 S, \tag{79}$$

where $\delta S = 0$ and

$$\delta^2 S = -2ij \int_{-\beta/2}^{\beta/2} \sum_{j=1}^{N} \left(\delta\theta_j \delta\dot{\phi}_j \sin\theta_j\right) d\tau + \int_{-\beta/2}^{\beta/2} \delta\mathbf{\Omega}\, \mathscr{H}\, \delta\mathbf{\Omega}^T d\tau. \tag{80}$$

$\mathscr{H}$ is the Hessian matrix of the energy surface $U(\mathbf{\Omega})$ at the saddle point $\mathbf{\Omega}^\dagger$. As $\varepsilon \to 0$, $\delta^2 S$ becomes a quadratic form of the Hessian, $\mathscr{H}$, which has one and only one real negative eigenvalue.

The task is to find the temperature at which $\mathbf{\Omega}$ becomes an instanton, *i.e.* a saddle point at the action surface with quantum delocalization. At that point, a zero mode appears corresponding to displacement along the path and thus constant S. This signals the transition from thermally activated jumps to quantum tunneling [74, 26].

Since the instanton is a closed path, $\delta\theta_k$ and $\delta\phi_k$ can be expanded in a Fourier series and $\delta^2 S$ in eqn.(80) rewritten as

$$\frac{1}{2}\delta^2 S(\theta^\dagger, \phi^\dagger) = \beta \sum_{n=0}^{\infty} \left(\sum_{k=0}^{N} \left[\frac{2\pi j \sin\theta_k^\dagger}{\beta} n(\phi_n^k \theta_n^{k^*} - \phi_n^{k^*} \theta_n^k) \right] + \sum_{j,k} \left[a\theta_n^k \theta_n^{j^*} + b\left(\phi_n^k \theta_n^{j^*} + \phi_n^{k^*} \theta_n^j\right) + c\phi_n^k \phi_n^{j^*} \right] \right) \tag{81}$$

The matrix representing the quadratic form of the action is infinite and has a block

diagonal form

$$G = \begin{pmatrix} \gamma_0 & & & & & \\ & \gamma_1 & & & & \\ & & \ddots & & & \\ & & & \gamma_n & & \\ & & & & \ddots & \end{pmatrix}, \tag{82}$$

where

$$\gamma_n = \mathscr{H} + \left(\begin{array}{ccc|ccc} 0 & \cdots & 0 & -k_1^n & \cdots & 0 \\ 0 & \ddots & 0 & 0 & \ddots & 0 \\ 0 & \cdots & 0 & 0 & \cdots & -k_N^n \\ \hline k_1^n & \cdots & 0 & 0 & \cdots & 0 \\ 0 & \ddots & 0 & 0 & \ddots & 0 \\ 0 & \cdots & k_N^n & 0 & \cdots & 0 \end{array}\right), \tag{83}$$

where $k_j^n = 2\pi n T j \sin\theta_j^\dagger$.

An expression for the onset temperature for tunneling can be obtained by analyzing the determinant of G

$$\det(G) = \prod_{n=0}^{\infty} \det(\gamma_n). \tag{84}$$

Consider first γ_0 which is the Hessian of the energy surface at the first order saddle point. There, γ_0 contains one negative eigenvalue so $\det(\gamma_0) < 0$. However, the other blocks, γ_n (for $n > 0$), depend on temperature and at $T >> T_c$ are positive definite

$$\det(\gamma_n) \sim (2\pi jn)^{2N} \prod_{j=1}^{N} sin^2\theta_j^\dagger > 0 \tag{85}$$

and $\det(G) < 0$. As the temperature is lowered to T_c, a zero of G appears signalling a stationary point involving quantum delocalization.

This must arise from γ_1 since the temperature in each γ_n is scaled by n and blocks with $n > 1$ thus have zeros at even lower temperature. The onset temperature for tunneling is, therefore, found by solving

$$\det(\gamma_1(T_c)) = 0. \tag{86}$$

This can be easily done numerically for multi-spin systems. All that is required for the calculation are the second derivatives of the energy at the first order saddle point corresponding to the over-the-barrier mechanism.

For a single-spin system, an analytical expression for the onset temperature can be obtained

$$T_c = \frac{\sqrt{b^2 - ac}}{2\pi j k_B \sin\theta^\dagger}. \tag{87}$$

where

$$a \equiv \left.\frac{\partial^2 E(\theta^\dagger,\phi^\dagger)}{\partial\theta^2}\right|_{\theta^\dagger,\phi^\dagger}, c \equiv \left.\frac{\partial^2 E(\theta^\dagger,\phi^\dagger)}{\partial\phi^2}\right|_{\theta^\dagger,\phi^\dagger}, b \equiv \left.\frac{\partial^2 E(\theta^\dagger,\phi^\dagger)}{\partial\theta\partial\phi}\right|_{\theta^\dagger,\phi^\dagger}. \tag{88}$$

4.2 Applications

4.2.1 Mn_4 molecular magnet

In this section we consider some application of the formula for the crossover temperature calculation. Recently, the formula (86) was applied to both the monomer[32] and the dimer[75] of the Mn_4 molecular magnet compounds and both the high temperature jump rate and the onset temperature for tunneling were calculated and compared with the experimental data[24, 25]. Both compounds were described by spin Hamiltonians with quartic terms. Calculations for the jump rate were performed using the HTST formula (4) with ZPE corrections. An excellent agreement was achieved. The results of these calculations are shown in figure 4.8

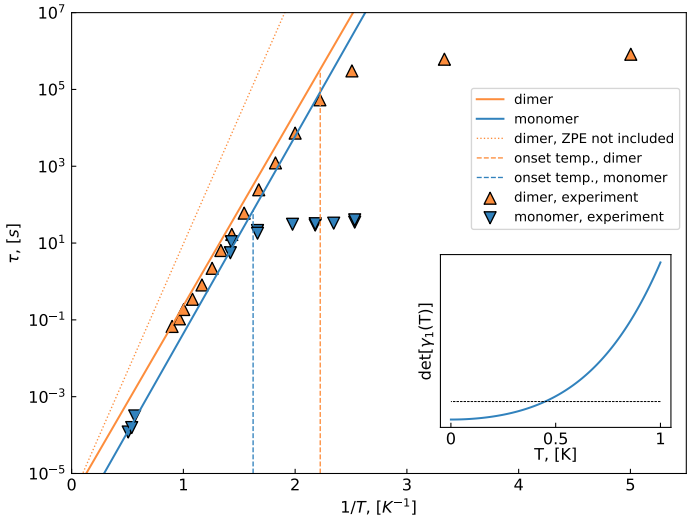

Figure 4.8. The calculated lifetime for a monomer and a dimer of molecular magnets containing Mn_4 groups. Results of calculations using harmonic transition state theory with zero point energy correction for the monomer (solid blue line) and the dimer (solid orange line) are shown. Calculated lifetime for the dimer without ZPE correction (dashed line) is also shown for comparison. Calculated values for the onset temperature for tunneling calculated for the monomer and for the dimer (dashed vertical lines) with parameters taken from experimental measurements. Experimentally measured transition rate for the monomer[32] is shown with blue triangles and for the dimer[75] with orange triangles. Below T_c, the tunneling rate is expected to be similar to the HTST rate at T_c. Excellent agreement is obtained between the calculated and measured results. Inset: The determinant of the γ_1 matrix block for the dimer, showing how it becomes negative at T_c.

4.2.2 Magnetic skyrmion

As another example, the onset temperature for tunneling of a magnetic skyrmion to a ferromagnetic state was calculated. Magnetic skyrmions are localized, noncollinear multi-spin configurations that have a soliton-like behavior. Skyrmions have been proposed in the context of elementary particles as configurations of continuous fields with topological charge. In a continuum limit, topological protection makes them stable against arbitrarily large fluctuations. However, in discrete systems where the spins are localized on atoms, the topological protection is not strict. In reality, a skyrmion state is isolated from the topologically simple (e.g., ferromagnetic) state by a finite energy barrier that defines its stability.

The model we used here can be described by the Hamiltonian

$$\hat{H} = \sum_{\langle i,j \rangle} \left[-J\hat{\mathbf{S}}_i \cdot \hat{\mathbf{S}}_j + \mathbf{d}_{ij} \cdot (\hat{\mathbf{S}}_i \times \hat{\mathbf{S}}_j) \right] - \sum_i K(\hat{S}_i^z)^2 - g\mu_0 \sum_i \hat{\mathbf{S}}_i \cdot \mathbf{B}, \tag{89}$$

where J is the isotropic Heisenberg exchange, $\mathbf{d}_{ij} = D(\mathbf{u}_{ij} \times \hat{\mathbf{z}})$ is a vector representing Dyaloshinsky-Moria interaction, K describes the anisotropy and B is the applied magnetic field, all parameters are taken from [76]. The calculated crossover temperature for this system is $T_c = 1.8$ K. However, the lifetime, calculated using (4), at T_c is predicted to be 7.1×10^{17} seconds, what makes the crossover to be unobservable. To find the set of parameters for the system (89) corresponding to the lifetime of minutes or hours we have calculated for the various values of anisotropy and Dyaloshinsky-Moria interaction, see figure 4.9.

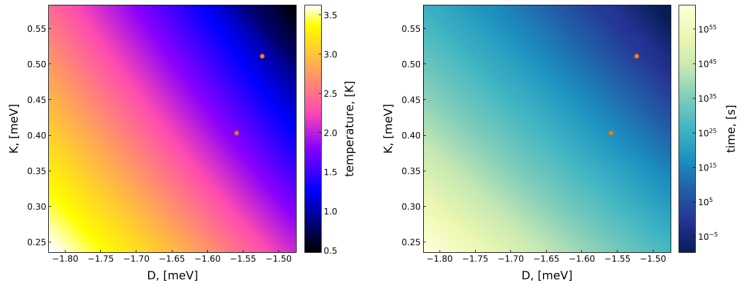

Figure 4.9. ***Left:*** *Calculated crossover temperature for a magnetic skyrmion.* ***Right:*** *Calculated lifetime for the magnetic skyrmion at the crossover temperature, the values of T_c taken from the left panel. In both panels, orange star corresponds to the set of parameters from [76], orange circle corresponds to the system with a lifetime, T_c, of is ca. 10 min.*

The parameters are chosen to be following: D $= -1.523$ meV, K $= 0.511$ meV, J $= 5.88$ meV and B $= 3$ T. Figure 4.10 shows the minimum energy path (MEP) for skyrmion nucleation. The maximum along the MEP is the saddle point of the energy surface.

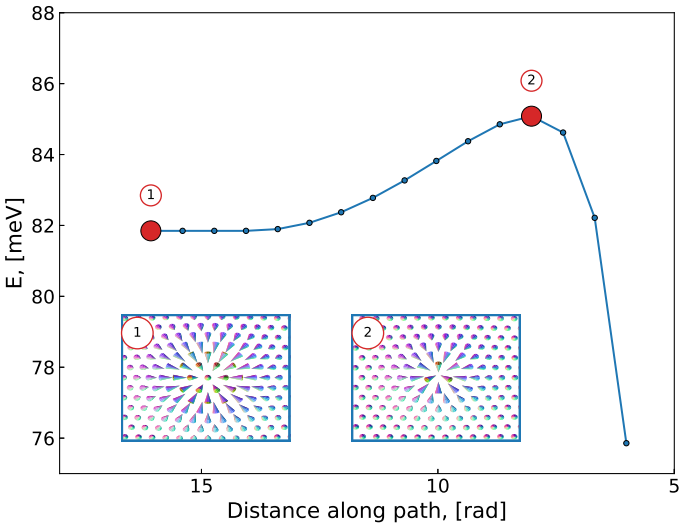

Figure 4.10. Energy as a function of the total displacement along the minimum energy path for the annihilation of a magnetic skyrmion to a ferromagnetic state (from right to left). The filled circles correspond to images in the geodesic nudged elastic band calculation, with end points and first order saddle point marked separately (in red). Insets: configurations of the spins in the skyrmion state, the ferromagnetic state, and at the saddle point.

At the crossover temperature, $T_c = 1.1$ K, the system has finite lifetime, ca. 10 min., see fig. 4.11. This makes it possible to observe the crossover from classical to quantum tunneling for this system.

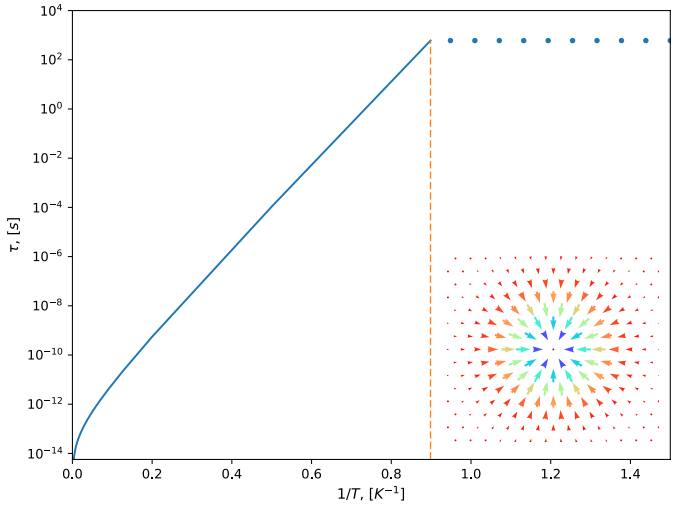

Figure 4.11. Lifetime of a magnetic skyrmion calculated using harmonic transition state theory (solid line) predicted onset temperature for annihilation by quantum mechanical tunneling, 1.1 *K (dashed line), and corresponding tunneling rate (dots). The lifetime of the skyrmion at the onset temperature for tunneling is about 10 minutes so the crossover in mechanism should be observable in the laboratory for this set of parameters.*

5 Conclusions

This thesis presents a method for calculating the onset temperature for thermally activated tunneling in magnetic systems. The method provides a general expression based on calculations of second derivatives of the energy at the first-order saddle point. Several model systems, as well as the Mn_4 molecular magnet and the magnetic skyrmion, were investigated and the crossover temperature for tunneling calculated. In the case of the Mn_4 molecular magnet, excellent agreement with experimental data was obtained.

An efficient method was developed for finding instantons in magnetic systems at finite temperature – optimal paths corresponding to tunneling from one magnetic state to another. The method requires analytical continuation of the energy function to allow for complex values of the angle variables. First, a set of discretization points are placed equally spaced on a chosen energy contour. Then, an estimate of the corresponding temperature is obtained using Landau-Lifshitz dynamics in imaginary time along the contour. Finally, the distribution of the discretization points, as well as the energy, are systematically refined by converging on the nearest stationary point of the Euclidean action, thereby obtaining a discrete representation of the closest instanton at the given temperature. The method is illustrated with an application to a model system consisting of a single spin subject to uniaxial anisotropy and transverse external magnetic field. First-order and second-order crossovers from over-the-barrier mechanism to tunneling are found depending on the applied field, and the difference in the dependence of the instanton temperature on the energy illustrated for the two cases. By comparing the Boltzmann factors for over-the-barrier and tunneling transitions, the crossover temperature between the two mechanisms is estimated for both first- and second-order crossover.

There are, admittedly, still tasks to be done. First of all, the full and comprehensive instanton theory – a harmonic quantum transition state theory – that allows calculating quantum-mechanical tunneling rate for magnetic systems needs to be developed.

Article I

Classical to quantum mechanical tunneling mechanism crossover in thermal transitions between magnetic states

Sergei Vlasov, Pavel F. Bessarab, Valery M. Uzdin, and Hannes Jónsson

Faraday discussions **195**, 93 (2016)

Faraday Discussions

Cite this: *Faraday Discuss.*, 2016, **195**, 93

PAPER View Article Online
View Journal | View Issue

Classical to quantum mechanical tunneling mechanism crossover in thermal transitions between magnetic states

Sergei Vlasov,[ab] Pavel F. Bessarab,[cd] Valery M. Uzdin[bd] and Hannes Jónsson*[ae]

Received 16th May 2016, Accepted 21st June 2016
DOI: 10.1039/c6fd00136j

Transitions between states of a magnetic system can occur by jumps over an energy barrier or by quantum mechanical tunneling through the energy barrier. The rate of such transitions is an important consideration when the stability of magnetic states is assessed for example for nanoscale candidates for data storage devices. The shift in transition mechanism from jumps to tunneling as the temperature is lowered is analyzed and a general expression derived for the crossover temperature. The jump rate is evaluated using a harmonic approximation to transition state theory. First, the minimum energy path for the transition is found with the geodesic nudged elastic band method. The activation energy for the jumps is obtained from the maximum along the path, a saddle point on the energy surface, and the eigenvalues of the Hessian matrix at that point as well as at the initial state minimum used to estimate the entropic pre-exponential factor. The crossover temperature for quantum mechanical tunneling is evaluated from the second derivatives of the energy with respect to orientation of the spin vector at the saddle point. The resulting expression is applied to test problems where analytical results have previously been derived, namely uniaxial and biaxial spin systems with two-fold anisotropy. The effect of adding four-fold anisotropy on the crossover temperature is demonstrated. Calculations of the jump rate and crossover temperature for tunneling are also made for a molecular magnet containing an Mn_4 group. The results are in excellent agreement with previously reported experimental measurements on this system.

1 Introduction

The assessment of the stability of magnetic states with respect to thermal fluctuations is an important problem in the theory of magnetism. The preparation of

[a]*Science Institute and Faculty of Physical Sciences, University of Iceland VR-III, 107 Reykjavík, Iceland. E-mail: hj@hi.is; Tel: +354 525 4643*
[b]*Department of Natural Sciences, University ITMO, St. Petersburg, 197101 Russia*
[c]*Department of Materials and Nanophysics, Royal Institute of Technology (KTH), Electrum 229, SE-16440 Kista, Sweden*
[d]*Department of Physics, St. Petersburg State University, St. Petersburg, 198504 Russia*
[e]*Department of Applied Physics, Aalto University, Espoo, FI-00076, Finland*

a magnetic system in a particular state can be destroyed by thermally-activated transitions to other available states.[1,2] Thermal activation also needs to be taken into account when assessing the stability of a system with respect to external perturbations such as a magnetic field, contributing, for example, to the temperature dependence of hysteresis loops.[3] Thermal stability is a particularly important issue in the context of novel information storage devices. As the size of such devices is reduced, the thermal stability of the magnetic states decreases. Methods for estimating the rate of magnetic transitions are, therefore, important tools when designing such systems.

Thermally-activated magnetic transitions involving a jump over an energy barrier are typically rare events on the time scale of oscillations of the magnetic moments, making direct simulations of spin dynamics an impractical way to calculate transition rates. This separation of time scales, however, makes it possible to apply statistical approaches such as transition state theory (TST)[4] or Kramers theory.[5] Within the harmonic approximation to TST (HTST)[6] and within Kramers theory, the activation energy of a transition is given by the energy difference between the local minimum on the energy surface corresponding to the initial state and the highest energy on the minimum energy path connecting the initial and final state minima. In adaptions of these rate theories to magnetic systems,[1,2,7–10] the magnitude of the magnetic vectors is either assumed to be constant as orientation changes, or it is treated as a fast variable obtained from self-consistency calculations for fixed values of the slow variables that specify orientation.[11] The energy surface of a system of N magnetic moments is then a function of $2N$ degrees of freedom defining the orientation of the magnetic moments.

The mechanism of magnetic transitions can involve the formation of a temporary domain wall or soliton.[2,9,12] This results in a flat energy barrier, *i.e.* the energy is practically constant along the minimum energy path in the region of high energy. An illustration of this is given below for Fe islands on a tungsten substrate. Kramers theory then overestimates the importance of recrossings and underestimates the transition rate. The transition state theory approach followed by explicit dynamical corrections is then preferable over Kramers' approach. Similar flat barrier issues arise in polymer escape problems where HTST followed by recrossing corrections has been shown to be a useful approach for estimating the transition rate.[13]

At low enough temperature, quantum tunneling through the energy barrier becomes the dominant transition mechanism and the rate can eventually become temperature independent. It is important to have a way to estimate the crossover temperature for tunneling when assessing the stability of a magnetic state. Quantum tunneling in spin systems has been a subject of a great deal of theoretical[14–16] and experimental work[17–19] over the past few decades. Molecular magnets have, in particular, been a focus of such studies. One example of a molecular magnet that has been studied extensively is the $Mn_4O_3Cl(O_2CCH_3)_3(dbm)_3$ molecule[20] which has three Mn^{3+} ions and one Mn^{4+} and a total spin of $s = 9/2$. Experimental measurements of the rate of transitions between its magnetic states have been carried out as a function of temperature and reveal a crossover from activated transitions to nearly non-activated transitions. This experimental data is analyzed by classical and quantum mechanical calculations below.

View Article Online
Paper Faraday Discussions

The crossover from jumps to tunneling is in some cases abrupt, as in a first-order phase transition, but in other cases smooth, as in a second-order transition. In the latter the tunneling is thermally assisted. The shape of the energy barrier affects how sharp the transition is.[21] A spin system can in some cases be mapped onto a particle system and methods developed for particles used to estimate the tunneling rate.[22] Several theoretical studies of the crossover in uniaxial and biaxial spin models with two-fold anisotropy in a transverse magnetic field have been carried out using this approach.[23–26] The presence of higher-order anisotropy can strongly affect the tunneling rate[18,27] but is not included in this mapping approach.[28] So far, systems with higher-order anisotropy have only been studied numerically by direct diagonalisation of the Hamiltonian.[29,30]

Here, a general approach for calculating the crossover temperature for thermally assisted tunneling involving uniform rotation of the spin vectors (the macro-spin approximation) is presented, and an equation derived in terms of the second derivatives of the energy of the system with respect to the orientation of the magnetic vector at the saddle point on the energy surface. For systems that are small enough compared to the correlation length determined by the strength of the exchange interaction between the spins, such as the molecular magnets discussed here, the uniform rotation mechanism is preferred over a mechanism where a temporary domain wall forms.[2,12] By saddle point, we are referring to a first-order saddle point where the Hessian has one and only one negative eigenvalue. The formula reduces to known analytical solutions for simple spin systems with low order anisotropy, but can also be applied to more complex systems where the energy is evaluated using self-consistent field calculations.

The article is organized as follows: the methodology for estimating the jump rate based on harmonic transition state theory for magnetic systems is briefly reviewed for completeness in the following section, Section 2. Then, the crossover temperature for quantum mechanical tunneling is derived in Section 3. Applications are presented in Section 4, first to uniaxial and then biaxial systems, both with and without four-fold anisotropy, and finally to a molecular magnet which has been studied experimentally. A summary is presented in Section 5.

2 Jump rate

In order to set the stage for the discussion of the crossover temperature for tunneling, we first review briefly the methodology we use to calculate the mechanism and rate of thermally-activated jumps over the energy barrier.

The initial and final states of the system are characterized by local minima on the energy surface representing the system. The transition is characterized by the path on the energy surface for which the energy is at a minimum with respect to all orthogonal directions. Such a path is referred to as a minimum energy path (MEP). The MEP reveals the mechanism of the transition, for example whether the spins all rotate in a concerted way, a uniform rotation, or whether some rotate first and then others, the so-called temporary domain wall or soliton mechanism.[2,9] Examples of the latter are shown in Fig. 1 for monolayer thick iron islands on a W(110) surface. In one case the island is elongated along the anisotropy axis, in the other case it is elongated perpendicular to the anisotropy axis. In either case, the energy barrier has small curvature at the top.

The minimum energy path is calculated using the geodesic nudged elastic band (GNEB) method,[31] which is an adaption of the nudged elastic band method[32,33] to magnetic systems where the variables correspond to orientation of magnetic vectors and the MEP maps onto a path in a configuration space represented by a curved manifold due to the constraints on the length of the magnetic vectors. Such constraints arise when the length of the magnetic vectors is either fixed, as in a Heisenberg-type model, or is determined from self-consistent field calculations such as *ab initio* or semi-empirical models. Compared with the NEB method, GNEB involves an additional projection of the force vector to ensure that the magnetic constraints are satisfied and that a projection of the path tangent on the local tangent space of the configuration space properly decouples the spring force from the component of the energy gradient perpendicular to the path.

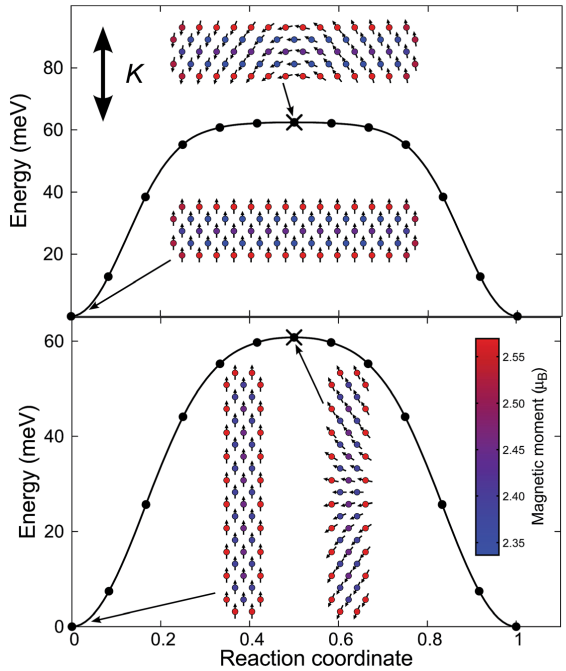

Fig. 1 Calculated minimum energy paths for magnetization reversal in Fe islands on a W(110) surface. The magnetic moments are calculated in a self-consistent way using the NCAA method.[11] The direction of the anisotropy axis, *K*, is shown as well as a color coding for the size of the magnetic moment of each Fe atom. The island is elongated perpendicular (upper panel) or parallel (lower panel) to the anisotropy axis. In both cases, the minimum energy path is nearly flat at the maximum because the energy does not change much as the temporary domain wall propagates along the island.

View Article Online
Paper Faraday Discussions

Within HTST, the maximum energy along the MEP, $E^{\dagger}$, which corresponds to a saddle point, $(\theta, \phi) = (\theta^{\dagger}, \phi^{\dagger})$, on the energy surface, gives the activation energy of the transition as $E_a = E^{\dagger} - E^{m}$, where E^{m} is the energy of the initial state minimum. This gives the exponential dependence of the rate on temperature. The pre-exponential factor can be estimated by evaluating the Hessian and calculating its eigenvalues at the saddle point, $\varepsilon_{\dagger,j}$, and at the initial state minimum, $\varepsilon_{m,j}$. The HTST estimate of the rate of magnetic transitions is[9,10]

$$k^{\mathrm{HTST}} = \frac{1}{2\pi}\frac{J_{\dagger}}{J_{m}}\sqrt{\sum_{j=2}^{D}\frac{a_j^{2}}{\varepsilon_{\dagger,j}}}\,\frac{\prod_{i=1}^{D}\sqrt{\varepsilon_{m,i}}}{\prod_{i=2}^{D}\sqrt{\varepsilon_{\dagger,i}}}\,e^{-\beta\left(E^{\dagger}-E^{m}\right)}, \tag{1}$$

where $J_{\dagger} = J(\theta^{\dagger}, \phi^{\dagger})$ is a Jacobian evaluated at the saddle point, while J_m is evaluated at the initial state minimum,[9] and $\beta = 1/k_B T$. The lowest eigenvalue of the Hessian at the saddle point, $\varepsilon_{\dagger,1}$, is negative and is skipped in the summation in (1). The calculated rate of magnetization reversals using this approach for Fe islands of various size and shape on the W(110) surface[12] is in close agreement with experimentally measured rates,[34] even an observed maximum in the pre-exponential factor for islands of intermediate size that have nearly equal numbers of atoms on each side. The calculations have been carried out using both Heisenberg-type Hamiltonians as well as self-consistent field calculations based on a non-collinear extension of the Alexander–Anderson (NCAA) model[11] (see Fig. 1).

In Kramers theory the rate estimate includes the curvature of the energy barrier at the saddle point. This results from a harmonic approximation in the estimate of the effect of recrossings due to fluctuating forces from the thermal bath.[1,5] When the energy barrier is flat, as for example in magnetic transitions involving a transient domain wall, this rate estimate is too low because the harmonic approximation at the saddle point in the direction of the MEP is inaccurate. The HTST approach is more accurate in such cases, but should also be followed by calculation of the recrossing correction using short time scale dynamics simulations.[35]

3 Onset of quantum mechanical tunneling

The thermally-averaged transition rate is

$$\Gamma(T) = \frac{1}{Z_0}\sum_i \Gamma_i \exp(-\beta E_i), \tag{2}$$

where Z_0 is the partition function of the initial state and Γ_i is the quantum mechanical transition probability from state i with energy E_i. Statistical Feynman path integrals can be used to write the rate in terms of the imaginary-time ($\tau = it$) action, S.[36] A stationary phase approximation[37,38] then gives an estimate of the transition rate as

$$\Gamma \propto \exp(-S[\mathbf{q}(\tau)]_{\mathrm{inst}}/\hbar), \tag{3}$$

where $\mathbf{q}(\tau)$ is a periodic trajectory with period $\tau = \beta\hbar$. This special trajectory, often referred to as the instanton, corresponds to a stationary point of the action, a saddle point on the action surface.[36,39,40]

For a spin of length s, the action is given by[41–43]

$$S(\theta,\phi)=\int_{-\beta/2}^{\beta/2}\mathrm{d}\tau\big[-is(1-\cos\theta)\dot{\phi}+U(\theta,\phi)\big], \tag{4}$$

where $U(\theta, \phi)$ is the energy surface. From here on we use atomic units with $\hbar = 1$, $\mu_B = 1/2$ and the mass and charge of an electron have unit magnitude, $e = -1$ and $m_e = 1$. A scaled gyromagnetic ratio is defined as $\tilde{g} = g/2$. The first term in (4) is related to Berry phase[44,45]

$$A[\mathbf{n}]=-is\int_{\gamma}(1-\cos\theta)\mathrm{d}\phi=-is\Omega, \tag{5}$$

where Ω is an area of a surface bounded by γ.

To find paths for which $S(\theta, \phi)$ is stationary, we consider the first order variation of the action

$$\delta S=\int_{-\beta/2}^{\beta/2}\mathrm{d}\tau\left[\left(-is\sin\theta\dot{\phi}+\frac{\partial U(\theta,\phi)}{\partial\theta}\right)\delta\theta+\left(is\sin\theta\dot{\theta}+\frac{\partial U(\theta,\phi)}{\partial\phi}\right)\delta\phi\right]. \tag{6}$$

Setting $\delta S = 0$ gives classical equations of motion which correspond to Landau–Lifshitz equations in imaginary time:

$$\dot{\theta}=\frac{i}{s\sin\theta}\frac{\partial U(\theta,\phi)}{\partial\phi}, \tag{7}$$

$$\dot{\phi}=\frac{-i}{s\sin\theta}\frac{\partial U(\theta,\phi)}{\partial\theta}. \tag{8}$$

These equations have two types of solutions. The first one is trivial, $\theta = \theta_0$ and $\phi = \phi_0$, corresponding to a stationary point of the potential, $U_0 \equiv U(\theta_0, \phi_0)$. If the stationary point is taken to be the saddle point $(\theta^\dagger, \phi^\dagger)$,

$$S_{\mathrm{jump}}=\beta U(\theta^\dagger,\phi^\dagger)=\beta E^\dagger, \tag{9}$$

this trivial solution corresponds to the high-temperature jump mechanism.

The second solution is the instanton – a closed path corresponding to constant energy. In the limit of zero temperature, $T \to 0$, *i.e.* $\beta \to \infty$, it corresponds to quantum tunnelling from the ground state. As the temperature is increased, the amplitude of the instanton trajectory decreases until it becomes infinitesimal:

$$\theta(\tau)=\theta^\dagger+\delta\theta,\ \phi(\tau)=\phi^\dagger+\delta\phi, \tag{10}$$

just below the crossover temperature. The instanton eventually collapses to the saddle point on the energy surface, $(\theta^\dagger, \phi^\dagger)$ at $T = T_c$.

In order to find the crossover temperature, T_c, the action is expanded to second order around the saddle point on the energy surface,

$$S(\theta^\dagger,\phi^\dagger)=\beta U_{\theta^\dagger,\phi^\dagger}+\delta S+\frac{1}{2}\delta^2 S. \tag{11}$$

Since $\delta S = 0$ at the saddle point, we focus on $\delta^2 S$:

View Article Online
Paper Faraday Discussions

$$\delta^2 S = \int_{-\beta/2}^{\beta/2} \mathrm{d}\tau \left[-2is\delta\theta\delta\dot{\phi} \sin\theta + \left(a\delta^2\theta + 2b\delta\theta\delta\phi + c\delta^2\phi\right)\right], \tag{12}$$

where

$$a \equiv \left.\frac{\partial^2 U(\theta^\dagger,\phi^\dagger)}{\partial\theta^2}\right|_{\theta^\dagger,\phi^\dagger}, \quad c \equiv \left.\frac{\partial^2 U(\theta^\dagger,\phi^\dagger)}{\partial\phi^2}\right|_{\theta^\dagger,\phi^\dagger}, \quad b \equiv \left.\frac{\partial^2 U(\theta^\dagger,\phi^\dagger)}{\partial\theta\partial\phi}\right|_{\theta^\dagger,\phi^\dagger}. \tag{13}$$

At the saddle point, $\delta^2 S$ is a quadratic form of the Hessian which has one and only one negative eigenvalue. As the temperature decreases below T_c, a second negative eigenvalue of $\delta^2 S$ appears, corresponding to the quantum delocalization. This signals the transition from thermally-activated jumps to quantum tunnelling.

Since the instanton is a closed trajectory, $\delta\theta$ and $\delta\phi$ can be expanded in Fourier series:

$$\delta\theta = \sum_{n=-\infty}^{\infty} \theta_n e^{i2\pi n\tau/\beta}, \quad \delta\phi = \sum_{n=-\infty}^{\infty} \phi_n e^{i2\pi n\tau/\beta}. \tag{14}$$

Here, ϕ_n and θ_n are complex numbers that satisfy

$$\phi_n = \phi_{-n}^*, \quad \theta_n = \theta_{-n}^*, \tag{15}$$

since $\delta\theta$ and $\delta\phi$ are real. $\delta^2 S$ from (12) can now be rewritten using (14) as

$$\frac{1}{2}\delta^2 S(\theta^\dagger,\phi^\dagger) = \beta \sum_{n=0}^{\infty} \left[\frac{2\pi s \sin\theta^\dagger}{\beta} n\left(\phi_n\theta_n^* - \phi_n^*\theta_n\right) + a\theta_n\theta_n^* + b\left(\phi_n\theta_n^* + \phi_n^*\theta_n\right) + c\phi_n\phi_n^* \right]. \tag{16}$$

The matrix representing the quadratic form of the action has a block form

$$G = \left[\begin{array}{cccc|cccc} a & & & & b & & & \\ & a & & & & -k+b & & \\ & & a & & & & -2k+b & \\ & & & \ddots & & & & \ddots \\ \hline b & & & & c & & & \\ & k+b & & & & c & & \\ & & 2k+b & & & & c & \\ & & & \ddots & & & & \ddots \end{array}\right], \tag{17}$$

where $k = 2\pi s \sin\theta^\dagger/\beta$. To obtain the eigenvalues of this matrix we need to solve the equation

$$\det(G - \lambda) = 0. \tag{18}$$

After some algebra, one obtains

$$\lambda_m = \frac{a+c}{2} \pm \frac{\sqrt{(a-c)^2 + 4b^2 - 4k^2m^2}}{2}. \tag{19}$$

In order to determine the temperature at which two eigenvalues are negative, we first inspect the two eigenvalues corresponding to $m = 0$:

$$\lambda_{0+} = \frac{a+c}{2} + \frac{\sqrt{(a-c)^2 + 4b^2}}{2}, \tag{20}$$

$$\lambda_{0-} = \frac{a+c}{2} - \frac{\sqrt{(a-c)^2 + 4b^2}}{2}. \tag{21}$$

Clearly $\lambda_{0+} > 0$, but λ_{0-} is negative if

$$\frac{a+c}{2} - \frac{\sqrt{(a-c)^2 + 4b^2}}{2} \leq 0,\ a + c \leq \sqrt{(a-c)^2 + 4b^2},\ \ ac - b^2 \leq 0. \tag{22}$$

Since $ac - b^2$ is the determinant of the Hessian at the saddle point, this condition is fulfilled. The second negative eigenvalue must come from $m > 1$. Substitution of $\beta = 1/k_B T$ and the expression for k into the negative branch, $\lambda_{m,-}$, in (19), gives

$$T \leq \frac{\sqrt{b^2 - ac}}{2\pi s m k_B \sin\theta^\dagger}. \tag{23}$$

The highest temperature for which a second negative eigenvalue exists can be determined from the $m = 1$ case:

$$T_c = \frac{\sqrt{b^2 - ac}}{2\pi s k_B \sin\theta^\dagger}. \tag{24}$$

This equation can be rewritten as

$$T_c = \frac{\omega}{2\pi k_B}, \tag{25}$$

where

$$\omega^2 = \frac{b^2 - ac}{s^2 \sin^2\theta^\dagger} \tag{26}$$

and a, b, c are the second derivatives defined in (13). This provides an estimate of the crossover temperature for tunneling in terms of second derivatives of the energy evaluated at the saddle point. For model Hamiltonians, the derivatives can typically be evaluated analytically. For more complicated descriptions of the magnetic system, such as self-consistent field calculations, the derivatives can be evaluated numerically from the forces, which in turn can be obtained using a force theorem.[11]

This expression for the crossover temperature of spin tunneling can be compared with the corresponding equation for particle tunneling,[46]

$$T_c = \frac{\omega_p}{2\pi k_B}, \quad \omega_p{}^2 = -\frac{U''(x_{sp})}{\mu}, \tag{27}$$

where now the second derivative is taken along the unstable mode at the saddle point of the energy surface and μ is the effective mass corresponding to the unstable mode.

4 Applications

In this section, the crossover temperature for various spin models is calculated. When only a two-fold anisotropy axis is included in the model, analytical solutions are available for comparison. But when four-fold anisotropy is included, so as to better represent physical systems, only numerical solutions based on direct diagonalization of the Hamiltonian have been presented so far. Here, analytical expressions in terms of the second derivatives of the energy are obtained also for such models. Finally, the jump rate as well as the crossover temperature is evaluated for a model of the Mn_4 molecular magnet and the results compared with experimental measurements.

4.1 Uniaxial systems with two- and four-fold anisotropy

A Hamiltonian which has, for example, been used to describe the Mn_{12} – *ac* molecular magnet[17,19] and has been studied theoretically[47] can be written as

$$H = -DS_z^2 - BS_z^4 - \tilde{g}H_xS_x - C(S_-^4 + S_+^4), \quad (28)$$

where D, B and C are the anisotropy constants. The third term is the Zeeman energy associated with an applied field H_x. The last term corresponds to transverse anisotropy. The z-axis is the easy axis (the orientation for which the energy is minimal) and has four-fold symmetry, while the x- and y-axis are medium axes, and $y = \pm x$ is the hard axis (the orientation for which the energy is maximal). The corresponding energy surface is

$$U(\theta, \phi) = -Ds^2(\cos^2\theta + k_1 s^2\cos^4\theta + 2k_2 s^2\sin^4\theta\cos(4\phi) + 2h_x\sin\theta\cos\phi), \quad (29)$$

where

$$k_1 \equiv B/D,\ k_2 \equiv C/D,\ h_x \equiv \tilde{g}H_x/2Ds. \quad (30)$$

The saddle point on the potential surface is located at $\theta^\dagger = \pi/2$, $\phi^\dagger = 0$. At a certain critical field, H_c, the energy barrier disappears. Applying the condition $\partial U/\partial\theta|_{\theta^\dagger} = \partial^2 U/\partial\theta^2|_{\theta^\dagger} = 0$ gives the critical field as

$$H_c = 2Ds - 8Cs^3. \quad (31)$$

The second derivatives at the saddle point are

$$a = 8Cs^4 + \tilde{g}sH_x - 2Ds^2,$$

$$c = 32Cs^4 + \tilde{g}sH_x,$$

$$b = 0,$$

$$k = 2\pi s k_B T.$$

After computing the coefficients of the quadratic form of the action, the formula for the crossover temperature in the presence of an applied field H_x is obtained:

$$T_c = \frac{\sqrt{(\tilde{g}H_x + 32Cs^3)(2Ds - 8Cs^3 - \tilde{g}H_x)}}{2\pi k_B}. \quad (32)$$

Fig. 2 shows the calculated crossover temperature as a function of the strength of the applied magnetic field for the following choice of parameters: $D/k_B = 0.548K$, $B/k_B = 1.17 \times 10^{-3}K$ and $C/k_B = 2.19 \times 10^{-5}K$. These are the same parameter values as considered by Park.[47] If the four-fold anisotropy parameter, C, is set to zero and the system only contains two-fold anisotropy, the crossover temperature is zero in the absence of a magnetic field. Even a small higher-order anisotropy term has a large effect on the crossover temperature.

If the model only contains two-fold anisotropy, $B = C = 0$, the potential surface becomes

$$U(\theta, \phi) = -Ds^2(\cos^2\theta + 2h_x \sin\theta \cos\phi). \quad (33)$$

The spin problem can then be mapped onto a particle in a one-dimensional potential,

$$U(x) = \left(s + \frac{1}{2}\right)^2 D\left(\tilde{h}_x{}^2 \sinh^2 x - 2\tilde{h}_x \cosh x\right), \quad \tilde{h}_x \equiv \frac{H_x}{(2s+1)D}, \quad (34)$$

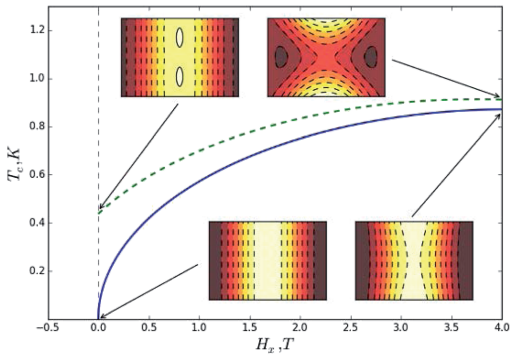

Fig. 2 Crossover temperature T_c for a uniaxial system with two-fold and four-fold anisotropy as a function of the strength of an applied magnetic field, H. The Hamiltonian is given by (28). The solid line shows results for a system with two-fold anisotropy, $C = 0$, while the dashed line shows results for a system with four-fold anisotropy. All parameters are taken from ref. 47. By adding higher-order anisotropy, the crossover temperature becomes finite even in the absence of a magnetic field. The insets show contour graphs of the energy surfaces (two-fold anisotropy below, four-fold above) at zero field and at a field of 4T.

and an analytical expression obtained for the crossover temperature for the particle.[23] Here, (32) simplifies to (by setting $C = 0$ in (32))

$$T_c = \frac{\sqrt{H_x(2Ds - H_x)}}{2\pi k_B}, \tag{35}$$

which is the same result as has been obtained previously using the particle mapping method by Garanin *et al.* (see eqn (13) in ref. 48).

Another spin Hamiltonian for which the crossover temperature has been estimated using the particle mapping method is[49]

$$H = -DS_z^2 + BS_y^2 - H_xS_x. \tag{36}$$

The corresponding particle model is unusual in that it involves coordinate-dependent mass.

The energy surface for the spin vector is

$$U(\theta, \phi) = Ds^2(-\cos^2\theta + \lambda \sin^2\theta \sin^2\phi - 2h_x \sin\theta \cos\phi),\ h_x \equiv H_x/2Ds,\ \lambda \equiv B/D. \tag{37}$$

By evaluating the second derivatives, a, b and c at the saddle point, $\theta^\dagger = \pi/2$, $\phi^\dagger = 0$ gives

$$a = -2Ds^2,$$

$$c = 2Ds^2\lambda,$$

$$b = 0.$$

The resulting expression for the crossover temperature is

$$T_c = \frac{Ds\sqrt{(\lambda + h_x)(1 - h_x)}}{\pi k_B}, \tag{38}$$

which coincides with the results obtained by the mapping to a particle model (see eqn (18) in ref. 49). Again, this is an illustration that for simple systems, our method gives results that agree with those obtained previously by other methods. Our approach has the advantage that it can also be applied to more complicated models, including for example Hamiltonians with a four-fold anisotropy axis in Heisenberg-type models and self-consistent field calculations, as illustrated in Fig. 2.

4.2 Biaxial system with two- and four-fold anisotropy

Another interesting case is the biaxial system with four-fold transverse anisotropy and a magnetic field applied along the hard direction. This has been used to describe the Fe_8 molecular magnet.[27] The Hamiltonian is

$$H = -DS_z^2 + B(S_x^2 - S_y^2) - \tilde{g}H_xS_x + C(S_-^4 + S_+^4), \tag{39}$$

where D, B and C are anisotropy constants. In this case, the z-axis is the easy axis, the y-axis is the medium axis and the x-axis is the hard axis. The corresponding energy surface is

$$U(\theta, \phi) = -Ds^2(\cos^2\theta + k_1 \sin^2\theta \cos 2\phi + k_2 \sin^4\theta \cos 4\phi + 2h_x \sin\theta \cos\phi), \quad (40)$$

where

$$k_1 \equiv B/D,\ k_2 \equiv 2Cs^2/D,\ h_x \equiv H_x/2Ds. \quad (41)$$

The saddle point is located at ($\theta^\dagger = \pi/2$ and $\phi^\dagger = \phi_0$), where ϕ_0 can be found as a solution of a third-order algebraic equation,

$$-16k_2 \cos^3\phi_0 + (8k_2 - 2k_1)\cos\phi_0 + h_x = 0. \quad (42)$$

The second derivatives at the saddle point are

$$a = -2Ds^2(1 - k_1 \cos 2\phi_0 + 2k_2 \cos 4\phi_0 - h_x \cos\phi_0),$$

$$c = -2Ds^2(2 - k_1 \cos 2\phi_0 + 8k_2 \cos 4\phi_0 - h_x \cos\phi_0),$$

$$b = 0,$$

and the expression for the crossover temperature becomes

$$T_c = \frac{Ds}{\pi k_B}\sqrt{1 - k_1 \cos 2\phi_0 + 2k_2 \cos 4\phi_0 - h_x \cos\phi_0} \times \sqrt{-2k_1 \cos 2\phi_0 + 8k_2 \cos 4\phi_0 - h_x \cos\phi_0}, \quad (43)$$

where ϕ_0 is the real solution of (42).

Fig. 3 shows the dependence of T_c on the applied magnetic field for parameters that are chosen to represent an Fe_8 molecular magnet, $D/k_B = 0.292K$, $B/k_B = 0.046K$ and $C/k_B = -2.9 \times 10^{-5}K$.[50] The calculated crossover temperature is in the

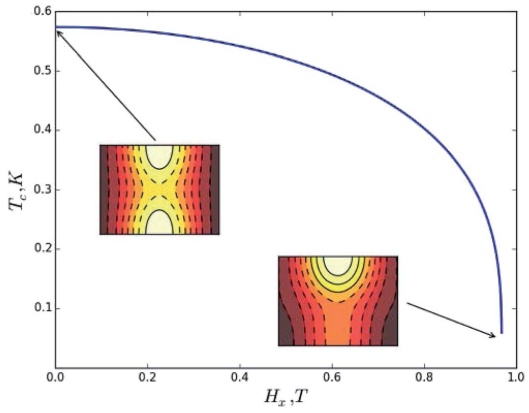

Fig. 3 Dependence of T_c on the applied field H_x for a biaxial spin model with four-fold transverse anisotropy. The parameters are chosen to represent the Fe_8 molecular magnet.[50] Insets show the energy surface at particular values of the applied magnetic field.

range between 0.4 and 0.7 K which agrees well with experimental results on the Fe_8 molecular magnet.[27,51,52]

4.3 Molecular Mn_4 magnet

The transition rate has been experimentally measured as a function of temperature for the Mn_4 molecular magnet by Aubin *et al.*[20] and a crossover observed. The full chemical formula for the molecule is $Mn_4O_3Cl(O_2CCH_3)_3(dbm)_3$. It is a trigonal pyramidal complex with one Mn^{4+} and three Mn^{3+} ions. The spins of the Mn^{3+} ions point in the same direction but the spin of Mn^{4+} points in the opposite direction (see inset in Fig. 4). The total spin is 9/2 and the transitions correspond to uniform rotation of the four spins.

Various experimental measurements of this molecular magnet have established the following Hamiltonian model for the system:

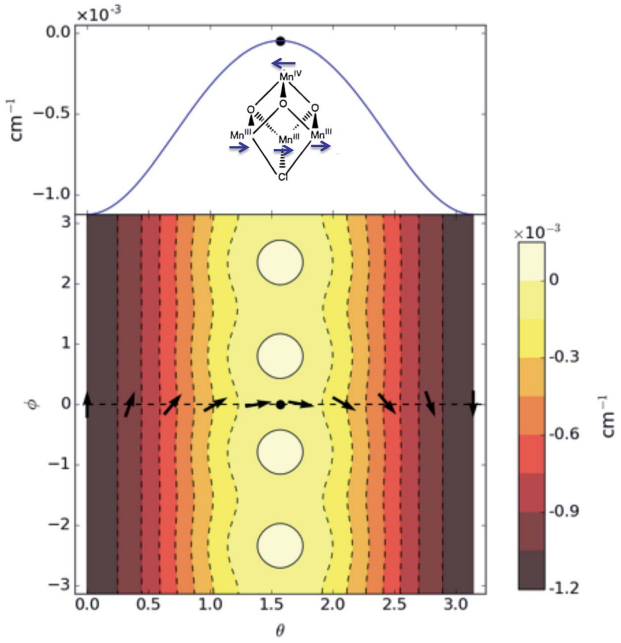

Fig. 4 Characterization of the spin Hamiltonian for the Mn_4 molecular magnet ($Mn_4O_3Cl(O_2CCH_3)_3(dbm)_3$). Upper: Minimum energy path for the rotation of the total spin $s = 9/2$ vector. The energy along the path is given in units of 10^{-3} cm^{-1}. The inset shows the structure of the Mn_4 core of the molecule with the one Mn^{4+} and three Mn^{3+} ions and the orientation of the four spins at the saddle point configuration. Lower: Contour graph of the energy surface $U(\theta, \phi)$. One of the four equivalent minimum energy paths is shown with a dashed line and the orientation of the magnetic momentum vector indicated at a few points along the path. The saddle point is indicated with a filled circle both in the upper and lower panels.

$$H = D\left[S_z^2 - \frac{1}{3}s(s+1)\right] + B_4^0 O_4^0 + B_4^4 O_4^4, \tag{44}$$

where $O_4^0 = 35S_z^4 - 30s(s+1)S_z^2 + 25S_z^2 + 6s(s+1)$ and $O_4^4 = \frac{1}{2}(S_+^4 + S_-^4)$. The parameters D and B_4^0 have been determined from various experiments (not rate measurements) by Aubin *et al.*[20] to be -0.53 cm^{-1} and -7.4×10^{-5} cm^{-1}, respectively. The last term in the Hamiltonian corresponds to four-fold anisotropy and the parameter B_4^4 can be chosen to have a similar, small value as has been determined for analogous molecular magnets.[53–56] Without it, the tunneling rate is zero because of a Kramers degeneracy.[20]

Both the calculated high temperature jump rate as well as the crossover temperature can be compared with the measured rate for this molecular magnet. The energy surface corresponding to the Mn_4 Hamiltonian is

$$U(\theta,\phi) = D\left[s^2\cos^2\theta - \frac{1}{3}s(s+1)\right] + B_4^0\left[35s^4\cos^4\theta - 5s^2\cos^2\theta\left(6s^2+6s-5\right) + 6s(s+1)\right] + B_4^4\left[\sin^4\theta\cos 4\phi\right]. \tag{45}$$

The system has four equivalent saddle points on the energy surface: $\theta^\dagger = \pi/2$, $\phi^\dagger = 0, \pi/2, \pi, 3\pi/2$, see Fig. 4. Here, the value of D is slightly smaller than the value estimated by Aubin *et al.*,[20] $D = -0.41$ cm^{-1}, and the value of B_4^4 is taken to be -8.5×10^{-4} cm^{-1}. The jump rate calculated using HTST is $\Gamma(T) = 2.3 \times 10^6 H_z \exp(-11.5K/T)$ and is shown in Fig. 5.

The second derivatives needed to estimate the crossover temperature are

$$a = 2Ds^2 - 60B_4^0 s^3(s+1) + 50B_4^0 s^2 - 4B_4^4 s^4,\ c = -32B_4^4 s^4,\ b = 0. \tag{46}$$

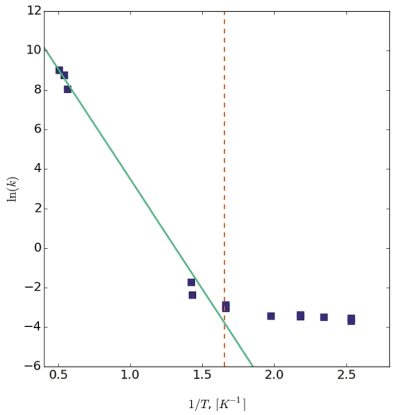

Fig. 5 The calculated jump rate using harmonic transition state theory (green line), given by (1), and the crossover temperature (dashed red line) given by (25) using the Hamiltonian in (44) and parameters chosen to represent the Mn_4 molecular magnet. The experimentally measured[20] transition rate is shown with filled squares. Excellent agreement is obtained between the calculated and measured results.

View Article Online
Paper Faraday Discussions

Inserting the values of the parameters gives a crossover temperature of

$$T_c = 0.6K, \tag{47}$$

which is in close agreement with the reported experimental data[20] as shown in Fig. 5.

Therefore, both the high-temperature jump rate obtained from HTST and the crossover temperature obtained from the formula presented here are in close agreement with the experimental measurements.

5 Summary

A method is presented for finding the crossover temperature of thermally-activated tunneling in a magnetic system that is characterized by a spin vector with orientation prescribed by continuous angular variables. Several model systems are used to verify that the general equation derived here in terms of second derivatives of the energy at the saddle point agrees with analytical results previously obtained for specific, simple Hamiltonians. More complicated Hamiltonians including four-fold anisotropy so as to better describe molecular magnets are also studied, and analytical equations for the crossover temperature presented. A more detailed study is made of the Mn_4 molecular magnet where both the high-temperature jump rate and the crossover temperature for tunneling are calculated and compared with experimental data. Excellent agreement is obtained.

The crossover temperature for tunneling in molecular magnets is low partly because the energy barriers are small. For larger systems, such as metal islands on substrates, the energy barriers can be significantly larger and the onset of tunneling can be expected to occur at higher temperature. The method presented here makes it possible to estimate the crossover temperature for tunneling in a magnetic system described by a single spin vector as long as the second derivatives of the energy with respect to the angles describing the orientation of the vector can be evaluated at the saddle point on the energy surface.

The equation derived here for the crossover temperature for tunneling in a magnetic system is significantly different from the analogous equation for a particle system in that all second derivatives of the energy at the saddle point are included, while only the second derivative along the unstable mode enters the particle equation. The essential difference between the two systems is the separation of the particle Hamiltonian into a kinetic and potential energy part, which does not occur for the magnetic systems. As a result, the magnetic systems' Hamiltonians are more difficult to deal with. The derivation of the crossover temperature for systems where the transition mechanism is not a uniform rotation as well as a method for calculating the rate of thermally-activated tunneling remain to be completed, but are being developed using an approach that is analogous to previous studies of atomic systems[57,58] and will be presented at a later time.

Acknowledgements

This work was supported by the Government of Russian Federation (Grant 074-U01), RFBR (Grant 14-02-00102), the Icelandic Research Fund, the Göran

Gustafsson Foundation for Research in Natural Sciences and Medicine (Grant 1303A) and the Academy of Finland FiDiPro program (grant 263294).

References

1 W. F. Brown Jr, *IEEE Trans. Magn.*, 1979, **15**, 1196.
2 H.-B. Braun, *J. Appl. Phys.*, 1994, **76**, 6310.
3 M. Moskalenko, P. F. Bessarab, V. M. Uzdin and H. Jónsson, *AIP Adv.*, 2016, **6**, 025213.
4 H. Pelzer and E. Wigner, *Z. Phys. Chem., Abt. B*, 1932, **15**, 445; E. Wigner, *Trans. Faraday Soc.*, 1938, **34**, 29.
5 H. A. Kramers, *Physica*, 1940, **7**, 284.
6 G. H. Vineyard, *J. Phys. Chem. Solids*, 1957, **3**, 121.
7 P. B. Visscher and R. Zhu, *Phys. B*, 2012, **407**, 1340.
8 G. Fiedler, J. Fidler, J. Lee, T. Schrefl, R. L. Stamps, H. B. Braun and D. Suess, *J. Appl. Phys.*, 2012, **111**, 093917.
9 P. F. Bessarab, V. M. Uzdin and H. Jónsson, *Phys. Rev. B: Condens. Matter Mater. Phys.*, 2012, **85**, 184409.
10 P. F. Bessarab, V. M. Uzdin and H. Jónsson, *Z. Phys. Chem.*, 2013, **227**, 1543.
11 P. F. Bessarab, V. M. Uzdin and H. Jónsson, *Phys. Rev. B: Condens. Matter Mater. Phys.*, 2014, **89**, 214424.
12 P. F. Bessarab, V. M. Uzdin and H. Jónsson, *Phys. Rev. Lett.*, 2013, **110**, 020604.
13 H. Mökkönen, T. Ikonen, T. Ala-Nissila and H. Jónsson, *J. Chem. Phys.*, 2015, **142**, 224906.
14 *Quantum Tunneling of Magnetization – QTM'94*, ed. L. Gunther and B. Barbara, Kluwer Academic, Dordrecht, 1995.
15 E. M. Chudnovsky and J. Tejada, *Macroscopic Quantum Tunneling of the Magnetic Moment*, Cambridge University Press, New York, 1998.
16 D. Gatteschi, R. Sessoli and J. Villain, *Molecular Nanomagnets*, Oxford University Press, New York, 2006.
17 L. Bokacheva, A. D. Kent and M. A. Walters, *Phys. Rev. Lett.*, 2000, **85**, 4803.
18 K. M. Mertes, Y. Zhong, M. P. Sarachik, *et al.*, *Europhys. Lett.*, 2001, **55**, 874.
19 W. Wernsdorfer, M. Murugesu and G. Christou, *Phys. Rev. Lett.*, 2006, **96**, 057208.
20 S. M. J. Aubin, *et al.*, *J. Am. Chem. Soc.*, 1998, **120**, 4991.
21 E. M. Chudnovsky, *Phys. Rev. A*, 1992, **46**, 8011.
22 V. V. Ulyanov and O. B. Zaslavskii, *Phys. Rep.*, 1992, **214**, 179.
23 E. M. Chudnovsky and D. A. Garanin, *Phys. Rev. Lett.*, 1997, **79**, 4469.
24 C.-S. Park, S.-K. Yoo and D.-H. Yoon, *Phys. Rev. B: Condens. Matter Mater. Phys.*, 2000, **61**, 11618.
25 G.-H. Kim and E. M. Chudnovsky, *Europhys. Lett.*, 2000, **52**, 681.
26 D. A. Garanin and E. M. Chudnovsky, *Phys. Rev. B: Condens. Matter Mater. Phys.*, 2000, **63**, 024418.
27 W. Wernsdorfer and R. Sessoli, *Science*, 1999, **284**, 133.
28 S. A. Owerre and M. B. Paranjape, *Phys. Rep.*, 2015, **546**, 1.
29 D. H. Kang and G.-H. Kim, *Phys. Rev. B: Condens. Matter Mater. Phys.*, 2006, **74**, 184418.
30 G. H. Kim, D. H. Kang and M. C. Shin, *Eur. Phys. J. B*, 2011, **83**, 63.

31 P. F. Bessarab, V. M. Uzdin and H. Jónsson, *Comput. Phys. Commun.*, 2015, **196**, 335.
32 G. Mills, H. Jónsson and G. Schenter, *Surf. Sci.*, 1995, **324**, 305.
33 H. Jónsson, G. Mills and K. W. Jacobsen, Nudged Elastic Band Method for Finding Minimum Energy Paths of Transitions, in *Classical and Quantum Dynamics in Condensed Phase Simulations*, ed. B. J. Berne, G. Ciccotti and D. F. Coker, World Scientific, 1998, p. 385.
34 S. Krause, G. Herzog, T. Stapelfeldt, L. Berbil-Bautista, M. Bode, E. Y. Vedmedenko and R. Wiesendanger, *Phys. Rev. Lett.*, 2009, **103**, 127202.
35 J. C. Keck, *Adv. Chem. Phys.*, 1967, **13**, 85.
36 V. A. Benderskii, V. I. Goldanskii and D. E. Makarov, *Phys. Rep.*, 1993, **233**, 195.
37 W. H. Miller, *J. Chem. Phys.*, 1975, **62**, 1899.
38 C. Callen and S. Coleman, *Phys. Rev. D: Part. Fields*, 1977, **16**, 1762.
39 G. Mills, G. K. Schenter, D. E. Makarov and H. Jónsson, *Chem. Phys. Lett.*, 1997, **278**, 91.
40 G. Mills, G. K. Schenter, D. E. Makarov and H. Jónsson, RAW Quantum transition state theory, in *Classical and Quantum Dynamics in Condensed Phase Simulations*, ed. B. J. Berne, G. Ciccotti and D. F. Coker, World Scientific, 1998, p. 405.
41 J. KIauder, *Phys. Rev. D: Part. Fields*, 1979, **19**, 2349.
42 E. Kochetov, *J. Math. Phys.*, 1995, **36**, 4667.
43 E. Fradkin, *Field Theories of Condensed Matter Physics*, Cambridge University Press, New York, 2013, ch 7.2.
44 M. V. Berry, *Proc. R. Soc. London, Ser. A*, 1984, **392**, 45.
45 A. Garg, *Am. J. Phys.*, 2010, **78**, 661.
46 V. I. Goldanskii, *Sov. Phys. Dokl.*, 1959, **4**, 74.
47 C.-S. Park, *J. Magn. Magn. Mater.*, 2003, **267**, 281.
48 D. A. Garanin, X. Martinez Hidalgo and E. M. Chudnovsky, *Phys. Rev. B: Condens. Matter Mater. Phys.*, 1998, **57**, 13639.
49 G.-H. Kim, *Phys. Rev. B: Condens. Matter Mater. Phys.*, 1999, **59**, 11847.
50 R. Caciuffo, *et al.*, *Phys. Rev. Lett.*, 1998, **81**, 4744.
51 C. Sangregorio, T. Ohm, C. Paulsen, R. Sessoli and D. Gatteschi, *Phys. Rev. Lett.*, 1997, **78**, 4645.
52 A. Caneschi, *et al.*, *J. Magn. Magn. Mater.*, 1998, **177**, 1330.
53 A. L. Barra, D. Gatteschi and R. Sessoli, *Phys. Rev. B: Condens. Matter Mater. Phys.*, 1997, **56**, 8192.
54 I. Mirebeau, M. Hennion, H. Casalta, H. Anders, H.-U. Güdel, A. V. Irodova and A. Caneschi, *Phys. Rev. Lett.*, 1999, **83**, 628.
55 S. Hill, J. A. A. J. Perenboom, N. S. Dalal, T. Hathaway, T. Stalcup and J. S. Brooks, *Phys. Rev. Lett.*, 1998, **80**, 2453.
56 E. Del Barco, A. D. Kent, S. Hill, J. M. North, N. S. Dalal, E. M. Rumberger, D. N. Hendrikson, N. Chakov and G. Christou, *J. Low Temp. Phys.*, 2005, **140**, 119.
57 H. Jónsson, *Proc. Natl. Acad. Sci. U. S. A.*, 2011, **108**, 944.
58 D. M. Einarsdóttir, A. Arnaldsson, F. Óskarsson and H. Jónsson, *Lect. Notes. Comput. Sci.*, 2012, **7134**, 45.

Article II

Calculations of the onset temperature for tunneling in multispin systems

Sergei M. Vlasov, Pavel F. Bessarab, Valery M. Uzdin, and Hannes Jónsson
Nanosystems: Physics, Chemistry, Mathematics **8**, 454 (2017)

NANOSYSTEMS: PHYSICS, CHEMISTRY, MATHEMATICS, 2017, 8 (4), P. 454–461

Calculations of the onset temperature for tunneling in multispin systems

S. M. Vlasov[1,2], P. F. Bessarab[1,2], V. M. Uzdin[1,3], H. Jónsson[2,4]

[1]ITMO University, Kronverkskiy, 49, St. Petersburg, 197101, Russia

[2]Science Institute and Faculty of Physical Sciences, Univ. of Iceland, 107 Reykjavík, Iceland

[3]St. Petersburg State University, St. Petersburg, 198504, Russia

[4]Department of Applied Physics, Aalto University, Espoo, FIN-00076, Finland

v_uzdin@mail.ru

PACS 75.45.+j , 82.20.Xr **DOI 10.17586/2220-8054-2017-8-4-454-461**

Transitions between magnetic states of a system coupled to a heat bath can occur by exceeding the energy barrier, but as temperature is lowered quantum mechanical tunneling through the barrier becomes the dominant transition mechanism. A method is presented for estimating the onset temperature for tunneling in a system with an arbitrary number of spins using the second derivatives of the energy with respect to the orientation of the magnetic vectors at the first order saddle point on the energy surface characterizing the over-the-barrier mechanism. An application to a monomer and a dimer of molecular magnets containing a Mn_4 group is presented and the result found to be in excellent agreement with reported experimental measurements.

Keywords: magnetic transitions, tunneling, rate theory, molecular magnet.

Received: 5 August 2017

Revised: 15 August 2017

1. Introduction

An assessment of the stability of magnetic states is an important problem in the theory of magnetism [1, 2]. Magnetic nanosystems are candidates for spintronics and high density storage devices where a critical issue is the lifetime of prepared magnetic states. A given magnetic state of a nanosystem coupled to a heat bath can have a finite lifetime because of thermally activated transitions involving leaps over an energy barrier separating it from other magnetic states of the system. But, at low enough temperature, quantum mechanical tunneling through the barrier will become the dominant transition mechanism. It is important to have a tool to estimate the temperature at which the tunneling mechanism becomes predominant, thereby reducing the lifetime from what would be expected based on the over-the-barrier mechanism.

Quantum tunneling in spin systems has been the topic of many theoretical [3] and experimental studies [4–7] over the past few decades. At high enough temperature, quantum effects are not significant and transitions are due to thermal activation described by the Arrhenius law. However, in the limit of zero temperature, only tunneling out of the lowest energy level of the initial state can occur. In an intermediate temperature range, tunneling can be thermally assisted, i.e. occurring from thermally activated levels of the initial state. The crossover from over-the-barrier to quantum tunneling can, in such cases, be relatively smooth. The shape of the energy surface affects how sharp this crossover is [8].

Several theoretical studies of the crossover in simple spin models containing one [9–12] or two [13] spins have been carried out using the effective potential method [14]. The effective potential method uses an exact mapping of a spin system onto a particle system with an effective potential and mass that can be coordinate dependent. However, this method is not general and can only be applied to simple model systems. High-order anisotropy terms, such as $(\hat{S}_+^2 + \hat{S}_-^2)$ and $(\hat{S}_+^4 + \hat{S}_-^4)$, have not been incorporated in the mapping approach [15], but can significantly affect the tunneling rate [5, 16]. So far, systems with high-order anisotropy have only been studied numerically by direct diagonalization of the Hamiltonian [17, 18].

Here, a method for calculating the onset temperature of thermally assisted tunneling in a multispin system is presented and applied to two systems: a monomer and a dimer of molecular magnets containing Mn_4 groups. The method involves an analysis of the shape of the energy surface in the vicinity of the first order saddle point on the energy surface representing the transition state of the over-the-barrier mechanism. The present article extends a previous report on systems consisting of a single magnetic vector (a single spin, or multiple spins within the macro-spin approximation) [19]. With the present formulation, the onset temperature for tunneling in systems consisting of an arbitrary number of spins can be estimated.

The article is organized as follows: In the next section, the methodology for estimating the lifetime of a magnetic state due to over-the-barrier transitions is briefly reviewed. Then, the expression for the onset temperature for quantum mechanical tunneling is derived in section 3. Applications are presented in section 4, first to a monomer and then to a dimer of molecular magnets. The article concludes with a summary in section 5.

2. Over-the-barrier transitions

A system of N spins is described by the orientation of each of the spins, $\omega = \{\theta_1, \phi_1, \theta_2, \dots \phi_N, \}$, where θ and ϕ are spherical polar coordinates. The energy as a function of these variables, $U(\omega)$, represents an energy surface and the magnetic states of the system correspond to local minima on this surface. The mechanism of a transition from one state to another involving a jump over an energy barrier is characterized by a minimum energy path (MEP) connecting the corresponding minima. At every point on an MEP, the gradient of the energy point is along the path. The MEP is a transition path with maximal statistical weight, assuming a Boltzmann distribution is established and maintained in the initial state. The MEP can be found using the geodesic nudged elastic band method where the path is discretized by generating a set of replicas of the system and an optimization algorithm is used to bring the replicas from some initial location to an MEP [20].

The point of highest energy along the MEP, $\omega^\dagger$, represents a first order saddle point on the energy surface, a point where the Hessian has one and only one negative eigenvalue. Within harmonic transition state theory (HTST), the transition state is taken to be a hyperplane going through the saddle point with normal pointing along the direction of the unstable mode (the eigenvector corresponding to the negative eigenvalue of the Hessian) [21,22]. An estimate of the activation energy for the transition is then obtained as $\Delta E = U(\omega^\dagger) - U(\omega_m)$, where $U(\omega^\dagger)$ is the energy at the first order saddle point and $U(\omega_m)$ is the energy of the initial state minimum.

The rate of thermally activated transitions involving jumps over the energy barrier can be estimated using HTST for magnetic systems [21]

$$\Gamma^{HTST} = \nu_0 e^{-\Delta E/k_B T}, \tag{1}$$

where ν_0 is a pre-exponential factor that depends on the Hessian evaluated at the saddle point and at the minimum of the energy surface. Calculations of transition rates in magnetic systems using this approach have been carried out in studies of, for example, remagnetization in small islands adsorbed on a solid surface [23], analysis of temperature dependence of hysteresis loops [24], annihilation of magnetic skyrmions [25,26] and interaction of a magnetic tip with a solid surface [27].

Quantum mechanical effects can influence the transition rate even at temperature above the onset temperature for tunneling. This occurs because of the zero point energy (ZPE) which can raise the energy of the initial state and the transition state to a different extent. Within the harmonic approximation, the correction is obtained by adding the ZPE for each vibrational (magnon) mode to the initial state energy and the saddle point energy. As there is one fewer vibrational mode at the transition state than at the initial state, this effect tends to reduce the energy barrier and lower the activation energy for the transition, analogous to the so-called kinetic isotope effect in atomic rearrangements (chemical reactions and atom diffusion). The ZPE corrected activation energy is

$$\Delta E^{ZPEC} = \left(U(\omega^\dagger) + \frac{1}{2}\sum_{i=1}^{N-1} \nu_{\dagger,i} \right) - \left(U(\omega_m) + \frac{1}{2}\sum_{i=1}^{N} \nu_{m,i} \right), \tag{2}$$

where $\nu_{\dagger,i}$ and $\nu_{m,i}$ are the vibrational frequencies [28,29] calculated at the saddle point and at the minimum, respectively. As can be seen from the molecular magnet example below, the ZPE correction can significantly change the acitvation energy and thereby the slope in the Arrhenius graf.

3. Onset temperature for tunneling

Tunneling through an energy barrier can take place because of quantum mechanical delocalization which enables the system to avoid the top of the energy barrier. In a thermalized system, the effect of delocalization can be described in a convenient way using statistical Feynman Path Integrals. The instanton technique can be used to identify when quantum delocalization becomes large enough to make tunneling the dominant transition mechanism. In instanton theory the transition rate is written in terms of the imaginary-time ($\tau = it$) action, S, and a stationary phase approximation [30–32]. The transition rate constant can be expressed as

$$\Gamma = D \exp\left(-S[\omega(\tau)]_{inst}/\hbar\right), \tag{3}$$

where $\omega(\tau)$ is a path corresponding to a periodic trajectory with period $\tau = \beta\hbar$ satisfying $\omega(0) = \omega(\beta\hbar)$, and the pre-factor D takes into account the probability of paths deviating from $\omega(\tau)$. This special path, often referred to

as the instanton, corresponds to a stationary point of the action, a saddle point on the action surface where the path is extended, corresponding to quantum delocalization [32–34].

In our previous work [19], we considered systems with a single spin. Here, a generalization to many-spin systems is described. The Hilbert space of a many-spin system is a tensor product of the Hilbert space of the individual spins. The Euclidean (imaginary-time) action for a system with N spins of length s is defined by [35–37]

$$S(\mathbf{\Omega}) = -is \int_{-\beta/2}^{\beta/2} \sum_{j=1}^{N} (1 - \cos\theta_j)\dot{\phi}_j d\tau + \int_{-\beta/2}^{\beta/2} U(\omega(\tau)) d\tau, \tag{4}$$

where the first term is the sum of the Berry phase of the individual spins and $\mathbf{\Omega} = \omega(\tau)$ represents a closed trajectory with period β.

From here on we use atomic units with $\hbar = 1$, $\mu_B = 1/2$ and the mass and charge of an electron have unit value, $e = 1$ and $m_e = 1$. A scaled gyromagnetic ratio is defined as $\bar{g} = g/2$.

In order to find the onset temperature for tunneling, T_c, the action is expanded to second order in the vicinity of the first order saddle point on the energy surface, $\mathbf{\Omega} = \omega^\dagger + \epsilon\delta\mathbf{\Omega}$,

$$S(\mathbf{\Omega}) = \beta U(\omega^\dagger) + \delta S + \frac{1}{2}\delta^2 S, \tag{5}$$

$$\delta^2 S = -2is \int_{-\beta/2}^{\beta/2} \sum_{j=1}^{N} \left(\delta\theta_j \delta\dot{\phi}_j \sin\theta_j\right) d\tau + \int_{-\beta/2}^{\beta/2} \delta\mathbf{\Omega}\ \mathcal{H}\ \delta\mathbf{\Omega}^T d\tau, \tag{6}$$

where $\mathcal{H}$ is the Hessian matrix of the energy surface $U(\omega)$ at the saddle point $\omega^\dagger$. As $\epsilon \to 0$, $\delta^2 S$ becomes a quadratic form of the Hessian, $\mathcal{H}$, which has one and only one real negative eigenvalue.

The task is to find the temperature at which $\mathbf{\Omega}$ becomes an instanton, *i.e.* a saddle point at the action surface with quantum delocalization. At that point, a zero mode appears corresponding to displacement along the path and thus constant S. This signals the transition from thermally activated jumps to quantum tunneling [32, 33].

Since the instanton is a closed path, $\delta\theta_k$ and $\delta\phi_k$ can be expanded in a Fourier series and $\delta^2 S$ in eqn. (6) rewritten as

$$\frac{1}{2}\delta^2 S(\theta^\dagger, \phi^\dagger) = \beta \sum_{n=0}^{\infty} \left(\sum_{k=0}^{N} \left[\frac{2\pi s \sin\theta_k^\dagger}{\beta} n(\phi_n^k \theta_n^{k^*} - \phi_n^{k^*}\theta_n^k) \right] + \sum_{j,k} \left[a\theta_n^k \theta_n^{j^*} + b\left(\phi_n^k \theta_n^{j^*} + \phi_n^{k^*}\theta_n^j\right) + c\phi_n^k \phi_n^{j^*} \right] \right). \tag{7}$$

The matrix representing the quadratic form of the action is infinite and has a block diagonal form

$$G = \begin{pmatrix} \gamma_0 & & & & \\ & \gamma_1 & & & \\ & & \ddots & & \\ & & & \gamma_n & \\ & & & & \ddots \end{pmatrix}, \tag{8}$$

where

$$\gamma_n = \mathcal{H} + \left(\begin{array}{ccc|ccc} 0 & \cdots & 0 & -k_1^n & \cdots & 0 \\ 0 & \ddots & 0 & 0 & \ddots & 0 \\ 0 & \cdots & 0 & 0 & \cdots & -k_N^n \\ \hline k_1^n & \cdots & 0 & 0 & \cdots & 0 \\ 0 & \ddots & 0 & 0 & \ddots & 0 \\ 0 & \cdots & k_N^n & 0 & \cdots & 0 \end{array}\right), \tag{9}$$

where $k_j^n = 2\pi n T s \sin\theta_j^\dagger$.

An expression for the onset temperature for tunneling can be obtained by analyzing the determinant of G:

$$\det(G) = \prod_{n=0}^{\infty} \det(\gamma_n). \tag{10}$$

Consider first γ_0 which is the Hessian of the energy surface at the first order saddle point. There, γ_0 contains one negative eigenvalue so $\det(\gamma_0) < 0$. However, the other blocks, γ_n (for $n > 0$), depend on temperature and at $T \gg T_c$ are positive definite

$$\det(\gamma_n) \sim (2\pi sn)^{2N} \prod_{j=1}^{N} \sin^2 \theta_j^{\dagger} > 0, \tag{11}$$

and $\det(G) < 0$. As the temperature is lowered to T_c, a zero of G appears signaling a stationary point involving quantum delocalization. This must arise from γ_1 since the temperature in each γ_n is scaled by n and blocks with $n > 1$ thus have zeros at even lower temperature. The onset temperature for tunneling is, therefore, found by solving

$$\det(\gamma_1(T_c)) = 0. \tag{12}$$

This can be easily done numerically for multi-spin systems. All that is required for the calculation are the second derivatives of the energy at the first order saddle point corresponding to the over-the-barrier mechanism.

For a single-spin system, an analytical expression for the onset temperature can be obtained

$$T_c = \frac{\sqrt{b^2 - ac}}{2\pi s k_B \sin\theta^{\dagger}}, \tag{13}$$

where

$$a \equiv \left.\frac{\partial^2 U(\theta^{\dagger}, \phi^{\dagger})}{\partial \theta^2}\right|_{\theta^{\dagger}, \phi^{\dagger}}, \; c \equiv \left.\frac{\partial^2 U(\theta^{\dagger}, \phi^{\dagger})}{\partial \phi^2}\right|_{\theta^{\dagger}, \phi^{\dagger}}, \; b \equiv \left.\frac{\partial^2 U(\theta^{\dagger}, \phi^{\dagger})}{\partial \theta \partial \phi}\right|_{\theta^{\dagger}, \phi^{\dagger}}. \tag{14}$$

The pair of eigenvalues of the γ_1 block are

$$\lambda = \frac{a+c}{2} \pm \frac{\sqrt{(a-c)^2 + 4b^2 - 4k^2}}{2}. \tag{15}$$

In addition to the crossover temperature, we can define the temperature T_0 at which the two eigenvalues become complex conjugates

$$T_0 = \frac{\sqrt{(a-c)^2 + 4b^2}}{4\pi s k_B \sin\theta^{\dagger}}. \tag{16}$$

At this temperature, both eigenvalues are equal to $(a + c)/2$ and could be negative. At higher temperature, the eigenvalues are complex. In the temperature range between T_c and T_0 the two eigenvalues are real, either both are positive or both are negative.

4. Applications. Molecular magnets

Previously, we have presented calculations and compared with experimental results for the single molecular magnet containing a Mn_4 group [19]. We briefly review those calculations here before discussing the dimer. The molecular magnet has a total spin of $s = 9/2$ and can be described with the following Hamiltonian

$$\hat{H} = -D\hat{S}_z^2 - B\hat{S}_z^4 - g\mu_0 \hat{\mathbf{S}} \cdot \mathbf{H} + \hat{H}_{trans}, \tag{17}$$

where D and B are axial anisotropy constants, B is an applied magnetic field and H_{trans} gives the in-plane anisotropy which is small compared with D. The values of the parameters have been determined from experimental measurements (not involving tunneling) [38]: $D = 0.74$ K, $B = -3.8$ mK and $g = 2$. The transverse term is chosen to be fourth-order $E(\hat{S}_+^4 + \hat{S}_-^4$ with $E = 9.8 \times 10^{-4}$ K [38].

For the single molecular magnet it is possible to give an analytical formula for the onset temperature. Expanding (12) with the Mn_4 system Hamiltonian (17) at the saddle point gives

$$T_c = \frac{4s^2\sqrt{DE - 4E^2 s^2}}{\pi}, \tag{18}$$

and $T_c = 0.61$ K. This result is in close agreement with the reported experimental results giving 0.67 K [38]. The dependence of eigenvalues on temperature is shown in Fig. 1.

The calculated transition rate using HTST (applicable for $T > T_c$) and the predicted onset temperature for tunneling in the monomer are shown in Fig. 2, along with experimental data. At temperature below T_c, the tunneling rate is expected to be similar to the HTST rate at T_c. The agreement between the calculations and measurements is good.

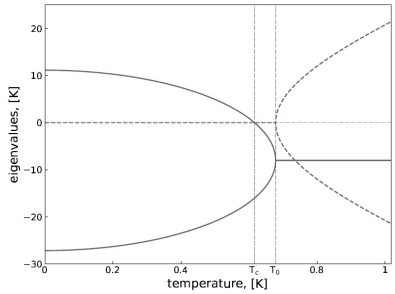

FIG. 1. Eigenvalues of the γ_1 matrix block for the monomer (eq. (17)) Mn_4 molecular magnet. Solid line: real part. Dashed line: imaginary part. At temperature above T_0 the eigenvalues are complex conjugates and give a positive contribution into the determinant. At temperature below the T_c, γ_1 has only one negative eigenvalue, therefore the determinant changes sign at T_c. In the temperature interval $T_c < T < T_0$ γ_1 has two negative eigenvalues

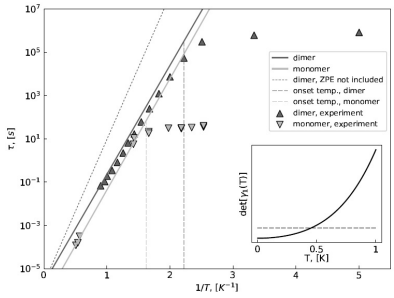

FIG. 2. The calculated lifetime for a monomer and a dimer of molecular magnets containing Mn_4 groups. Results of calculations using harmonic transition state theory with zero point energy correction for the monomer (solid gray line) and the dimer (solid black line) are shown. Calculated lifetime for the dimer without ZPE correction (dashed line) is also shown for comparison. Calculated values for the onset temperature for tunneling calculated from (18) using the Hamiltonian in (17) for the monomer and (19) for the dimer (dashed vertical lines) with parameters taken from experimental measurements are also shown. Experimentally measured transition rate for the monomer [38] is shown with gray triangles and for the dimer [40] with black triangles. Below T_c, the tunneling rate is expected to be similar to the HTST rate at T_c. Excellent agreement is obtained between the calculated and measured results. Inset: The determinant of the γ_1 matrix block for the dimer, showing how it becomes negative at T_c

We turn now to calculations for a dimer of Mn_4 molecular magnets and compare with experimental measurements on $[Mn_4O_3Cl_4(O_2CEt)_3(py)_3]_2$. Each unit of the dimer is described with a magnetic moment of $s = 9/2$, and the Hamiltonian of the system is taken to be

$$\hat{H} = \hat{H}_1 + \hat{H}_2 + J\hat{\mathbf{S}}_1 \cdot \hat{\mathbf{S}}_2, \tag{19}$$

where both $\hat{H}_1$ and $\hat{H}_2$ have the same form as (17) with the parameters taken from [39] and $J = 0.12$ K is isotropic superexchange [40]. The transverse term is chosen to include both 4th- and 2nd-order anisotropies: $C(\hat{S}_+^2 + \hat{S}_-^2)$ and $E(\hat{S}_+^4 + \hat{S}_-^4)$, with $C = 0.032$ K and $E = -7.5 \times 10^{-5}$ K, in order to match the experimental results of the rate above T_c. The energy surface and a minimum energy path for a transition are shown in Fig. 3.

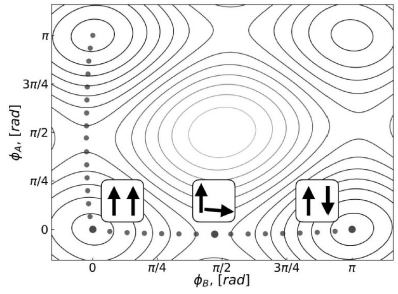

FIG. 3. Energy surface for a dimer molecular magnets containing Mn_4 group when $\theta_A = \theta_B = \pi/2$. The minimum energy path for a remagnetization transition is shown with black dots. The insets show the orientation of the $9/2$ spins of each Mn_4 unit at the initial state (left), first order saddle point (middle), and product state (right).

The calculated crossover temperature for the dimer is $T_c = 0.40$ K in close agreement with experimental measurements [40]. Due to the weak exchange interaction every spin flips almost independently.

In order to see the effect of coupling between the two units more clearly, we also calculated and analyzed a system with larger exchange interaction, taken to be of the same order as the anisotropy, $J = 0.6$ K. The calculated onset temperature for the tunneling is found to be $T_c = 0.35$ K. Due to the strong exchange interaction between spins eigenvalues of γ_1 behave differently, but we still can see the temperature at which one of them crosses zero (see Fig. 4).

The result of calculation of the HTST transition rate and onset temperature for tunneling of the dimer (19) using experimentally determined parameter values is shown in Fig. 2. The ZPE correction changes the slope in the Arrhenius graph, bringing the calculated HTST results closer to the experimental values.

5. Summary

A method is presented for finding the onset temperature of thermally activated tunneling in magnetic systems that are characterized by spin vectors with orientation prescribed by continuous angular variables. A study is made for the Mn_4 molecular magnets where both the high temperature jump rate and the onset temperature for tunneling are calculated and compared with experimental data. Excellent agreement is obtained. The rate calculated above the onset temperature for tunneling includes zero point energy correction. The onset temperature for tunneling is found by analyzing eigenvalues of the γ_1 matrix block at the first order saddle point on the energy surface.

Previously, the onset temperature for tunneling in single-spin or simple (without higher-order anisotropy) two-spin systems can be assessed by other methods, such as the effective potential method or numerical methods involving direct diagonalization of the Hamiltonian, but the method presented here is applicable to systems with an arbitrary number of spins. The method presented here, makes it possible to estimate the onset temperature for tunneling in a magnetic system described by spin vectors as long as the second derivatives of the energy with respect to the angles describing the orientation of vectors can be evaluated at the saddle point on the energy surface.

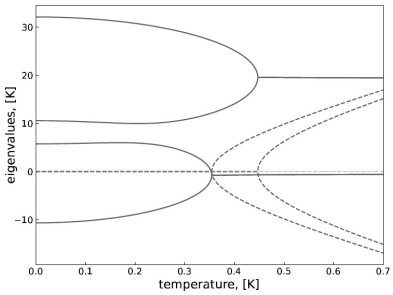

FIG. 4. Eigenvalues of the γ_1 matrix block of the dimer (eq. (19)) when the exchange parameter is chosen to be $J = 0.6$ K. Solid line: real part. Dashed line: imaginary part. The eigenvalues depend on temperature in a similar way as is shown for the monomer in Fig. 1. A pair of eigenvalues becomes real and remains positive, while a second pair of eigenvalues changes sign at T_c from negative to positive as temperature is lowered

The most peculiar characteristic of magnetic systems is that the onset temperature for tunneling depends not only on second derivatives along the unstable mode at the first order saddle point, as in particle systems, but on the curvature of the energy surface at the first order saddle point. This is due to the inseparability of the spin Hamiltonian.

Acknowledgements

This work was supported by the Icelandic Research Fund and the Academy of Finland (grant 278260) and partially financially supported by the Government of the Russian Federation (grant 074-U01).

References

[1] Brown, Jr. W.F. Thermal Fluctuations of Fine Ferromagnetic Particles. *IEEE Transactions on Magnetics*, 1979, **MAG-15**, P. 1196–1208.
[2] Braun H.-B. Kramers's rate theory, broken symmetries and magnetization reversal. *J. Appl. Physics*, 1994, **76**, P. 6310–6315.
[3] Chudnovsky E.M., Tejada J. *Macroscopic Quantum Tunneling of the Magnetic Moment.* Cambridge University Press, New York.: 1998.
[4] Bokacheva L., Kent A.D. and Walters M.A. Crossover between Thermally Assisted and Pure Quantum Tunneling in Molecular Magnet Mn_{12}-Acetate. *Phys. Rev. Lett.*, 2000, **85**, P. 4803–4806.
[5] Mertes K.M., Zhong Y., *et al.* Abrupt crossover between thermally activated relaxation and quantum tunneling in a molecular magnet. *Europhys. Lett.*, 2001, **55**, P. 874–879.
[6] Wernsdorfer W., Murugesu M. and Christou G. Resonant Tunneling in Truly Axial Symmetry Mn_{12} Single-Molecule Magnets: Sharp Crossover between Thermally Assisted and Pure Quantum Tunneling. *Phys. Rev. Lett.*, 2006, **96**, 057208 (4 pp.)
[7] Loth S., Baumann S., *et al.* Bistability in atomic-scale antiferromagnets. *Science*, 2012, **335**, P. 196–199.
[8] Chudnovsky E.M. Phase transitions in the problem of the decay of a metastable state. *Phys. Rev. A*, 1992, **46**, P. 8011–8014.
[9] Chudnovsky E. M., Garanin D. A. First- and Second-Order Transitions between Quantum and Classical Regimes for the Escape Rate of a Spin System. *Phys. Rev. Lett.*, 1997, **79**, P. 4469–4472.
[10] Park C.-S., Yoo S.-K. and Yoon D.-H. Quantum-classical crossover of the escape rate in a biaxial spin system with an arbitrarily directed magnetic field. *Phys. Rev. B*, 2000, **61**, P. 11618–11624.
[11] Kim G.-H. and Chudnovsky E.M. Escape-rate crossover between quantum and classical regimes in molecular magnets: A diagonalization approach. *Europhys. Lett.*, 2000, **52**, P. 681–687.
[12] Garanin D.A. and Chudnovsky E.M. Quantum statistical metastability for a finite spin. *Phys. Rev. B*, 2000, **63**, 024418 (7 pp.)
[13] Owerre S. A. and Paranjape M. B. Phase transition between quantum and classical regimes for the escape rate of dimeric molecular nanomagnets in a staggered magnetic field. *Phys. Lett. A*, 2014, **378**, P. 1407–1412.
[14] Ulyanov V.V. and Zaslavskii O.B. New methods in the theory of quantum spin systems. *Phys. Rep.*, 1992, **216**, P. 179–251.
[15] Owerre S. A., Paranjape M. B. Macroscopic quantum tunneling and quantum-classical phase transitions of the escape rate in large spin systems. *Phys. Rep.*, 2015, **546**, P. 1–60.
[16] Wernsdorfer W. and Sessoli R. Quantum Phase Interference and Parity Effects in Magnetic Molecular Clusters. *Science*, 1999, **284**, P. 133–135.
[17] Kang D.H. and Kim G.-H. Theoretical study of abrupt or gradual crossover of the escape rate in single-molecule magnets. *Phys. Rev. B*, 2006, **74**, 184418 (5 pp.)

[18] Kim G.-H., Kang D.H. and Shin M.C. Quantum-classical crossover of the escape rate in the biaxial nanomagnets with a higher order symmetry. *Eur. Phys. J. B*, 2011, **83**, P. 63–67.

[19] Vlasov S., Bessarab P.F., Uzdin V.M. and Jónsson H. Classical to quantum mechanical tunneling mechanism crossover in thermal transitions between magnetic states. *Faraday Discuss.*, 2016, **195**, P. 93–109.

[20] Bessarab P.F., Uzdin V.M. and Jónsson H. Method for finding mechanism and activation energy of magnetic transitions, applied to skyrmion and antivortex annihilation. *Comp. Phys. Commun.*, 2015, **196**, P. 335–347.

[21] Bessarab P.F., Uzdin V.M. and Jónsson H. Harmonic Transition State Theory of Thermal Spin Transitions. *Phys. Rev. B*, 2012, **85**, 184409 (4 pp.)

[22] Bessarab P.F., Uzdin V.M. and Jónsson H. Potential Energy Surfaces and Rates of Spin Transitions. *Z. Phys. Chem.*, 2013, **227**, P. 1543–1557

[23] Bessarab P.F., Uzdin V.M. and Jónsson H. Size and Shape Dependence of Thermal Spin Transitions in Nanoislands. *Phys. Rev. Lett.*, 2013, **110**, 020604 (5 pp.)

[24] Moskalenko M. , Bessarab P.F., Uzdin V.M. and Jónsson H. Qualitative Insight and Quantitative Analysis of the Effect of Temperature on the Coercivity of a Magnetic System. *AIP Advances*, 2016, **6**, 025213 (8 pp.)

[25] Lobanov I., Jónsson H. and Uzdin V. M. Mechanism and activation energy of magnetic skyrmion annihilation obtained from minimum energy path calculations. *Phys. Rev. B*, 2016, **94**, 174418 (7 pp.)

[26] Bessarab P.F. Comment on "Path to collapse for an isolated Néel skyrmion". *Phys. Rev. B*, **95**, 2017, 136401 (2 pp.)

[27] Ivanov A. , Bessarab P.F., Uzdin V.M. and Jónsson H. Magnetic exchange force microscopy: Theoretical analysis of induced magnetization reversals. *Nanoscale*, 2017, Accepted Manuscript, DOI: 10.1039/C7NR04036A

[28] Smit J., Beljers H. Ferromagnetic resonance absorption in $BaFe_{12}O_{19}$, a highly anisotropic crystal. *Philips Res. Rep.*, 1955, **10**, P. 113–130.

[29] Suhl H. Ferromagnetic resonance in nickel ferrite between one and two kilomegacycles. *Phys. Rev.*, 1955, **97**, P. 555–557.

[30] Miller W.H. Semiclassical limit of quantum mechanical transition state theory for nonseparable systems. *J. Chem. Phys.*, 1975, **62**, P. 1899–1906.

[31] Callen C., Coleman S. Fate of the false vacuum. II. First quantum corrections. *Phys. Rev. D*, 1977, **16**, P. 1762–1768

[32] Benderskii V. A., Goldanskii V. I. and Makarov D. E. Quantum dynamics in low-temperature chemistry. *Phys. Rep.*, 1993, **233**, P. 195–339.

[33] Mills G., Schenter G. K., Makarov D. E. and Jónsson H. Generalized path integral based quantum transition state theory. *Chem. Phys. Letters*, 1997, **278**, P. 91–96.

[34] Mills G., Schenter G. K., Makarov D. E. and Jónsson H. RAW Quantum transition state theory. proceeding of "Classical and Quantum Dynamics in Condensed Phase Simulations", Villa Marigola, Lerici, Italy, 1997, 405 pp.

[35] KIauder J. Path integrals and stationary-phase approximations. *Phys. Rev. D*, 1979, **19**, P. 2349–2356.

[36] Kochetov E. SU(2) coherentstate path integral. *J. Math. Phys.*, 1995, **36**, P. 4667–4679.

[37] Fradkin E. *Field Theories of Condensed Matter Physics.* Cambridge University Press, New York.: 2013, 190 pp.

[38] Aubin S. M. J. *et. al.* Resonant Magnetization Tunneling in the Trigonal Pyramidal $Mn^{IV}Mn_3^{II}$ Complex $[Mn_4O_3Cl(O_2CCH_3)_3(dbm)_3]$. *J. Am. Chem. Soc.*, 1998, **120**, P. 4991–5004.

[39] Edwards R. S., Hill S., *et. al.* A comparative high frequency EPR study of monomeric and dimeric Mn_4 single-molecule magnets, *Polyhedron*, 2003, **22**, P. 1911–1916.

[40] Wernsdorfer W., Aliaga-Alcalde N., Hendrickson D. N., Christou G. Exchange-biased quantum tunnelling in a supramolecular dimer of single-molecule magnets. *Nature*, 2002, **416**, P. 406–409.

Article III

Instantons describing tunneling between magnetic states at finite temperature

Sergei M. Vlasov, Pavel F. Bessarab, Valery M. Uzdin, and Hannes Jónsson

Nanosystems: Physics, Chemistry, Mathematics (accepted for publication)

NANOSYSTEMS: PHYSICS, CHEMISTRY, MATHEMATICS, 2017, 0 (0), P. 1–17

Instantons describing tunneling between magnetic states at finite temperature

S. M. Vlasov[1,2], P. F. Bessarab[1,2], V. M. Uzdin[2,3], H. Jónsson[1,4]

[1]Science Institute and Faculty of Physical Sciences, Univ. of Iceland
107 Reykjavík, Iceland
[2]ITMO University, Kronverkskiy, 49, St. Petersburg, 197101, Russia
[3]St. Petersburg State University, St. Petersburg, 198504, Russia
[4]Center for Nonlinear Studies, Los Alamos, NM 87545, USA

A method is presented for finding instantons in magnetic systems – optimal paths corresponding to tunneling from one magnetic state to another at a finite temperature. The method involves analytical continuation of the energy to allow for complex values of the angle variables. First, a set of discretization points are placed equally spaced on a chosen energy contour. Then, an estimate of the corresponding temperature is obtained using Landau-Lifshitz dynamics in imaginary time along the contour. Finally, the distribution of the discretization points as well as the energy are systematically refined by converging on the nearest stationary point of the Euclidean action, thereby obtaining a discrete representation of the closest instanton at the given temperature. The method is illustrated with an application to a system consisting of a single spin subject to uniaxial anisotropy and transverse external magnetic field. First-order and second-order crossovers from over-the-barrier mechanism to tunneling are found depending on the applied field, and the difference in the dependence of the instanton temperature on the energy illustrated for the two cases. By comparing the Boltzmann factors for over-the-barrier and tunneling transitions, the crossover temperature between the two mechanisms is estimated for both first- and second-order crossover.

Keywords: magnetic transitions, tunneling, instanton, path optimization.

1. Introduction

Transitions between (meta)stable states of atomic systems are typically thermally activated, i.e. they occur as a result of thermal fluctuations due to coupling to a heat bath. The states are separated and can be identified because of an energy barrier, an energy ridge on the multidimensional energy surface. At high enough temperature, the transitions rely on large energy fluctuations in the right degrees of freedom that enable the system to overcome the energy barrier. This is referred to as over-the-barrier transition mechanism. For high barriers, these are rare events compared with the timescale of vibrations. The rate of such rare events can be estimated from statistical rate theories, in particular, transition state theory and Kramers/Langer theory [1–3]. These theoretical tools make it possible to predict and analyze the typically observed Arrhenius dependence of the transition rate on temperature, where the activation energy is essentially the height of the energy barrier. This methodology was initially developed in the context of atomic rearrangements such as chemical reactions, diffusion events and conformational changes of molecules. More recently, statistical rate theories have been extended to describe transitions from one magnetic state to another [4–8]. More generally, atomic coordinates and orientation of magnetic moments should be treated on an equal footing.

At low enough temperature a different transition mechanism will eventually become dominant. There, the system advances from one state to another by quantum mechanical tunneling through the energy barrier. The crossover from over-the-barrier mechanism to

tunneling is evident from a rapid drop in the activation energy as the temperature is lowered. For atomic rearrangements and temperature close to room temperature, this kind of behavior is mostly observed in transitions involving light atoms, such as hydrogen. Transition state theory for atomic rearrangements has been extended by use of Feynman path integrals to take into account the possibility of tunneling [9–13]. Full free energy calculations for determining transition rates have been carried out as well as sampling based on dynamical approaches [14–17].

Most of the time, transition state theory is used within the harmonic approximation where the calculations are simplified by approximating the energy surface with a quadratic expansion in the vicinity of the initial state minimum and at a first-order saddle point on the energy ridge separating the initial state from the final state(s). For over-the-barrier transitions, this leads to the widely used harmonic transition state theory expression for the rate constant [18]. The main challenge in such calculations is finding the relevant first-order saddle point(s) and evaluating the energy there as well as its second derivatives. If both the initial and final states of the transition are known, the minimum energy path on the energy surface connecting the two local energy minima can be found and thereby the first-order saddle point – the highest energy point on that path. The nudged elastic band (NEB) method is commonly used for this task [19–21]. A more challenging task is to find saddle points on the energy ridge given only the initial state minimum. For this, the minimum mode following method can, for example, be used [22, 23].

An analogous harmonic approximation to quantum transition state theory has been developed [10–13, 24]. It relies on finding special transition paths corresponding to thermally activated tunneling. Such paths are first-order saddle points on an extended quantum mechanical energy surface underlying the statistical properties of Feynman path integrals. These first-order saddle points are often referred to as 'instantons'. The evaluation of the rate of thermally activated tunneling within instanton theory requires much fewer computations than full quantum transition state theory calculations. Efficient implementations of instanton theory calculations for atomic rearrangements have recently been presented and applied to various chemical reactions [25–27]. Instantons can be found by using saddle point search methods, such as the minimum mode following method, or by using a line integral extension of the NEB method.

Much less has been done on quantum mechanical rate theory for magnetic transitions. Most of the work has relied on a mapping of the magnetic system onto a particle system with an effective Hamiltonian but this can only be done for certain simple spin systems [28, 29]. One such system consists of a single spin with uniaxial anisotropy and a transverse magnetic field [30]. In the particle mapping method, a spin wave function using the $\hat{S}_z$ eigenstates is constructed and then transformed to an eigenvalue equation $\hat{H}|\psi\rangle = E|\psi\rangle$, a Schrödinger equation with an effective potential and possibly coordinate dependent mass. The energy spectrum of the spin system coincides with the first 2j+1 levels of the corresponding particle system, where j is the quantum number giving the length of the magnetic momentum vector. Thereby, one can use techniques developed for particle systems to study spin systems. This approach, however, is not universal, since a general way to construct the corresponding particle Hamiltonian is not known. In fact, there are no known strategies for systems with multiple spins. Also, single spin systems with a Hamiltonian containing higher-order terms (cubic and higher) as is often the case in molecular magnets, for example [31, 32]. As far as we know, there is only one study based on spin-particle mapping for a two-spin system [33]. Furthermore, the action of the corresponding particle system does not contain a topological term (14) that affects quantum interference in magnetic systems [34–36]. An efficient method

for finding instantons for magnetic systems without relying on spin-particle mapping is, therefore, needed.

Interesting results have, nevertheless, been obtained from studies using the spin-particle mapping technique. It has, in particular, been shown that crossover from over-the-barrier to tunneling mechanism can be of two different types, a smooth second-order crossover where the activation energy changes rather gradually and a more abrupt first-order crossover where the activation energy drops suddenly as temperature is lowered [30]. A general expression has been presented recently for the second-order crossover temperature applicable to any system for which the energy can be evaluated, including self-consistent field calculations [37, 38]. The calculations can be carried out based on the second derivatives of the energy at the first-order saddle point. Such an estimate of the crossover temperature can be useful when assessing the lifetime of magnetic states since it shows whether tunneling needs to be taken into account, while classical rate theory would overestimate the lifetime. An estimate of a first-order crossover temperature is more difficult, however, since it cannot be obtained from the vicinity of the first-order saddle point. For this purpose, it is necessary to find the magnetic instantons for the temperature of interest, but we are not aware of such calculations in the literature.

In this article, we present a method for finding instantons representing tunneling in magnetic systems. The formulation is based on the Euclidean action obtained from the coherent state path integral formulation of the partition function. A numerical technique is presented for finding instantons as stationary points of the action. This approach is applied to a system consisting of a single spin with uniaxial anisotropy in the presence of a transverse magnetic field, and a comparison made with results obtained from spin-particle mapping. The approach can in principle be applied to any magnetic system, including multiple spins, as long as the energy of the system can be described by an analytical function.

2. Theoretical background

A brief review of the theoretical background for coherent spin states and the formulation of path integrals and Euclidean action for spin systems is given below for completeness. The reader is referred to the work by Fradkin for more detailed discussion [39]. An alternative derivation has been given by Kochetov [40].

2.1. Coherent spin states

Coherent states are well known in the context of the quantum harmonic oscillator where they have been used to relate quantum mechanical dynamics as closely as possible to classical dynamics. They are in many cases a useful addition to other descriptions of a quantum mechanical system, but in the case of spins, they are the only known way to develop a path integral representation. The reason is that the Hilbert space of a spin does not have continuously parameterized eigenstates corresponding to classical variables such as coordinates and momenta. For a system with spin j, (for example, the total magnetic moment of an atom) there are $2j+1$ eigenstates of the $\hat{S}_z$ operator: $\hat{S}_z|\mu, j\rangle = \mu|\mu, j\rangle$, where μ runs from $-j$ to j. They can be used to construct coherent states, $|\hat{\mathbf{n}}\rangle$, that correspond to particular orientation of the spin specified by continuous spherical polar coordinates, θ and ϕ as

$$|\hat{\mathbf{n}}\rangle = |\theta, \phi\rangle = \sum_{m=-j}^{j} \sqrt{\frac{(2j)!}{(j+m)!(j-m)!}} \left(\sin\frac{\theta}{2}\right)^{j+m} \left(\cos\frac{\theta}{2}\right)^{j-m} e^{-i(j+m)\phi}|m, j\rangle. \quad (1)$$

The coherent states satisfy the following closure relation

$$1 = \frac{2j+1}{4\pi} \int d\hat{\mathbf{n}} \, |\hat{\mathbf{n}}\rangle\langle\hat{\mathbf{n}}|. \tag{2}$$

Matrix elements of the spin operators in terms of coherent states are

$$\langle \hat{S}_z \rangle = -j + 2j \sin^2 \frac{\theta}{2} = -j \cos\theta. \tag{3}$$

$$\begin{aligned} \langle \hat{S}_x \rangle &= -j \sin\theta \cos\phi, \\ \langle \hat{S}_y \rangle &= -j \sin\theta \sin\phi. \end{aligned} \tag{4}$$

2.2. Path integral representation of the partition function

The partition function for a spin system can be written as

$$Z = \mathrm{Tr}(e^{-\beta\hat{H}}) = \int d\hat{\mathbf{n}} \langle \hat{\mathbf{n}} | e^{-\beta\hat{H}} | \hat{\mathbf{n}} \rangle. \tag{5}$$

As for Feynman path integrals for particles, the interval β is divided up into N parts

$$\langle \hat{\mathbf{n}} | e^{-\beta\hat{H}} | \hat{\mathbf{n}} \rangle = \lim_{N\to\infty} \langle \hat{\mathbf{n}} | \left(1 - \epsilon\hat{H}\right)^N | \hat{\mathbf{n}} \rangle, \tag{6}$$

where $\epsilon = \beta/N$. Then, the resolution of the identity (2) is inserted between the segments of the interval and the expression for the partition function gets the form

$$Z = \lim_{N\to\infty} \int \prod_{k=1}^{N} d\mu(\hat{\mathbf{n}}_k) \langle \hat{\mathbf{n}}_k | \left(1 - \epsilon\hat{H}\right) | \hat{\mathbf{n}}_{k-1} \rangle, \tag{7}$$

where $d\mu(\hat{\mathbf{n}}_k) = \left(\frac{2j+1}{4\pi}\right) d\hat{\mathbf{n}} \delta(\mathbf{n}^2 - 1)$ is the invariant integration measure and $\hat{\mathbf{n}}_0 = \hat{\mathbf{n}}_N$, i.e. periodic boundary conditions are fulfilled.

2.3. Euclidean action

The matrix elements in (7) can be approximated up to quadratic terms as

$$\begin{aligned} \langle \hat{\mathbf{n}}_k | \left(1 - \epsilon\hat{H}\right) | \hat{\mathbf{n}}_{k-1} \rangle &= \langle \hat{\mathbf{n}}_k | \hat{\mathbf{n}}_{k-1} \rangle \left(1 - \epsilon \frac{\langle \hat{\mathbf{n}}_k | \hat{H} | \hat{\mathbf{n}}_{k-1} \rangle}{\langle \hat{\mathbf{n}}_k | \hat{\mathbf{n}}_{k-1} \rangle}\right) \\ &\simeq \langle \hat{\mathbf{n}}_k | \hat{\mathbf{n}}_{k-1} \rangle \exp\left(-\epsilon \frac{\langle \hat{\mathbf{n}}_k | \hat{H} | \hat{\mathbf{n}}_{k-1} \rangle}{\langle \hat{\mathbf{n}}_k | \hat{\mathbf{n}}_{k-1} \rangle}\right). \end{aligned} \tag{8}$$

The first term in (8) does not equal zero since coherent states are not orthogonal. It leads to an important feature of the spin path integral, a topological phase equivalent to Berry phase [41]. This term can be rewritten as

$$\langle \hat{\mathbf{n}}_k | \hat{\mathbf{n}}_{k-1} \rangle = 1 - \epsilon \frac{\langle \hat{\mathbf{n}}_k | (|\hat{\mathbf{n}}_k\rangle - |\hat{\mathbf{n}}_{k-1}\rangle)}{\epsilon} \simeq \exp\left(-\epsilon \frac{\langle \hat{\mathbf{n}}_k | (|\hat{\mathbf{n}}_k\rangle - |\hat{\mathbf{n}}_{k-1}\rangle)}{\epsilon}\right). \tag{9}$$

which in the limit $\epsilon \to 0$ gives the path integral expression for the partition function as

$$Z = \int D[\hat{\mathbf{n}}(\tau)] e^{-S_E}, \tag{10}$$

where the Euclidean action

$$S_E(\mathbf{\Omega}) = \int_0^\beta d\tau \left[\langle \hat{\mathbf{n}} | \frac{\partial}{\partial\tau} | \hat{\mathbf{n}} \rangle + \langle \hat{\mathbf{n}} | \hat{H} | \hat{\mathbf{n}} \rangle \right] \tag{11}$$

is an integral over a closed path $\mathbf{\Omega} = (\theta(\tau), \phi(\tau)) \equiv \omega(\tau)$ on the energy surface $E(\omega)$. The integration variable, τ, can be interpreted as imaginary time.

The first term in the integrand can be rewritten using the expression for the coherent states, (1), as

$$\langle \hat{\mathbf{n}}| = \sum_{p=0}^{2j} \sqrt{\frac{(2j)!}{p!(2j-p)!}} \left(\cos\frac{\theta}{2}\right)^{2j} \left(\tan\frac{\theta}{2}\right)^{p} e^{ip\phi} \langle -j+p, j|, \tag{12}$$

$$|\frac{\partial \hat{\mathbf{n}}}{\partial \tau}\rangle = \sum_{p=0}^{2j} \sqrt{\frac{(2j)!}{p!(2j-p)!}} \left(\cos\frac{\theta}{2}\right)^{2j} \left(\tan\frac{\theta}{2}\right)^{p} e^{-ip\phi} \left[\left(p\csc\theta - j\tan\frac{\theta}{2}\right)\dot{\theta} - ip\dot{\phi}\right] |-j+p, j\rangle, \tag{13}$$

and

$$\langle \hat{\mathbf{n}}|\frac{\partial}{\partial\tau}|\hat{\mathbf{n}}\rangle = -j\tan\frac{\theta}{2}\dot{\theta} + j\tan\frac{\theta}{2}\dot{\theta} - ij(1-\cos\theta)\dot{\phi} = -ij(1-\cos\theta)\dot{\phi}. \tag{14}$$

Hence, the partition function (10) gets the phase

$$\begin{aligned}\exp\left(\int_0^\beta d\tau \langle \hat{\mathbf{n}}|\frac{\partial}{\partial\tau}|\hat{\mathbf{n}}\rangle\right) &= \exp\left(-ij\int_0^\beta d\tau(1-\cos\theta)\dot{\phi}\right) \\ &= \exp\left(-ij\int_\Gamma (1-\cos\theta)d\phi\right),\end{aligned} \tag{15}$$

where Γ is a closed path described by the vector $\hat{\mathbf{n}} = \{\theta(\tau), \phi(\tau)\}$. This term has a geometric interpretation. It is proportional to the area bounded by the curve Γ.

The final expression for the Euclidean action of a system with a spin j can be written as

$$S[\mathbf{\Omega}] = \int_{-\beta/2}^{\beta/2} d\tau \left[-ij(1-\cos\theta)\dot{\phi} + E(\omega)\right]. \tag{16}$$

2.4. Instantons

Instantons are stationary paths for (16), i.e. they correspond to $\delta S = 0$. Differentiation gives the equations of motion

$$\begin{aligned}\dot{\theta} &= \frac{i}{j\sin\theta}\frac{\partial E}{\partial\phi}, \\ \dot{\phi} &= -\frac{i}{j\sin\theta}\frac{\partial E}{\partial\theta},\end{aligned} \tag{17}$$

where θ and ϕ satisfy the boundary condition $\mathbf{\Omega}(0) = \mathbf{\Omega}(\beta)$. These are the Landau-Lifshitz equations for spin dynamics in imaginary time.

These equations of motion have two types of solutions. The first type corresponds simply to a stationary point on the energy surface, $\mathbf{\Omega} = \omega_0$, with energy $\mathrm{E}(\omega_0)$. This can, in particular, be the first-order saddle point on the energy surface $\omega^\dagger = (\theta^\dagger, \phi^\dagger)$. The corresponding action is

$$S_{jump} = \beta E(\omega^\dagger) = \beta E^\dagger. \tag{18}$$

This solution characterizes the classical over-the-barrier transition mechanism that dominates at high enough temperature.

The second type of solutions are extended closed paths, so-called instantons. They correspond to tunneling between two potential wells. In the limit of zero temperature $T \to 0$,

i.e. $\beta \to \infty$, the instanton corresponds to tunneling from the ground state, but at finite temperature, it corresponds to thermally assisted tunneling. An instanton is a trajectory in imaginary time that conserves energy (analogous to Landau-Lifshitz dynamics in real time) as can be shown by taking the time derivative of E and inserting into (17). This gives

$$\frac{dE}{d\tau} = \frac{\partial E}{\partial \theta}\dot{\theta} + \frac{\partial E}{\partial \phi}\dot{\phi} = \frac{i}{j \sin\theta}\frac{\partial E}{\partial \phi}\frac{\partial E}{\partial \theta} - \frac{i}{j \sin\theta}\frac{\partial E}{\partial \theta}\frac{\partial E}{\partial \phi} = 0. \tag{19}$$

In contrast to particle systems, magnetic systems have no kinetic energy. As a result, in order to find paths that satisfy the boundary conditions and solve (17), it is necessary to analytically continue the function $E(\omega)$ to allow for complex values of the angles, ω.

3. Method for finding magnetic instantons

This section describes the method we have developed for finding instantons for magnetic transitions. Since the instanton corresponds to a stationary point of the action, it corresponds to a periodic orbit described by Landau-Lifshitz equations in imaginary time. As the dynamics conserve energy, the instantons lie on equienergy contours. The first step is, therefore, to identify the contour for a given value of the energy. In order to map out the dependence on temperature, the calculations need to be carried out for a grid of energy values in the interval from the initial state minimum to the first-order saddle point. Once the energy contour has been identified and represented by a set of discretization points, the corresponding temperature is estimated by evaluating the period of the Landau-Lifshitz dynamics along the closed contour. The distribution of the discretization points along the energy contour as well as a refinement of the value of the energy is then carried out using iterative zeroing of the derivatives of the action. The resulting distribution of discretization points then represents an instanton for the given temperature.

3.1. Energy contours

The method for finding and representing energy contours with an even distribution of discretization points is essentially the one presented previously by Einarsdóttir *et al.* [26]. It is a modification of the NEB method [19, 20]. The contour is represented with a set of discretization points, k={1,N}. Each point corresponds to a configuration of the system, i.e. a value of all variables, ω_k. For a system with a single magnetic moment, $\omega_k = (\theta_k, \phi_k)$. More generally, for systems with more than one magnetic moment, ω_k is a vector with values of θ and ϕ for each one of the magnetic moments. For simplicity, the presentation here will be for a system with a single magnetic moment, but it can be generalized easily. In order to find non-trivial instantons, the angles need to be able to have complex values so a configuration can be written as $\omega_k = (\theta_k^R, \theta_k^I, \phi_k^R, \phi_k^I)$. The energy of the system is some known function of the orientation, E(ω), analytically continued to the complex plane.

In order to find the energy contour corresponding to some particular value of the energy, E′, an objective function, S^{iso}, is defined as the sum of quadratic deviations of the energy

$$S^{iso}(\omega_1, \ldots, \omega_N) = \frac{1}{2}\sum_{k=0}^{N} |E(\omega_k) - E'|^2. \tag{20}$$

Given some initial distribution of the discretization points, an iterative algorithm is used to converge on the energy contour corresponding to energy E′. The iterative algorithm is based on zeroing the derivatives of S^{iso} with respect to the variables.

The negative gradient of the objective function with respect to the variables ω_k

$$g_k = -\nabla_k S^{iso} = -(E(\omega_k) - E')\nabla_k E(\omega_k). \tag{21}$$

gives the direction of steepest descent for discretization point k. It represents a force acting on the discretization point that can be used to move it towards the energy contour. As in the NEB method, the displacements of the discretization point parallel and perpendicular to the path are treated separately. A tangent to the path, $\hat{t}_k$, described by the current location of discretization points is evaluated as in the NEB method [42]. It is used to distinguish between displacements that represent changes in the shape of the path and displacements that are related to the distribution of the discretization points along the path. The component of the gradient representing a change in the shape of the path is given by the force component perpendicular to the path

$$g_k^{\perp} = g_k - (g_k \cdot \hat{t}_k)\hat{t}_k. \tag{22}$$

An even distribution of the discretization points along the path is obtained by including a spring force between adjacent images in the direction parallel to the tangent

$$g_k^{sp} = (k_{sp}(|\omega_{k+1} - \omega_k| - |\omega_k - \omega_{k-1}|))\,\hat{t}_k \tag{23}$$

where k_{sp} is a spring force chosen in such a way that g_k^{sp} is roughly of the same magnitude as $g_k^{\perp}$.

The total force acting on each discretization point is then

$$g_k^{opt} = g_k^{\perp} + g_k^{sp}. \tag{24}$$

A minimization procedure based on the velocity Verlet algorithm is then used to move all the discretization points simultaneously in the direction given by the total force, analogous to what is often done in NEB calculations of minimum energy paths [20].

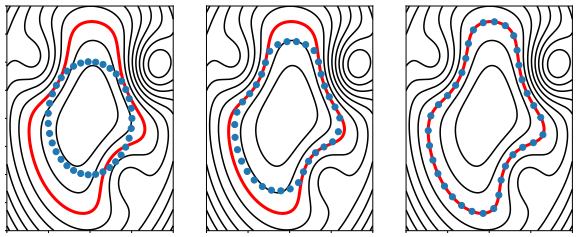

FIG. 1. Illustration of the method for finding and representing an energy contour of a model energy surface. The target contour is shown by the bold red line. Starting with a discrete representation of a circle in configuration space (left), the iterative algorithm moves the discretization points towards the specified energy contour (middle) and eventually converges on it (right).

Fig. 1 shows an example calculation where an energy contour is found using the algorithm described above. First, the discretization points are arranged arbitrarily in a circle. Then, they are moved iteratively in the direction of g_k^{opt} until an even distribution is obtained on the desired energy contour. This is an arbitrary test case where the energy surface is generated by adding up a few Gaussians for illustration purposes only.

3.2. Temperature estimate

Given an even distribution of discretization points along an energy contour, the next task is to estimate what temperature an instanton on this energy contour would correspond to. For this purpose, an approximate Landau-Lifshitz dynamics calculation is carried out to estimate the imaginary time it takes to go from one discretization point to another. From the total time it takes to go along the full path, the period, τ, can be estimated, and then the temperature as T=1/τ.

Let the closed path described by the set of N discretization points be denoted as $\mathbf{\Omega}^{iso} = \{\omega_1^{iso}, \omega_2^{iso} \dots \omega_N^{iso}\}$. The time it takes to go from one discretization point to another can be estimated as

$$\Delta\tau_i = \frac{|v_i|}{|d_i|} \tag{25}$$

where the distance between the two points is $|d_i| = |\omega_{i+1}^{iso} - \omega_i^{iso}|$ and the velocity can be estimated from Landau-Lifshitz equations as

$$v_i = \begin{pmatrix} \frac{i}{j \sin\theta_i} \frac{\partial E}{\partial \phi_i} \\ \\ \frac{-i}{j \sin\theta_i} \frac{\partial E}{\partial \theta_i} \end{pmatrix}. \tag{26}$$

Recall that θ and ϕ are complex variables. The total time period corresponding to the closed path along the contour is

$$\tau = \sum_{i=1}^{N} \Delta\tau_i. \tag{27}$$

This approximate calculation gives an estimate of the instanton temperature associated with the given energy contour. The even distribution of the discretization points along the contour and the temperature estimate are subsequently used as initial conditions for a calculation where an accurate distribution of the discretization points corresponding to an instanton is found, as well as a revised value of the energy for which the obtained temperature value corresponds more closely. This refinement is described in the following section.

3.3. Refinement of discretization points and energy

Given the even distribution of discretization points along an energy contour and the value of the temperature obtained as described above, a refinement calculation is carried out where the temperature is kept fixed but the distribution of the discretization points and the value of the energy are refined so as to converge on a stationary point of the action. This is done by zeroing the derivatives of the action with respect to all variables describing the path, $\mathbf{\Omega} = \{\omega_1, \omega_2 \dots \omega_N\}$.

The scaled action, $\tilde{S} \equiv \beta S(\mathbf{\Omega})$, is approximated using the set of N discretization points

$$\tilde{S}(\mathbf{\Omega}) = \sum_{k=1}^{N} \left[k(T) \left(1 - \frac{\cos\theta_k + \cos\theta_{k+1}}{2} \right) (\phi_{k+1} - \phi_k) + \frac{E(\theta_k, \phi_k) + E(\theta_{k+1}, \phi_{k+1})}{2N} \right], \tag{28}$$

where $k(T) = -ijTk_B$. The task is to find a stationary point of the function $\tilde{S}$ for a given value of T, that is, to solve the system of differential equations

$$\begin{aligned}\frac{\partial \tilde{S}}{\partial \theta_k} &= \frac{1}{2}k(T)\sin\theta_k(\phi_{k+1}-\phi_{k-1}) + \frac{\partial E}{\partial \theta_k} = 0,\\ \frac{\partial \tilde{S}}{\partial \phi_k} &= \frac{1}{2}k(T)(\cos\theta_{k+1}-\cos\theta_{k-1}) + \frac{\partial E}{\partial \phi_k} = 0, \quad k \in [1,N].\end{aligned} \tag{29}$$

Since the action is complex, it is convenient here to define a real objective function, F($\mathbf{\Omega}$), by summing up the magnitude squared of the derivatives of $\tilde{S}$ with respect to all the variables. The minimum value of F is zero and corresponds to a stationary point of the action. Standard minimization techniques can be applied to find the minimum of F since it is a real function.

Defining first the vector function $f(\tilde{\mathbf{\Omega}})$ as

$$f(\mathbf{\Omega}) = \begin{pmatrix} \frac{\partial S(\mathbf{\Omega})}{\partial \theta_1} \\ \vdots \\ \frac{\partial S(\mathbf{\Omega})}{\partial \phi_N}, \end{pmatrix} \tag{30}$$

the objective function can be written as the squared norm of $f(\mathbf{\Omega})$

$$F(\mathbf{\Omega}) \equiv \frac{1}{2}\bar{f}(\mathbf{\Omega})\cdot f(\mathbf{\Omega}), \tag{31}$$

The task is to find the N discretization points that give F($\mathbf{\Omega}$)=0 for the given temperature value (obtained as described in the previous section). Since the temperature estimate does not correspond exactly to the energy contour initially chosen, the discretization points will converge on a slightly different energy contour and their distribution will not be uniform.

The BFGS algorithm is used for the iterative minimization of F. It is important to start with the discretization points located on a contour of roughly the right energy to avoid converging on the trivial solution where the discretization points are all at the same location (the classical limit).

The BFGS algorithm requires the first derivatives of F with respect to all the variables. These, in turn, involve the second derivatives of $\tilde{S}$

$$\begin{cases} \frac{\partial F}{\partial \theta_j^R} = \sum_{k=1}^{N} \Re\frac{\partial \tilde{S}}{\partial \theta_k}\Re\frac{\partial^2 \tilde{S}}{\partial \theta_k \partial \theta_j} + \Im\frac{\partial \tilde{S}}{\partial \theta_k}\Im\frac{\partial^2 \tilde{S}}{\partial \theta_k \partial \theta_j} + \Re\frac{\partial \tilde{S}}{\partial \phi_k}\Re\frac{\partial^2 \tilde{S}}{\partial \phi_k \partial \theta_j} + \Im\frac{\partial \tilde{S}}{\partial \phi_k}\Im\frac{\partial^2 \tilde{S}}{\partial \phi_k \partial \theta_j},\\ \frac{\partial F}{\partial \theta_j^I} = \sum_{k=1}^{N} \Im\frac{\partial \tilde{S}}{\partial \theta_k}\Re\frac{\partial^2 \tilde{S}}{\partial \theta_k \partial \theta_j} - \Re\frac{\partial \tilde{S}}{\partial \theta_k}\Im\frac{\partial^2 \tilde{S}}{\partial \theta_k \partial \theta_j} + \Im\frac{\partial \tilde{S}}{\partial \phi_k}\Re\frac{\partial^2 \tilde{S}}{\partial \phi_k \partial \theta_j} - \Re\frac{\partial \tilde{S}}{\partial \phi_k}\Im\frac{\partial^2 \tilde{S}}{\partial \phi_k \partial \theta_j},\\ \frac{\partial F}{\partial \phi_j^R} = \sum_{k=1}^{N} \Re\frac{\partial \tilde{S}}{\partial \theta_k}\Re\frac{\partial^2 \tilde{S}}{\partial \theta_k \partial \phi_j} + \Im\frac{\partial \tilde{S}}{\partial \theta_k}\Im\frac{\partial^2 \tilde{S}}{\partial \theta_k \partial \phi_j} + \Re\frac{\partial \tilde{S}}{\partial \phi_k}\Re\frac{\partial^2 \tilde{S}}{\partial \phi_k \partial \phi_j} + \Im\frac{\partial \tilde{S}}{\partial \phi_k}\Im\frac{\partial^2 \tilde{S}}{\partial \phi_k \partial \phi_j},\\ \frac{\partial F}{\partial \phi_j^I} = \sum_{k=1}^{N} \Im\frac{\partial \tilde{S}}{\partial \theta_k}\Re\frac{\partial^2 \tilde{S}}{\partial \theta_k \partial \phi_j} - \Re\frac{\partial \tilde{S}}{\partial \theta_k}\Im\frac{\partial^2 \tilde{S}}{\partial \theta_k \partial \phi_j} + \Im\frac{\partial \tilde{S}}{\partial \phi_k}\Re\frac{\partial^2 \tilde{S}}{\partial \phi_k \partial \phi_j} - \Re\frac{\partial \tilde{S}}{\partial \phi_k}\Im\frac{\partial^2 \tilde{S}}{\partial \phi_k \partial \phi_j}, \end{cases}$$
$$\forall j \in [1,N] \quad . \tag{32}$$

4. Model

The methodology described above is applied to a uniaxial spin in transverse magnetic field. The anisotropy axis is taken to be the z-axis and the applied field is pointing along the x-axis. The Hamiltonian of the system is

$$\hat{H} = D\hat{S}_z^2 + B\hat{S}_x, \tag{33}$$

where D is the anisotropy constant and B the strength of the field.

The corresponding energy surface is

$$E(\theta,\phi) = Dj^2\cos^2\theta + Bj\sin\theta\cos\phi + Dj^2 + \frac{B^2}{4D}, \tag{34}$$

The energy is shifted here by the constant $\mathrm{Dj}^2+\mathrm{B}^2/4\mathrm{D}$ to set the minimum energy of the system to zero.

This system has been studied by Chudnovsky using the particle mapping technique [30]. For small field, B<0.5Dj, the crossover from over-the-barrier mechanism to tunneling is first-order, while it is second-order for larger field. The second-order crossover temperature can be obtained from the second derivatives of the energy at the first-order saddle point on the energy surface [37,38,43]. The expression is [43]

$$T_{(2)} = \frac{B(2Dj-B)}{2\pi k_B}. \tag{35}$$

The temperature for the first-order crossover can, however, only be found from calculations of the instantons, as illustrated below.

For convenience, the energy function is rather written in terms of dimensionless quantities

$$\tilde{E}(\theta,\phi) = -\cos^2\theta - 2h_x\sin\theta\cos\phi + 1 + h_x^2, \tag{36}$$

where $\tilde{E}$= Dj^2E is the scaled energy and h_x=B/2Dj is the scaled field strength.

The energy surface is shown in Fig. 2 for two values of the scaled field, h_x=0.50 and 0.05. The two minima corresponding to the ground states of the system as well as the minimum energy path connecting them are located at $\phi = 0$. The larger the field, the further away the minima are from the anisotropy axis.

The analytical continuation to complex angles is

$$\tilde{E}(\theta,\phi) = -\cos^2(\theta^R + i\theta^I) - 2h_x\sin(\theta^R + i\theta^I)\cos(\phi^R + i\phi^I) \tag{37}$$

where θ^R and ϕ^R are the real parts and θ^I and ϕ^I are the imaginary parts of the angular variables.

5. Results

Fig. 3 shows calculated instantons for an applied field of h_x=0.50 and 0.05. It turns out that $\phi^R = \theta^I = 0$ for all these instantons and the energy is real

$$\tilde{E} = E = -\cos^2(\theta^R) - 2h_x\sin(\theta^R)\cosh(\phi^I) \tag{38}$$

so the instantons can be visualized in the (θ^R,ϕ^I) plane. For the higher temperature values, the replicas are nearly equally distributed along the equipotential contours. But, for the lowest temperature, the distribution is distinctly uneven, with larger density of discretization points near the extreme values of θ^R.

The temperature corresponding to each of the instantons is given in the legend of Fig. 3. The classical first-order saddle point on the energy surface appears as a maximum in this plane. An instanton corresponding to a slightly lower energy contour has all discretization

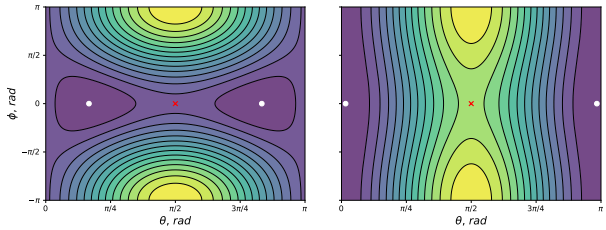

FIG. 2. The energy surface of a system with a single spin subject to anisotropy along the z-axis and an applied magnetic field in x-direction of magnitude h_x=B/2Dj =0.50 (left) and h_x=0.05 (right), see eqn. (34). The local minima corresponding to initial and final states are marked with a white ×. For the weaker field, they are located closer to the anisotropy axis. The minimum energy path for the transition is a straight line at $\phi = 0$ between the minima. The maximum along the minimum energy path, a first-order saddle point on the energy surface, is marked with a red ×.

points at nearly the same location, as the path just barely opens up. The corresponding temperature is denoted as $T_{(2)}$ (1.592 K for the higher field, 0.694 K for the lower field).

Instantons on lower energy contours correspond to lower temperature in the high field case. There is a monotonic decrease in the temperature as the energy is decreased. This behavior can be seen for the high field case in Fig. 4. The crossover from over-the-barrier mechanism to tunneling then occurs at a temperature of $T_{(2)}$ and this is referred to as second-order crossover. The relevant instantons for the onset of tunneling appear at an energy just below $E^{\dagger}$ and correspond to an energy contour lying in the vicinity of the classical first-order saddle point on the real energy surface. There is a continuous transition from over-the-barrier to tunneling mechanism. The value of $T_{(2)}$ can be obtained from the second derivatives of the energy at the saddle point [37, 38]. In the limit of zero energy, the temperature approaches zero and the instanton lies on the energy contour that goes through the initial and final state minima.

For the low field case, h_x=0.05, the situation is different. From Fig. 3 it can be seen that the shape of the instantons is quite different from the high field case. The change in the instanton temperature as the energy is lowered from the saddle point energy is non-monotonic. The temperature first increases as the energy is decreased, reaching a maximum at a value T_m (see Fig. 4) and then decreases, but eventually reaches zero at the energy of the initial state minimum. Two of the instantons shown in Fig. 3 for the low field case have a temperature that is higher than $T_{(2)}$. Even though the instantons are more spread out, and the corresponding periodic orbits longer, the imaginary time period is shorter. Apparently, this is related to the long vertical segments that can be seen in Fig. 3 for the instantons

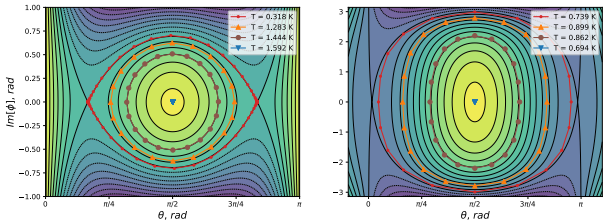

FIG. 3. Analytically continued energy surface in (θ^R,ϕ^I) plane for field strength of h_x=B/2Dj =0.50 (left) and 0.05 (right). For the system studied here, the instantons are at $\Re\phi$=0 and $\Im\theta$=0 so it is sufficient to show them in the ($\Im\phi, \Re\theta$) plane. Instantons for various energy contours are shown (red, orange, brown and blue lines with dots, upper triangles, and filled circles indicating the location of the discretization points) and the corresponding values of the temperature are given in the legend. The blue instantons are near the first-order saddle point on the real energy surface, corresponding to over-the-barrier mechanism and temperature close to the second-order crossover temperature, $T_{(2)}$. For the stronger field, h_x=0.50, the lower energy and more extended instantons correspond to longer period for the periodic orbit and lower temperature. The crossover from over-the-barrier mechanism to tunneling is second-order. For the weaker field, h_x=0.05, the period decreases and the temperature increases as the energy is lowered from the value at the first-order saddle point until a maximum is reached (notice the high temperature associated with the brown curve with circles). The crossover is first-order and occurs at a temperature $T_{(1)}$ that is higher than $T_{(2)}$.

in low field. There, the partial derivative of the energy with respect to θ^R is large and the acceleration in ϕ^I given by the Landau-Lifshitz equations has a correspondingly large magnitude.

Fig. 5 compares the exponents of the Boltzmann factors for the two mechanisms: over-the-barrier, $E^\dagger/k_BT$, and tunneling, S_{ins}/k_BT. The smaller this exponent is, the larger the transition rate. For the large field case, h_x=0.50, a smaller exponent is obtained for tunneling as the temperature drops below $T_{(2)}$, consistent with a second-order crossover from over-the-barrier to tunneling mechanism. After a slight increase in the value of S_{ins}/k_BT as the temperature is lowered below $T_{(2)}$, it remains relatively independent of temperature.

For the small field case, h_x=0.05, the instantons on energy contours just below the saddle point energy turn out to have a larger Boltzmann exponent than over-the-barrier transitions so they do not lead to crossover to tunneling. The instanton temperature continues to increase as the energy of the contour is lowered until a maximum value is obtained

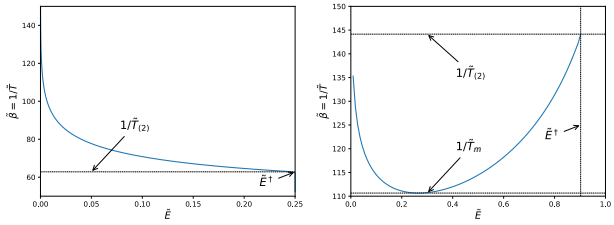

FIG. 4. Inverse scaled temperature, $1/\tilde{T}$= 2Dj/Tk$_B$, found from the period of Landau-Lifshitz orbits in imaginary time vs. scaled energy, $\tilde{E}$=Dj^{2}E, of the contour where the instanton lies for field strength of h$_x$=B/2Dj =0.50 (left) and 0.05 (right). $\tilde{E}^{\dagger}$ is the scaled energy of the first-order saddle point on the energy surface corresponding to the activation energy of the classical over-the-barrier mechanism. $\tilde{T}_{(2)}$ is the scaled temperature for an instanton at an energy contour just below $\tilde{E}^{\dagger}$. For strong field, h$_x$=0.50, this is the highest instanton temperature and a second-order crossover to tunneling occurs there. For weak field, h$_x$=0.05, the crossover is first-order and the instanton involved is not located near the saddle point. There, the instanton temperature increases as the energy is lowered from $\tilde{E}^{\dagger}$ and reaches a maximum of $\tilde{T}_m$ for an energy that is intermediate between that of the initial state and the first-order saddle point. The crossover temperature turns out to be higher than $\tilde{T}_{(2)}$ in this case (see Fig. 5).

at T$_m$. Further lowering of the energy then gives a second set of instantons for each temperature value between T$_{(2)}$ and T$_m$. The Boltzmann exponent for these instantons is smaller and at a certain temperature, T$_{(1)}$, an instanton has the same value of the exponent as the over-the-barrier mechanism, indicating a crossover to tunneling (see Fig. 5). The stationary point of the action that gives the fastest transition rate then changes abruptly from the classical saddle point to an instanton that has significantly lower energy.

Since the first-order crossover corresponds to an instanton that is far removed from the first-order saddle point on the energy surface, it is not possible to estimate T$_{(1)}$ from the energy and its derivatives at the saddle point, as can be done for second-order crossover. Identification of first-order crossover to tunneling requires the evaluation of instantons over the relevant energy range from E=0 to E†.

The difference between first and second-order crossover can be seen from calculations carried out at and slightly below the critical field, h_x=B/2Dj=0.25, as shown in Fig. 6. The second-order crossover is characterized by a monoton decrease of the instanton temperature as the energy decreases. On the other hand, the first-order crossover is characterized by non-monotone behavior. Over a certain range in temperature, instantons on two different energy contours correspond to the same value of the temperature. The instanton lying on the lower energy contour corresponds to a smaller exponent in the Boltzmann factor and therefore higher tunneling rate.

The critical value of h_x=0.25 between first- and second-order crossover had previously been determined for this system by Chudnovsky using the particle mapping technique [30].

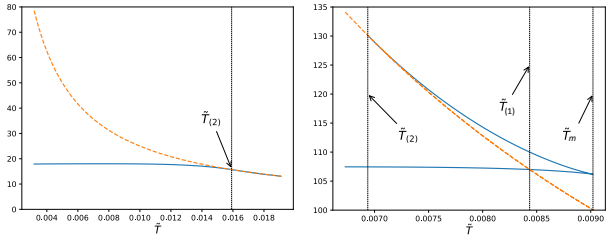

FIG. 5. Exponents of the Boltzmann factor, S_{ins}/k_BT for instantons (blue curve) and $E^{\dagger}/k_BT$ for over-the-barrier mechanism (dashed orange curve), as a function of scaled temperature, $\tilde{T} = Tk_B/2Dj$, for field strength of h_x=B/2Dj =0.50 (left) and 0.05 (right). For strong field, the highest temperature instanton is obtained for energy contour just below the saddle point energy and the crossover temperature, $T_{(2)}$, can be deduced from the second derivatives of the energy at the saddle point [37, 38]. For weak field, the instanton temperature increases as the energy is lowered from the saddle point energy and the Boltzmann exponent for those instantons is larger than for over-the-barrier transitions. After reaching a maximum at T_m, the instanton temperature decreases as the contour energy is lowered and at a temperature of $T_{(1)}$ the exponent for the instanton equals that of the over-the-barrier mechanism indicating a first-order crossover to tunneling.

The calculations presented here of finite temperature instantons are clearly in good agreement with this previous estimate.

6. Discussion

A method is presented for finding instantons corresponding to tunneling between magnetic states at finite temperature. The method is based on analytical continuation of the energy of the system to complex angular variables and identification of an energy contour, followed by evaluation of the corresponding temperature and finally refinement of the distribution of discretization points to converge on a stationary point of the action. This method takes advantage of the fact that the Landau-Lifshitz equations of motion for spin systems conserve energy. Since the instanton corresponds to a stationary point of the action, it also corresponds to a periodic orbit along an energy contour. The refinement is based on local minimization of the magnitude of the gradients of the action with respect to the degrees of freedom in the system. Since a good initial guess for this iterative refinement procedure can be obtained from an even distribution of discretization points along the energy contour, such a local minimization most likely will converge on the appropriate instanton, rather than some other stationary point of the action.

This method is quite different from the ones used to find instantons for atomic rearrangements [25, 26] where the equations of motion conserve the total energy, i.e. kinetic plus potential energy. In some sense, it is easier to find instantons for magnetic systems since their shape can so clearly be identified on the energy surface. The additional complication, however, lies in the analytical continuation of the energy expression to allow for complex

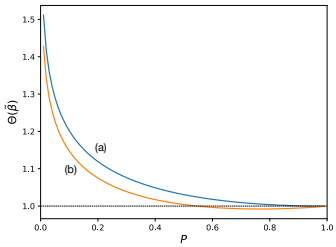

FIG. 6. Illustration of the change from first-order to second-order crossover to tunneling as the applied field is increased from h_x=B/2Dj =0.20 (orange line (b)) to 0.25 (blue line (a)). Scaled inverse temperature Θ=T_c/T is shown as a function of scaled energy P=E/$E^\dagger$. The instanton temperature is a monotone function of the energy when the the crossover to tunneling is second-order. When the crossover is first-order, the temperature corresponding to the instantons first increases as the energy of the contour is lowered below $E^\dagger$, but then decreases for even lower energy.

values of the angular variables. While this is relatively straightforward when the energy of the system is given by an analytical expression, it is not clear how to approach this problem when self-consistent calculations (such as the non-collinear Alexander-Andersson model [44]) are used to evaluate the energy.

By finding the instantons as a function of temperature, the crossover temperature for both first-order and second-order crossover can be estimated. Previously, a general expression for the second-order crossover temperature based on second derivatives of the energy at the first-order saddle point on the energy surface had been presented [37, 38], but a calculation of the first-order crossover temperature is more challenging because it does not relate directly to the first-order saddle point. There is not a continuous transition from the over-the-barrier to tunneling mechanism in that case. By finding the instantons, however, the first-order case can be treated.

The method has been illustrated here with an application to a system with a single spin. It is, however, easily generalized to systems with arbitrary number of spins. The method for finding the energy contour, an extension of the NEB method which is routinely used for multidimensional systems, the Landau-Lifshitz dynamics and the BFGS minimization of the magnitude of the gradient of the action can all be carried out in a straightforward way for many degrees of freedom. We anticipate that tunneling of, for example, magnetic skyrmions and other localized non-collinear states can be studied with the technique presented here.

7. Acknowledgements

We thank Igor Lobanov for helpful discussions. This work was supported by the Icelandic Research Fund, the Academy of Finland (grant 278260) and the Government of the Russian Federation (grant 074U01).

References

[1] Wigner E. The transition state method. *Trans. Faraday Soc.* 1938. **34**. 29–41.
[2] Kramers H. A. Brownian motion in a field of force and the diffusion model of chemical reactions. *Physica.* 1940. **7**(4). 284–304.
[3] Langer J. S. Statistical theory of the decay of metastable states. *Ann. Phys.* 1969. **54**. 258–275.
[4] Braun H.-B. Kramers's rate theory, broken symmetries and magnetization reversal. *J. Appl. Physics* 1994. **76**. 6310–6315.
[5] Coffey W. T., Garanin D. A. and McCarthy D. J. Crossover formulas in the Kramers theory of thermally activated escape rates-application to spin systems. *Adv. Chem. Phys.* 2001. **117**. 483–765.
[6] Fiedler G., Fidler J., Lee J., Schrefl T., Stamps R. L., Braun H. B.,Suess D. Direct calculation of the attempt frequency of magnetic structures using the finite element method. *J. Appl. Phys.* 2012. **111**(9). 093917 (7 pp.)
[7] Bessarab P. F., Uzdin V. M. and Jónsson H. Harmonic Transition State Theory of Thermal Spin Transitions. *Phys. Rev. B* 2012. **85**. 184409 (4 pp.)
[8] Bessarab P. F., Uzdin V. M. and Jónsson H. Potential Energy Surfaces and Rates of Spin Transitions. *Z. Phys. Chem.* 2013. **227**. 1543–1557.
[9] Feynman R. P., Hibbs A. R. *Quantum Mechanics and Path Integrals.* McGraw-Hill, NY, 1965.
[10] Miller W. H. Semiclassical limit of quantum mechanical transition state theory for nonseparable systems. *J. Chem. Phys.* 1975. **62**. 1899–1906.
[11] Coleman S. Fate of the false vacuum: Semiclassical theory *Phys. Rev. D.* 1977. **15**. 2929–2936.
[12] Callan C., Coleman S. Fate of the false vacuum. II. First quantum corrections. *Phys. Rev. D* 1977. **16**. 1762–1768.
[13] Benderskii V. A., Makarov D. E., Wight C. A. *Chemical dynamics at low temperatures.* John Wiley & Sons, New York.: 1994.
[14] Mills G., Schenter G. K., Makarov D. E. and Jónsson H. Generalized path integral based quantum transition state theory. *Chem. Phys. Letters* 1997. **278**. 91–96.
[15] Mills G., Schenter G. K., Makarov D. E., and Jónsson H. RAW quantum transition state theory. in *Classical and Quantum Dynamics in Condensed Phase Simulations*, edited by Berne B. J., Ciccotti G., and Coker D. F., World Scientific, 1998, 405–421.
[16] Craig I. R., Manolopoulos D. E. *J. Chem. Phys.* 2005. **123**. 034102.
[17] Habershon S., Manolopoulos D. E., Markland T. E. and Miller III T. F. *Annu. Rev. Phys. Chem.* 2013. **64**. 387–413.
[18] Vineyard G. H. Frequency factors and isotope effects in solid state rate processes. *J. Phys. Chem. Solids.* 1957. **3**(1). 121–127.
[19] Mills G., Jónsson H., and Schenter G. K. Reversible work based transition state theory: application to H_2 dissociative adsorption. *Surf. Sci.* 1995. **324**. 305–337.
[20] Jónsson H., Mills G., and Jacobsen K. W., "Nudged elastic band method for finding minimum energy paths of transitions," in *Classical and Quantum Dynamics in Condensed Phase Simulations*, edited by Berne B. J., Ciccotti G., and Coker D. F., World Scientific, 1998, 385–404.
[21] Bessarab P. F., Uzdin V. M. and Jónsson H. Method for finding mechanism and activation energy of magnetic transitions, applied to skyrmion and antivortex annihilation. *Comp. Phys. Commun.* 2015. **196**. 335–347.
[22] Henkelman G., Jónsson H. A Dimer Method for Finding Saddle Points on High Dimensional Potential Surfaces Using Only First Derivatives. *J. Chem. Phys.* 1999. **111**. 7010–7022.
[23] Gutiérrez M. P., Argáez C. and Jónsson H. Improved Minimum Mode Following Method for Finding First Order Saddle Points *J. Chem. Theor. Comput.* 2017. **13**. 125–134.
[24] Richardson J. O. Derivation of instanton rate theory from first principles. *J. Chem. Phys.* 2016. **144**. 114106 (5 pp.).

[25] Andersson S., Nyman G., Arnaldsson A., Manthe U. and Jónsson H. Comparison of Quantum Dynamics and Quantum Transition State Theory Estimates of the H + CH_4 Reaction Rate. *J. Phys. Chem. A*. 2009. **113** 4468–4478.

[26] Einarsdóttir D. M., Arnaldsson A., Óskarsson F. and Jónsson H. Path Optimization with Application to Tunneling. *Lecture Notes in Computer Science* 2012. **7134**. 45–55.

[27] Rommel J. B., Liu Y., Werner H.-J. and Kästner J. Role of tunneling in the enzyme glutamate mutase. *J. Phys. Chem. B* 2012. **116**. 13682–13689.

[28] Zaslavskii O. Spin tunneling and the effective potential method. *Phys. Lett. A* 1990. **145**(8). 471–475.

[29] Ulyanov V. V., Zaslavskii O. B. New methods in the theory of quantum spin systems. *Phys. Rep*. 1992. **216**. 179–251.

[30] Chudnovsky E. M., Garanin D. A. First- and Second-Order Transitions between Quantum and Classical Regimes for the Escape Rate of a Spin System. *Phys. Rev. Lett.* 1997. **79**. 4469–4472.

[31] Wernsdorfer W., Aliaga-Alcalde N., Hendrickson D. N., Christou G. Exchange-biased quantum tunnelling in a supramolecular dimer of single-molecule magnets. *Nature* 2002. **416**. 406–409.

[32] Wernsdorfer W., Murugesu M. and Christou G. Resonant Tunneling in Truly Axial Symmetry Mn_{12} Single-Molecule Magnets: Sharp Crossover between Thermally Assisted and Pure Quantum Tunneling. *Phys. Rev. Lett.* 2006. **96**. 057208 (4 pp.)

[33] Owerre S. A. and Paranjape M. B. Phase transition between quantum and classical regimes for the escape rate of dimeric molecular nanomagnets in a staggered magnetic field. *Phys. Lett. A* 2014. **378**. 1407–1412.

[34] von Delft J. and Henley C. L. Destructive quantum interference in spin tunneling problems. *Phys. Rev. Lett.* 1992. **69**. 3236–3239.

[35] Loss D., DiVincenzo D. P. and Grinstein G. Suppression of tunneling by interference in half-integer-spin particles. *Phys. Rev. Lett.* 1992. **69**. 3232–3236.

[36] Garg A. Topologically Quenched Tunnel Splitting in Spin Systems without Kramers Degeneracy. *Europhys. Lett.* 1993. **22**(3). 205–210.

[37] Vlasov S., Bessarab P. F., Uzdin V. M. and Jónsson H. Classical to quantum mechanical tunneling mechanism crossover in thermal transitions between magnetic states. *Faraday Discuss.* 2016. **195**. 93–109.

[38] Vlasov S. M., Bessarab P. F., Uzdin V. M. and Jónsson H. Calculations of the onset temperature for tunneling in multispin systems. *Nanosystems: Physics, Chemistry, Mathematics* 2017. **8**. 454–461.

[39] Fradkin E. *Field Theories of Condensed Matter Physics.* Cambridge University Press, New York.: 2013, 190 p.

[40] Kochetov E. SU(2) coherentstate path integral. *J. Math. Phys.* 1995. **36**. 4667–4679.

[41] Berry M. V. Quantal Phase Factors Accompanying Adiabatic Changes. *Proceedings of the Royal Society of London. Series A, Mathematical and Physical Sciences* 1984. **392**(1802). 45–57.

[42] Henkelman G., Jónsson H. Improved tangent estimate in the nudged elastic band method for finding minimum energy paths and saddle points. *J. Chem. Phys.* 2000. **113**. 9978–9985.

[43] Vlasov S. M., Bessarab P. F., Uzdin V. M. and Jónsson H. Crossover temperature for quantum tunnelling in spin systems. *J. Phys. Conf. Ser.* 2016. **741**. 012183 (5 pp.).

[44] Bessarab P. F., Uzdin V. M. Jónsson H. Calculations of magnetic states and minimum energy paths of transitions using a noncollinear extension of the Alexander-Anderson model and a magnetic force theorem. *Phys. Rev. B.* 2014. **89**(21). 214424 (12 pp.).

References

[1] **C. Joachim** and **M. A. Ratner**. *Molecular electronics: Some views on transport junctions and beyond*. Proceedings of the National Academy of Sciences of the United States of America, 102(25), (2005), 8801.

[2] **N. J. Tao**. *Electron transport in molecular junctions*. Nat Nano, 1(3), (2006), 173.

[3] **D. D. Awschalom** and **M. E. Flatte**. *Challenges for semiconductor spintronics*. Nat Phys, 3(3), (2007), 153.

[4] **H. Dery**, **P. Dalal**, **L. Cywinski** and **L. J. Sham**. *Spin-based logic in semiconductors for reconfigurable large-scale circuits*. Nature, 447(7144), (2007), 573.

[5] **Z. H. Xiong**, **D. Wu**, **Z. Valy Vardeny** and **J. Shi**. *Giant magnetoresistance in organic spin-valves*. Nature, 427(6977), (2004), 821.

[6] **W. F. Brown Jr**. *Thermal fluctuation of fine ferromagnetic particles*. IEEE Transactions on Magnetics, 15(5), (1979), 1196 .

[7] **H. Braun**. *Kramers's rate theory, broken symmetries, and magnetization reversal (invited)*. Journal of Applied Physics, 76(10), (1994), 6310.

[8] **P. Visscher** and **R. Zhu**. *Low-dimensionality energy landscapes: Magnetic switching mechanisms and rates*. Physica B: Condensed Matter, 407(9), (2012), 1340 . 8th International Symposium on Hysteresis Modeling and Micromagnetics (HMM 2011).

[9] **G. Fiedler**, **J. Fidler**, **J. Lee**, **T. Schrefl**, **R. L. Stamps**, **H. B. Braun** and **D. Suess**. *Direct calculation of the attempt frequency of magnetic structures using the finite element method*. Journal of Applied Physics, 111(9), (2012), 093917.

[10] **P. F. Bessarab**, **V. M. Uzdin** and **H. Jónsson**. *Harmonic transition-state theory of thermal spin transitions*. Phys. Rev. B, 85, (2012), 184409.

[11] **P. F. Bessarab**, **V. M. Uzdin** and **H. Jónsson**. *Size and Shape Dependence of Thermal Spin Transitions in Nanoislands*. Phys. Rev. Lett., 110, (2013), 020604.

[12] **P. F. Bessarab**, **V. M. Uzdin** and **H. Jónsson**. *Potential Energy Surfaces and Rates of Spin Transitions*. Zeitschrift für Physikalische Chemie, 227, (2013), 1543.

[13] **H. Mökkönen**, **T. Ikonen**, **T. Ala-Nissila** and **H. Jónsson**. *Transition state theory approach to polymer escape from a one dimensional potential well*. The Journal of Chemical Physics, 142(22), (2015), 224906.

[14] **E. M. Chudnovsky**. *Phase transitions in the problem of the decay of a metastable state*. Phys. Rev. A, 46, (1992), 8011.

[15] **V. Ulyanov** and **O. Zaslavskii**. *New methods in the theory of quantum spin systems*. Physics Reports, 216(4), (1992), 179 .

[16] **E. M. Chudnovsky** and **D. A. Garanin**. *First- and Second-Order Transitions between Quantum and Classical Regimes for the Escape Rate of a Spin System*. Phys. Rev. Lett., 79, (1997), 4469.

[17] **C.-S. Park**, **S.-K. Yoo** and **D.-H. Yoon**. *Quantum-classical crossover of the escape rate in a biaxial spin system with an arbitrarily directed magnetic field*. Phys. Rev. B, 61, (2000), 11618.

[18] **G.-H. Kim** and **E. M. Chudnovsky**. *Escape-rate crossover between quantum and classical regimes in molecular magnets: A diagonalization approach*. EPL (Europhysics Letters), 52(6), (2000), 681.

[19] **D. A. Garanin** and **E. M. Chudnovsky**. *Quantum statistical metastability for a finite spin*. Phys. Rev. B, 63, (2000), 024418.

[20] **S. Owerre** and **M. Paranjape**. *Phase transition between quantum and classical regimes for the escape rate of dimeric molecular nanomagnets in a staggered magnetic field*. Physics Letters A, 378(20), (2014), 1407 .

[21] **S. Owerre** and **M. Paranjape**. *Macroscopic quantum tunneling and quantum–classical phase transitions of the escape rate in large spin systems*. Physics Reports, 546(Supplement C), (2015), 1 . Macroscopic quantum tunneling and quantum–classical phase transitions of the escape rate in large spin systems.

[22] **K. M. Mertes**, **Y. Zhong**, **M. P. Sarachik**, **Y. Paltiel**, **H. Shtrikman**, **E. Zeldov**, **E. Rumberger**, **D. N. Hendrickson** and **G. Christou**. *Abrupt crossover between thermally activated relaxation and quantum tunneling in a molecular magnet*. EPL (Europhysics Letters), 55(6), (2001), 874.

[23] **W. Wernsdorfer** and **R. Sessoli**. *Quantum Phase Interference and Parity Effects in Magnetic Molecular Clusters*. Science, 284(5411), (1999), 133.

[24] **S. Vlasov**, **P. F. Bessarab**, **V. M. Uzdin** and **H. Jónsson**. *Classical to quantum mechanical tunneling mechanism crossover in thermal transitions between magnetic states*. Faraday discussions, 195, (2016), 93.

[25] **S. M. Vlasov**, **P. F. Bessarab**, **V. M. Uzdin** and **H. Jónsson**. *Calculations of the onset temperature for tunneling in multispin systems*. Nanosystems: Physics, Chemistry, Mathematics, 8(4), (2017), 454.

[26] **G. Mills**, **G. Schenter**, **D. Makarov** and **H. Jónsson**. *Generalized path integral based quantum transition state theory*. Chemical Physics Letters, 278(1), (1997), 91 .

[27] **E. Wigner**. *The transition state method*. Transactions of the Faraday Society, 34, (1938), 29.

[28] **H. Kramers**. *Brownian motion in a field of force and the diffusion model of chemical reactions*. Physica, 7(4), (1940), 284 .

[29] **J. Langer**. *Statistical theory of the decay of metastable states*. Annals of Physics, 54(2), (1969), 258 .

[30] **T. Lis**. *Preparation, structure, and magnetic properties of a dodecanuclear mixed-valence manganese carboxylate*. Acta Crystallographica Section B, 36(9), (1980), 2042.

[31] **K. Weighardt**, **K. Pohl**, **I. Jibril** and **G. Huttner**. *Hydrolysis Products of the Monomeric Amine Complex ($C_6H_15N_3$)$FeCl_3$: The Structure of the Octameric Iron(III) Cation of [($C_6H_15N_3$)$_6Fe_8(\mu_3$-$O)_2(\mu_2$-$OH)_12$]$Br_7(H_2O)Br{\cdot}8H_2O$*. Angewandte Chemie International Edition in English, 23(1), (1984), 77.

[32] **S. M. J. Aubin**, **N. R. Dilley**, **L. Pardi**, **J. Krzystek**, **M. W. Wemple**, **L.-C. Brunel**, **M. B. Maple**, **G. Christou** and **D. N. Hendrickson**. *Resonant Magnetization Tunneling in the Trigonal Pyramidal MnIVMnIII3 Complex [Mn4O3Cl(O2CCH3)3(dbm)3]*. Journal of the American Chemical Society, 120(20), (1998), 4991.

[33] **J. R. Friedman**, **M. P. Sarachik**, **J. Tejada** and **R. Ziolo**. *Macroscopic Measurement of Resonant Magnetization Tunneling in High-Spin Molecules*. Phys. Rev. Lett., 76, (1996), 3830.

[34] **L. Thomas**, **F. Lionti**, **R. Ballou**, **D. Gatteschi**, **R. Sessoli** and **B. Barbara**. *Macroscopic quantum tunnelling of magnetization in a single crystal of nanomagnets*. Nature, 383(6596), (1996), 145.

[35] **A. Ardavan**, **O. Rival**, **J. J. L. Morton**, **S. J. Blundell**, **A. M. Tyryshkin**, **G. A. Timco** and **R. E. P. Winpenny**. *Will Spin-Relaxation Times in Molecular Magnets Permit Quantum Information Processing?* Phys. Rev. Lett., 98, (2007), 057201.

[36] **I. Tupitsyn** and **B. Barbara**. *Quantum Tunneling of Magnetization in Molecular Complexes with Large Spins – Effect of the Environment*, chapter 4, pp. 109–168. Wiley-VCH Verlag GmbH Co. KGaA, 2001.

[37] **V. M. Uzdin**, **A. Vega**, **A. Khrenov**, **W. Keune**, **V. E. Kuncser**, **J. S. Jiang** and **S. D. Bader**. *Noncollinear Fe spin structure in (Sm-Co)/Fe exchange-spring bilayers: Layer-resolved ^{57}Fe Mössbauer spectroscopy and electronic structure calculations*. Phys. Rev. B, 85, (2012), 024409.

[38] **V. M. Uzdin**, **H. Zabel**, **A. Remhof** and **B. Hjörvarsson**. *Transition from spin-density-wave to layered antiferromagnetic state induced by hydrogen as a test for the origin of spin-density waves in chromium*. Phys. Rev. B, 80, (2009), 174418.

[39] **C. F. Hirjibehedin**, **C.-Y. Lin**, **A. F. Otte**, **M. Ternes**, **C. P. Lutz**, **B. A. Jones** and **A. J. Heinrich**. *Large Magnetic Anisotropy of a Single Atomic Spin Embedded in a Surface Molecular Network*. Science, 317(5842), (2007), 1199.

[40] **M. Mannini**, **F. Pineider**, **C. Danieli**, **F. Totti**, **L. Sorace**, **P. Sainctavit**, **M. A. Arrio**, **E. Otero**, **L. Joly**, **J. C. Cezar**, **A. Cornia** and **R. Sessoli**. *Quantum tunnelling of the magnetization in a monolayer of oriented single-molecule magnets*. Nature, 468(7322), (2010), 417.

[41] **G. Mills**, **H. Jónsson** and **G. K. Schenter**. *Reversible work transition state theory: application to dissociative adsorption of hydrogen*. Surface Science, 324(2), (1995), 305 .

[42] **H. Jónsson**, **G. Mills** and **K. W. Jacobsen**. *Nudged elastic band method for finding minimum energy paths of transitions*. In *Classical And Quantum Dynamics In Condensed Phase Simulations*, pp. 385–404. World Scientific, 1998.

[43] **P. F. Bessarab**, **V. M. Uzdin** and **H. Jónsson**. *Method for finding mechanism and activation energy of magnetic transitions, applied to skyrmion and antivortex annihilation*. Computer Physics Communications, 196(Supplement C), (2015), 335 .

[44] **G. Henkelman** and **H. Jónsson**. *A dimer method for finding saddle points on high dimensional potential surfaces using only first derivatives*. The Journal of Chemical Physics, 111(15), (1999), 7010.

[45] **R. Malek** and **N. Mousseau**. *Dynamics of Lennard-Jones clusters: A characterization of the activation-relaxation technique*. Physical Review E, 62(6), (2000), 7723.

[46] **L. J. Munro** and **D. J. Wales**. *Defect migration in crystalline silicon*. Physical Review B, 59(6), (1999), 3969.

[47] **M. J. S. Dewar**, **E. F. Healy** and **J. J. P. Stewart**. *Location of transition states in reaction mechanisms*. J. Chem. Soc., Faraday Trans. 2, 80, (1984), 227.

[48] **P. F. Bessarab**, **V. M. Uzdin** and **H. Jónsson**. *Calculations of magnetic states and minimum energy paths of transitions using a noncollinear extension of the Alexander-Anderson model and a magnetic force theorem*. Phys. Rev. B, 89, (2014), 214424.

[49] **S. Loth**, **S. Baumann**, **C. P. Lutz**, **D. M. Eigler** and **A. J. Heinrich**. *Bistability in Atomic-Scale Antiferromagnets*. Science, 335(6065), (2012), 196.

[50] **S. Krause**, **G. Herzog**, **T. Stapelfeldt**, **L. Berbil-Bautista**, **M. Bode**, **E. Y. Vedmedenko** and **R. Wiesendanger**. *Magnetization Reversal of Nanoscale Islands: How Size and Shape Affect the Arrhenius Prefactor*. Phys. Rev. Lett., 103, (2009), 127202.

[51] **M. Moskalenko**, **P. F. Bessarab**, **V. M. Uzdin** and **H. Jónsson**. *Qualitative insight and quantitative analysis of the effect of temperature on the coercivity of a magnetic system*. AIP Advances, 6(2), (2016), 025213.

[52] **I. S. Lobanov**, **H. Jónsson** and **V. M. Uzdin**. *Mechanism and activation energy of magnetic skyrmion annihilation obtained from minimum energy path calculations*. Phys. Rev. B, 94, (2016), 174418.

[53] **A. Ivanov**, **P. F. Bessarab**, **V. M. Uzdin** and **H. Jonsson**. *Magnetic exchange force microscopy: theoretical analysis of induced magnetization reversals*. Nanoscale, 9(35), (2017), 13320.

[54] **J. Smit** and **H. G. Beljers**. *Ferromagnetic resonance absorption in BaFe12O19, a highly anisotropic crystal*. Philips Res. Rep, 10(113), (1955), 31.

[55] **H. Suhl**. *Ferromagnetic Resonance in Nickel Ferrite Between One and Two Kilomegacycles*. Phys. Rev., 97, (1955), 555.

[56] **O. Zaslavskii**. *Spin tunneling and the effective potential method*. Physics Letters A, 145(8), (1990), 471 .

[57] **J. von Delft** and **C. L. Henley**. *Destructive quantum interference in spin tunneling problems*. Phys. Rev. Lett., 69, (1992), 3236.

[58] **D. Loss**, **D. P. DiVincenzo** and **G. Grinstein**. *Suppression of tunneling by interference in half-integer-spin particles*. Phys. Rev. Lett., 69, (1992), 3232.

[59] **A. Garg**. *Topologically Quenched Tunnel Splitting in Spin Systems without Kramers' Degeneracy*. EPL (Europhysics Letters), 22(3), (1993), 205.

[60] **R. J. Glauber**. *Coherent and Incoherent States of the Radiation Field*. Phys. Rev., 131, (1963), 2766.

[61] **A. Perelomov**. *Generalized coherent states and their applications*. Springer Science & Business Media, 2012.

[62] **E. Fradkin**. *Field Theories of Condensed Matter Physics*, chapter 7.2, p. 190. Cambridge University Press, New York, 2013.

[63] **E. Kochetov**. *SU(2) coherent-state path integral*. Journal of Mathematical Physics, 36(9), (1995), 4667.

[64] *Quantal phase factors accompanying adiabatic changes*. Proceedings of the Royal Society of London A: Mathematical, Physical and Engineering Sciences, 392(1802), (1984), 45.

[65] **S. Kirkpatrick**, **C. D. Gelatt**, **M. P. Vecchi** *et al. Optimization by simulated annealing*. science, 220(4598), (1983), 671.

[66] **M. Plasencia Gutiérrez**, **C. Argáez** and **H. Jónsson**. *Improved Minimum Mode Following Method for Finding First Order Saddle Points*. Journal of Chemical Theory and Computation, 13(1), (2017), 125. PMID: 27959552.

[67] **D. M. Einarsdóttir**, **A. Arnaldsson**, **F. Óskarsson** and **H. Jónsson**. *Path Optimization with Application to Tunneling*, pp. 45–55. Springer Berlin Heidelberg, Berlin, Heidelberg, 2012.

[68] **D. Sheppard**, **R. Terrell** and **G. Henkelman**. *Optimization methods for finding minimum energy paths*. The Journal of Chemical Physics, 128(13), (2008), 134106.

[69] **D. H. Kang** and **G.-H. Kim**. *Theoretical study of abrupt or gradual crossover of the escape rate in single-molecule magnets*. Phys. Rev. B, 74, (2006), 184418.

[70] **G. H. Kim**, **D. H. Kang** and **M. C. Shin**. *Quantum-classical crossover of the escape rate in the biaxial nanomagnets with a higher order symmetry*. The European Physical Journal B, 83(1), (2011), 63.

[71] **L. Bokacheva**, **A. D. Kent** and **M. A. Walters**. *Crossover between Thermally Assisted and Pure Quantum Tunneling in Molecular Magnet* Mn_{12}*-Acetate*. Phys. Rev. Lett., 85, (2000), 4803.

[72] **W. Wernsdorfer**, **M. Murugesu** and **G. Christou**. *Resonant Tunneling in Truly Axial Symmetry* Mn_{12} *Single-Molecule Magnets: Sharp Crossover between Thermally Assisted and Pure Quantum Tunneling*. Phys. Rev. Lett., 96, (2006), 057208.

[73] **V. I. Goldanskii**. Sov. Phys. Dokl., 4, (1959), 74.

[74] **V. Benderskii**, **V. Goldanskii** and **D. Makarov**. *Quantum dynamics in low-temperature chemistry*. Physics Reports, 233(4), (1993), 195 .

[75] **W. Wernsdorfer**, **N. Aliaga-Alcalde**, **D. N. Hendrickson** and **G. Christou**. *Exchange-biased quantum tunnelling in a supramolecular dimer of single-molecule magnets*. Nature, 416(6879), (2002), 406.

[76] **N. Romming**, **A. Kubetzka**, **C. Hanneken**, **K. von Bergmann** and **R. Wiesendanger**. *Field-dependent size and shape of single magnetic skyrmions*. Physical review letters, 114(17), (2015), 177203.